To the Graduate Council:

I am submitting herewith a thesis written by Michael L. Thompson entitled "On The Nature of Interaction Between Melittin of Bee Venom and Model Phospholipid Membranes." I recommend that it be accepted in partial fulfillment of the requirements for the degree of Master of Science, with a major in Radiation Biology.

Solon Georghiou, Major Professor

We have read this thesis and recommend its acceptance:

Accepted for the Council:

Vice Chancellor
Graduate Studies and Research

ON THE NATURE OF INTERACTION BETWEEN MELITTIN OF BEE VENOM AND MODEL PHOSPHOLIPID MEMBRANES

A Thesis

Presented for the

Master of Science

Degree

The University of Tennessee, Knoxville

Michael L. Thompson

December 1980

ACKNOWLEDGMENTS

My sincere thanks is extended to my major professor, Dr. Solon Georghiou, for his careful advice and extreme patience. He not only provided me with encouragement, but also instilled a professionalism, which made this research project possible. I would also like to thank the Institute of Radiation Biology for providing a teaching assistantship, which aided greatly in attaining my degree. Special thanks is extended to Dr. Ajay Mukhopadhyay for preparing the excellent membrane samples. I am also indebted to Dr. Jorge Churchich and Dr. Leaf Huang for making their laboratory facilities available. I also wish to acknowledge Mrs. Virginia Patterson, Mr. Don Broach, and Mr. Keith Brown for their diligent effort in assisting me with the computer analysis.

My deepest appreciation goes out to my parents, Walter and Doris Thompson, for their endless encouragement and financial support throughout my academic studies. My warmest thanks is extended to Miss Christine Royston for typing this thesis and for giving me that added incentive necessary to complete this project.

ABSTRACT

The single tryptophan residue of melittin, the major component of bee venom, has been utilized as an intrinsic fluorescence probe for investigating the nature of binding of melittin to model phospholipid membranes. A recent CD study showed that 0.15 M inorganic phosphate increases the α-helical content of melittin. The maximum of the fluorescence spectrum in 0.01 M Tris buffer (pH 7.0) is at 352 nm, virtually identical to that of free tryptophan in that buffer. Thus, the tryptophan residue is almost completely exposed to water. The spectrum blue-shifts to 336 nm upon addition of 0.5 M inorganic phosphate implying that the environment of the tryptophan residue becomes more hydrophobic. One molar NaCl causes similar results. The spectra for melittin are very similar with those in salt solutions. That is also the case for the absorption spectra that shift to the red by about 2 nm relative to that of free melittin. Free melittin has been found to exhibit very small time-resolved spectral shifts on the ns time scale and dependence of the fluorescence decay time on the emission wavelength resembling those exhibited by free tryptophan. For salt solutions and membranes, however, the effects are much more pronounced. The rotational correlation time, obtained from ns fluorescence depolarization measurements, increases from 1.1 ns for free melittin to 3.5 ns for 0.5 M K_2HPO_4, implying a different conformation in the salt solution. These findings can be rationalized in terms of aggregation of the protein in salt solutions and when bound to membranes in line with

the suggested in the literature tetrameric form of the protein at high ionic strength. Acrylamide quenching measurements indicate that the tryptophan residue is much less exposed to the solvent when in salt solutions and when bound to membranes than in Tris buffer. In all cases, fluorescence quenching occurs by both diffusion-controlled and instantaneous processes. It is inferred that the tryptophan residue does not penetrate into the hydrophobic core of the membranes, which contradicts published reports.

TABLE OF CONTENTS

LIST OF TABLES

LIST OF FIGURES

FIGURE PAGE

FIGURE PAGE

CHAPTER I

INTRODUCTION

Of the three amino acids which fluoresce (which are tyrosine, tryptophan, and phenylalanine), tryptophan is the principal fluorescing amino acid (Teale, 1960). Tryptophan contains an aromatic R group which is nonpolar or hydrophobic. Due to its aromaticity, tryptophan contains two types of bonds, σ-bonds and π-bonds. For every two atomic orbitals that combine, two molecular orbitals are produced—a bonding orbital and an antibonding orbital. The antibonding orbital is virtually devoid of electrons. Thus, if two s orbitals combine to form a σ-bonding orbital, a σ*-antibonding orbital is also produced. Similarly, if two p orbitals combine, a π-bonding orbital and a higher energy π*-antibonding orbital are produced. Since both σ-bonds and π-bonds exist in tryptophan, there also exists σ*-antibonding and π*-antibonding orbitals. Normally, the lower-energy bonding molecular orbitals are dealt with since these are the ones occupied by bonding electrons. Absorption of energy in the ultraviolet region results in the transition of an electron from the low-energy bonding orbital to the unoccupied high-energy antibonding orbital.

When ultraviolet light is shone on a molecule, energy absorption results and raises the molecule from the So singlet ground electronic state to one of the excited singlet states, i.e. S_1, S_2, S_3, etc. Usually, the molecule will go to the zero vibrational level of the first excited state, S_1, via a very fast radiationless transition.

The molecule can then emit light, undergo internal conversion, or undergo intersystem crossing. By emitting light, the molecule returns to the ground state. Internal conversion will also return the molecule to the ground state, but through a radiationless process. The molecule can also proceed to the triplet state by intersystem crossing. The emission of light resulting by a transition from a singlet state to the ground state is known as fluorescence, while emission accompanying a transition from a triplet state to the ground state is known as phosphorescence.

All of the above processes are unimolecular in nature. Bimolecular processes do occur and they should be considered. Birks (1970) categorizes the bimolecular processes into five distinct groups: (1) perturbation processes, (2) exciton migration and transfer processes, (3) complex formation in the ground state, (4) complex formation between an excited and an unexcited molecule, and (5) interaction between two excited molecules. The heavy atom effect is an example of a perturbation process. When a heavy atom is in the vicinity of an aromatic molecule, spin orbit coupling results which increases the rate of intersystem crossing and hence the rate of phosphorescence emission. Energy transfer processes have been extensively studied. These processes are not dealt with in this study because the protein melittin contains only one tryptophan residue and no tyrosine residues. The third group of bimolecular processes, complex formations in the ground state, has also been extensively studied. The complexes formed are called dark complexes because they develop in the ground state before light falls on the system.

Typical of the fourth group is exciplex and excimer formation. An exciplex is a complex which arises only in the excited state (it is fully dissociated in the ground state) between a solute and a solvent molecule, whereas an excimer is a complex formed in the excited state between identical molecular species. Interaction between two excited molecules can also take place. An example of this is when two identical molecules in the triplet state form one excited molecule in the ground state and an excited singlet state.

The optical properties of tryptophan are strongly dependent on the nature of the solvent. The fluorescence spectrum shifts to the red as the polarity of the solvent increases. The spectral maximum in water is at 352 nm. Walker et al. (1967) attributed this strong dependence of the optical properties of tryptophan on the solvent to exciplex formation. This solvent sensitivity is a desirable property for it allows the tryptophan residue to be used as an environmental probe.

There are two important parameters to consider in dealing with the fluorescence spectrum of a molecule: (1) the quantum yield and (2) the decay time. The fluorescence quantum yield is the ratio of photons emitted as fluorescence to the number of photons absorbed in the first excited state. It can be shown that fluorescence quantum yield q is given by

$$q = \frac{K_f}{K_f + K_i + K_{IC} + K_c \cdot [M]}$$

where K_f is the rate constant of fluorescence, K_i is the rate constant of internal conversion, K_{IC} is the rate constant of intersystem crossing,

and $K_c[M]$ is the rate constant of concentration quenching for a solute concentration [M]. Typical values for the rate constants K_f, K_i, and K_{IC} vary between 10^7 and 10^8 sec^{-1}. For $S_o \rightarrow S_1$ absorption, the molar extinction coefficient has values between 10^3 and 10^4 M^{-1} cm^{-1}. The extinction coefficient for $S_o \rightarrow T_1$ absorption, however, is approximately 10^{-8} times that for $S_o \rightarrow S_1$ absorption. Self-absorption must also be considered because this will distort the fluorescence spectrum. Self-absorption takes place when emitted photons are reabsorbed and subsequently re-emitted. This can be minimized by using dilute (10^{-5}M) and/or thin samples.

The fluorescence decay time τ is another important parameter to consider. It can be shown that

$$\tau = \frac{1}{K_f + K_i + K_{IC} + K_c\,[M]}.$$

In measuring the decay time of a sample, excitation is accomplished with a light pulse. The decay of the fluorescence intensity is observed and τ is obtained from the time difference between points corresponding to I(o) and I(o)/e where I(o) is the fluorescence intensity at time equal to zero. For relatively broad exciting light pulses, the fluorescence decay data needs to be deconvoluted to correct for the distortion of the data introduced by the exciting light. A typical fluorescence decay time is on order of 10 ns, whereas a typical phosphorescence decay time is much longer, usually between 10^{-3} sec and a few seconds.

The above considerations are necessary in order to understand the fluorescence properties of a protein such as melittin. Melittin is a

relatively small protein, which is the major component of bee venom. The protein is composed of twenty-six amino acid residues—residues 1 to 20 being hydrophobic and the rest being hydrophilic (See Fig. I-1). Melittin attacks and lyses cell membranes by destroying the phospholipid structure (Sessa et al., 1969).

Melittin contains only one tryptophan residue, which is located in the nineteenth position of the amino acid sequence. Tryptophan has been used extensively in the literature as an intrinsic fluorescence probe because of its sensitivity to environmental changes. In the case of melittin, tryptophan has been used as a "reporter" on the nature of binding to phospholipids (Mollay and Kreil, 1973, Mollay et al., 1976, Dufourcq, 1977).

Mollay and coworkers (1976) bound melittin to various lecithins and observed a shift in the fluorescence spectrum from 352 nm to 330 nm. They attributed the blue-shift to tryptophan moving from a water environment to a very hydrophobic environment. Dufourcq (1977) observed the same results but also determined that binding was dependent on the net electrical charge of the vesicle. A more recent study indicated that α - helicity of melittin greatly increases upon binding to egg lecithin (Dawson et al., 1978). A similar effect was also observed in 0.15 M inorganic phosphate (Drake and Hider, 1979).

There are two different classes of membrane proteins. Extrinsic proteins are bound to the outside of the membrane whereas intrinsic proteins are located in the hydrophobic core. Several studies have been done dealing with extrinsic proteins which undergo electrostatic

1	2	3	4	5	6	7	8	9	10	11	12	13	14
GLY	ILU	GLY	ALA	VAL	LEU	LYS	VAL	LEU	THR	THR	GLY	LEU	PRO

15	16	17	18	19	20	21	22	23	24	25	26
ALA	LEU	ILU	SER	TRP	ILU	LYS	ARG	LYS	ARG	GLN	GLN

Fig. I.1. Amino acid composition of melittin (from the Honey Bee: Apis Mellifera) (Dayhoff, 1968).

interactions with the polar head groups of phospholipids and to a lesser extent, intrinsic proteins which interact with the aliphatic chains (Dufourcq, 1977). The question as to whether melittin acts as an extrinsic or intrinsic protein is dealt with in this study.

Fluorescence quenching studies done with nonionic acrylamide provide information on the nature of the binding of protein to membranes. The degree of exposure of tryptophan in various proteins has been determined (Eftink and Ghiron, 1976a; Eftink and Ghiron, 1977). By applying this method to melittin bound to phospholipids, it is possible to obtain information on the degree of exposure of the segment of protein adjacent to the tryptophan residue to the solvent.

The purpose of this study is to investigate the interaction between melittin and model phospholipid membranes. This is accomplished by monitoring the fluorescence from the intrinsic probe, tryptophan. The results show that melittin undergoes a structural change upon binding and that the mode of binding appears to be electrostatic in nature.

CHAPTER II

MATERIALS AND METHODS

Melittin was obtained from the ICN Nutritional Biochemicals Company and the Sigma Chemical Company. Both samples were lypholized and chromatographically pure. The samples were compared using steady-state fluorescence and absorption measurements and found to be identical. Tryptophan was purchased from P-L Biochemicals and used without further purification. L-α-phosphatidylcholine from egg yolk (egg lecithin) and L-α-distearoyl phosphatidylcholine (DSL) were purchased from the Sigma Chemical Company. Propylene glycol was obtained from the J. T. Baker Chemical Company. All other chemicals, e.g. Tris, NaCl, K_2HPO_4, and nonionic acrylamide, were purchased from the Fisher Scientific Company and were of analytical grade.

Melittin was kept frozen (0°C) until ready for use. Fresh samples were made for each measurement by dissolving enough melittin in 0.01 M Tris buffer (pH = 7.0) to yield an absorbance of 0.1 at the excitation wavelength (298 nm) for the fluorescence nanosecond (ns) measurements. A Cary 14 recording spectrophotometer was used to determine the absorbance of all solutions. The 0.01 M Tris buffer was made as follows. First, a 0.1 M Tris solution was made by dissolving 0.6050 g of Tris in 50 ml of triply distilled water. Next, a 0.1 M HCl solution was made by diluting 0.83 ml of concentrated HCl acid to 100 ml with triply distilled water. Then, 26 ml of the Tris solution was added to 24 ml of HCl

solution and diluted to 500 ml to yield a 0.01 M Tris buffer solution of pH 7.0 (checked with a Fisher pH meter).

Some of the measurements required dissolving melittin in various K_2HPO_4 and NaCl solutions. In those cases, the solutions were prepared by adding the necessary amount of salt to 0.01 M Tris buffer and then readjusting the pH to 7.0.

In order to perform the fluorescence quenching experiments with acrylamide, melittin was dissolved in the proper salt solution and in liposomes to yield an absorbance of 0.05 at 305 nm (which is the excitation wavelength). The stock acrylamide solution was prepared in the presence of the liposomes for titrations involving artificial membranes.

All of the model phospholipids were prepared according to published procedures (Cogan et al., 1973; Kawato et al., 1977). A 10 ml volume of 2 mg/ml lipid solution was prepared in 0.01 M Tris buffer (pH 7.0). The suspension was rigorously stirred for 20 minutes and then sonicated for 20 minutes using a Heat System—Ultrasonics 20 kHz model W-375 sonifier equipped with a 0.5 in. tip at 50% full power. Finally, it was centrifuged at 65,000 g for 30 minutes. All procedures were carried out under nitrogen. In the case of distearoyllecithin, sonication was done at 61°C (above the transition temperature of 51°C) and at room temperature. Steady-state and nanosecond fluorometric techniques did not detect any fluorescence from liposomes which contained no melittin. Melittin was incubated in the phospholipid solution at room temperature for the case of egg lecithin and at 61°C and room temperature for

distearoyllecithin. The lipid-to-melittin ratio was about 400:1 which ensured that all the melittin was bound to the liposomes.

Fluorescence Measurements

All steady-state fluorescence measurements were made utilizing a right angle fluorometer (Georghiou, 1975). This fluorometer employs a 1000 watt xenon-mercury lamp as a source of exciting light. The light is passed through a mechanical chopper to a Bausch and Lomb 0.5 m monochromator before being focused on the sample. Fluorescence, viewed at right angles to the exciting beam, was passed through another Bausch and Lomb monochromator before entering the 9558 QB EMI photomultiplier. The output signal was fed into a Princeton Applied Research lock-in amplifier which was triggered by the chopper. The amplifier drove the Y-axis of a Honeywell X-Y recorder while the X-axis was driven by an automatic scanner on the emission monochromator. The emission bandwidth was 3.4 nm for spectral studies and 6.6 nm for quenching studies.

The acrylamide quenching experiments were done by measuring the fluorescence intensity of the tryptophan residue of melittin in the absence and presence of acrylamide. By using equation (1)

$$F_o/F = 1 + K_{sv}[Q] \qquad (1)$$

where F_o is the fluorescence intensity in absence of acrylamide, F is the fluorescence intensity in the presence of acrylamide, K_{sv} is the quenching constant, and [Q] is the concentration of the quencher, one can construct a Stern-Volmer plot to determine the K_{sv}. A curved line results, however, and the following modified equation (2)

$$(F_o/F)e^{-V[Q]} = 1 + K_{sv}[Q], \qquad (2)$$

where V is the instantaneous quenching constant, must be used to determine K_{sv} (Weller, 1961). A simple FORTRAN computer program accomplished this by varying the V value to obtain the best straight line as fitted to equation (2). The K_{sv} value was obtained as the slope of the plot.

The nanosecond fluorometer employed in this research project has been previously described (Badea and Georghiou, 1976). An Optitron high pressure lamp provided the exciting light. Ultra-pure N_2 gas was introduced into the lamp at about 200 psi. A 10 kHz pulse rate was achieved by applying 17.5 KV across the variable electrode gap. The exciting beam was passed through a specially constructed Pomfret Research Optics ultraviolet interference filter before being focused on the sample. The fluorescence was viewed at right angles to the exciting beam through a Corning 7-37 emission filter. A 56TUVP Amperex photomultiplier with S-20 response was used for detecting the fluorescence. The photomultiplier has a gain in excess of 10^8. The signal was processed by a Princeton Applied Research Model 162 boxcar averager. This model incorporates model 163 sampling heads and uses a digital storage plug-in unit for infinite data holding time. Essentially a single-channel analyzer, the boxcar averager achieves a high signal-to-noise ratio by averaging 10^3 samples and by additional smoothing at its output. The data acquisition time was typically 25 minutes. The Y-axis of a Hewlett-Packard X-Y recorder was driven by the boxcar averager while

the X-axis was driven by the sampling speed control. The boxcar averager was interfaced via a microprocessor to a teletype. The microprocessor allowed the sampling of up to 1000 data points, each point taken at 1 to 99 second intervals. Typically, 300 data points were taken with a 4 second interval between them.

The Pomfret excitation filter has its transmission maximum at 298 nm with a 6.5 nm FWHM. The Corning 7-37 emission filter has a transmission maximum at 360 nm. The transmission curves of the two filters are shown in Fig. II.1. For polarization studies, a 3-M type 105UVWRMR ultraviolet polarizer was placed in the excitation beam while a Polaroid HNP'B polarizer was placed in the emission light path. Time-resolved studies and wavelength-dependence measurements were performed on the nanosecond fluorometer utilizing a 0.25 Bausch and Lomb high intensity scanning monochromator (of 9.6 nm bandwidth) placed before the photomultiplier.

Computing Facilities and Data Analysis

The University of Tennessee Computing center provided the facilities for the analysis of the data. Each of the IBM 370/3031 computers has four million bytes of memory and runs under SVS (release 1.7 of OS/VS2) with HASP II Version 4. The DECsystem-10, Model 1090, is run under TOPS-10 with Galaxy-10 and is interfaced with the IBM 370/3031 computer. Also interfaced with the IBM 370/3031 is a California Computers (CALCOMP) plotter, Model 1051. This plotter was used to draw all of the nanosecond wavelength-dependence, nanosecond depolarization,

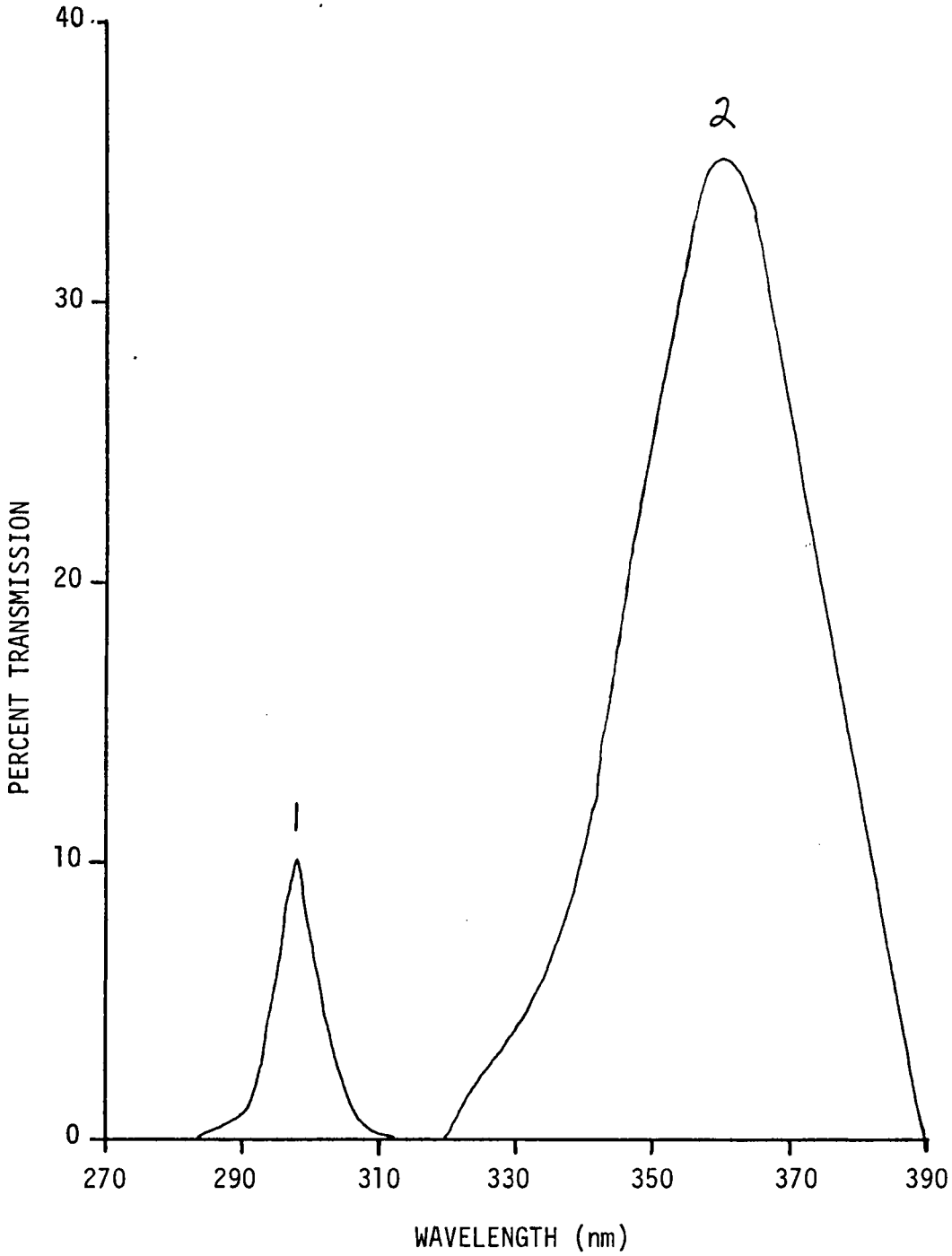

Fig. II.1. Transmission curves of (1) excitation filter and (2) emission filter for nanosecond fluorescence studies.

emission anisotropy, and acrylamide quenching plots. All of the nanosecond data were automatically punched on a paper tape by using a teletype interfaced with the nanosecond fluorometer. The data were entered on the DECsystem-10 computer by a telephone decoder where they were stored until the proper analysis could be performed.

For analyzing the fluorescence decay time data, the S.A.S. 79.3B computer language was employed. Specifically, the NLIN (nonlinear least-squares regression analysis) procedure allowed the convolution of the data (Lianos, 1978). This program took the profile of the lamp and convoluted a fluorescence decay profile by assuming the following equation for the true fluorescence decay profile:

$$F(t) = \sum_i Ai e^{-t/\tau i} \qquad (3)$$

where F(t) is the total fluorescence intensity, A_i is the fluorescence intensity of the i th component, and τ_i is the fluorescence decay time of the i th component. Then the regression analysis was performed by comparing the synthesized curve with the experimental decay curve. Plots of the residuals, percent residuals, and autocorrelation versus channel number were used to determine the goodness of fit. The autocorrelation plot, however, is the ultimate criterion due to its extreme sensitivity (Grinvald and Steinberg, 1974; Grinvald, 1976).

The depolarization data analysis was performed utilizing a special nonlinear regression analysis program written in FORTRAN and S.A.S. 79. In order to determine the emission anisotropy, r(t), one needs to consider the following equation for the excitation polarizer at the vertical position;

$$r(t) = \frac{I_V(t) - I_H(t)}{I_V(t) + 2(I_H(t))} . \qquad (4)$$

In (4), $I_V(t)$ is the fluorescence intensity at time t with the emission polarizer in the vertical position and $I_H(t)$ is the fluorescence in intensity at time t with the polarizer in the horizontal position. The emission anisotropy, r(t), may be assumed to have the form

$$r(t) = \sum_i r(o)_i e^{-t/\phi_i} \qquad (5)$$

where ϕ_i are the rotational correlation times and $r(o)_i$ are the zero-point anisotropy values. It should be noted that $I_V(t) + 2\ (I_H(t))$ represents the total decay and is, therefore, proportional to $\sum_i Ai e^{-t/\tau_i}$. The A_i and τ_i were determined by employing the NLIN program. It follows from (4) and (5) that

$$I_V(t) - I_H(t) = \sum_i r(o) e^{-t/\phi_i} \sum_i Ai e^{-t/\tau_i} . \qquad (6)$$

The computer program fitted the $I_V(t) - I_H(t)$ data with the known A_i and τ_i values and the determined values of ϕ_i and $r(o)_i$. Plots of the residuals, percent residuals, and autocorrelation were used to determine the goodness of fit in the same manner as in the NLIN procedure. Finally, a separate computer program used equation (5) to construct a plot of the actual anisotropy by using the values of ϕ_i and $r(o)_i$ obtained by the above convolution procedure.

CHAPTER III

RESULTS

Melittin is a small protein which contains only one tryptophan amino acid residue. By using the tryptophan residue as an intrinsic fluorescent probe, one can gain some understanding of the structural changes that melittin undergoes as its environment changes. A circular dichroism study showed that melittin undergoes a conformation change from a random coil to an α-helix in the presence of inorganic phosphate (Drake and Hider, 1979). Consequently, this research project was undertaken to study these structural changes in relation to the binding of melittin to phospholipid membranes. Nanosecond wavelength-dependence, nanosecond depolarization, time-resolved, and steady-state spectrofluorometric techniques were used in this project.

First, it was necessary to understand the optical properties of free tryptophan in its natural state, i.e. in the presence of an "inert" buffer. This was necessary before tryptophan could be effectively used as a fluorescent probe. Tryptophan was found in the present work to decay monoexponentially with fluorescence decay times (τ_o) of 2.5, 2.6, and 2.8 ns at emission wavelengths of 325, 350, and 380 nm, respectively. The data for the various emission wavelengths are shown in Figs. III.1 through III.3.

Time-resolved emission spectral studies performed on tryptophan show a minor shift to the red of about 2 nm. The red shift took place

Fig. III.1. Fluorescence decay profile of tryptophan in Tris buffer (emission wavelength = 325 nm). Curve (1) represents the lamp profile. Curve (2) represents the experimental fluorescence decay profile while curve (3) is the convoluted decay profile. Insert (A): Plot of the Residuals versus Channel Number. Insert (B): Plot of the Autocorrelation versus Channel Number. Channel width = 0.180 ns.

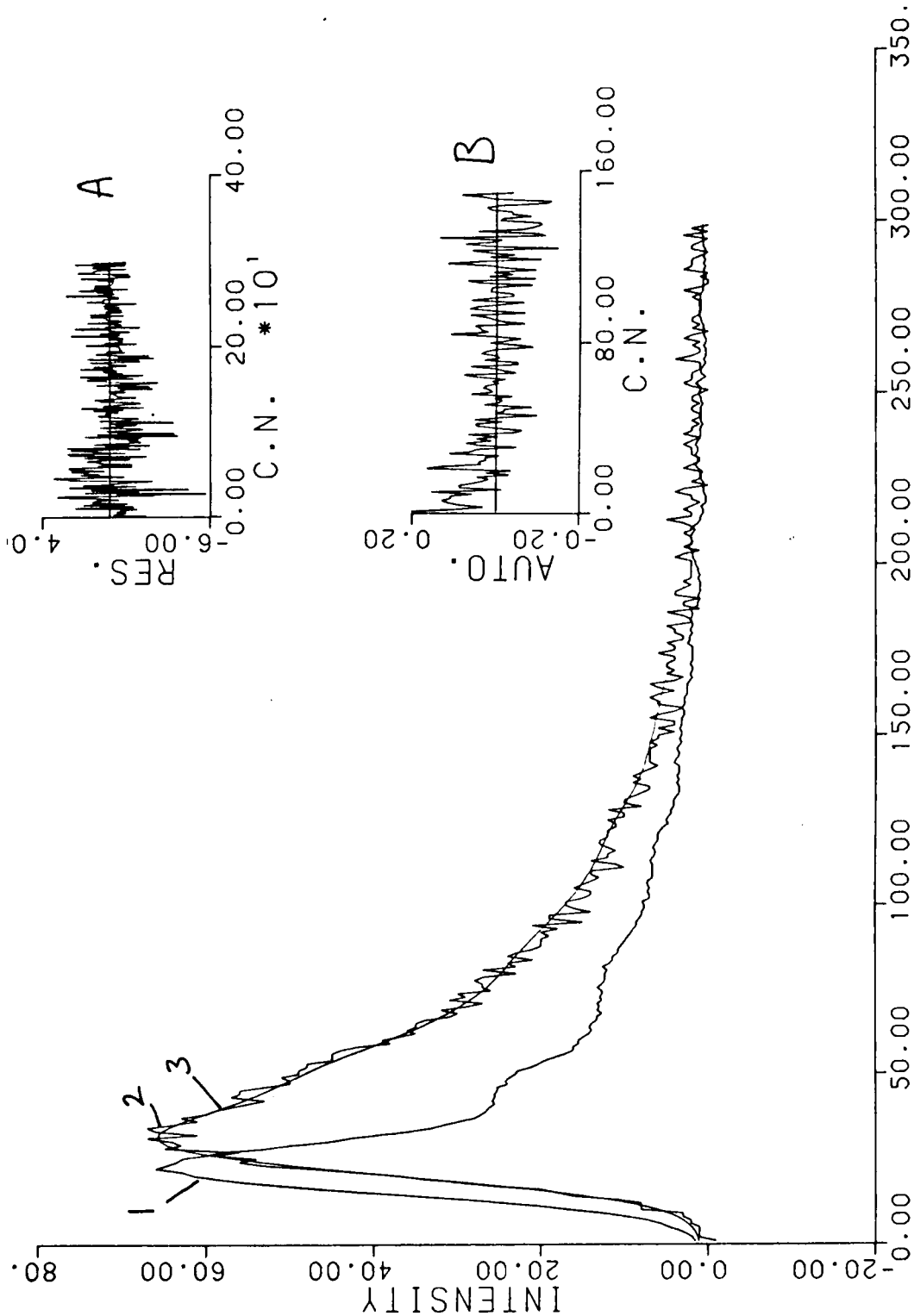
A
RES.
-6.00
4.0
0.00
20.00
40.00
C.N. *10'
B
AUTO.
-0.20
0.20
0.00
80.00
160.00
C.N.
INTENSITY
-20.00
0.00
20.00
40.00
60.00
80.
0.00
50.00
100.00
150.00
200.00
250.00
300.00
350.
CHANNEL NUMBER
1
2
3

Fig. III.1.

Fig. III.2. Fluorescence decay profile of tryptophan in Tris buffer (emission wavelength = 350 nm). Curve (1) represents the lamp profile. Curve (2) represents the experimental fluorescence decay profile while curve (3) is the convoluted decay profile. Insert (A): Plot of the Residuals versus Channel Number. Insert (B): Plot of the Autocorrelation versus Channel Number. Channel width = 0.180 ns.

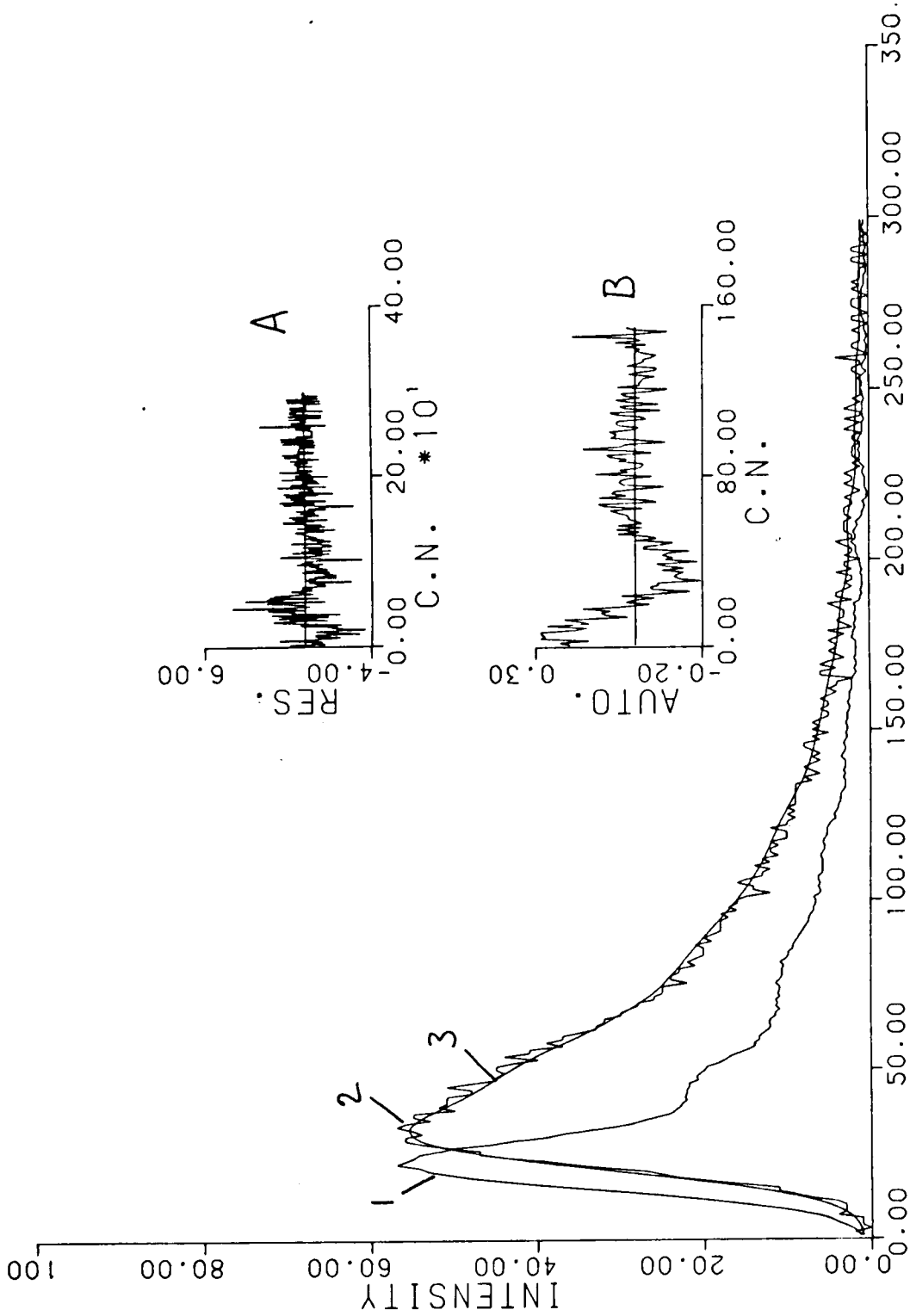
INTENSITY
0.00
20.00
40.00
60.00
80.00
100
0.00
50.00
100.00
150.00
200.00
250.00
300.00
350.
CHANNEL NUMBER
1
2
3
A
RES.
6.00
-4.00
0.00
20.00
40.00
C.N.
*10¹
B
AUTO.
0.30
-0.20
-0.00
80.00
160.00
C.N.

Fig. III.2.

Fig. III.3. Fluorescence decay profile of tryptophan in Tris buffer (emission wavelength = 380 nm). Curve (1) represents the lamp profile. Curve (2) represents the experimental fluorescence decay profile while curve (3) is the convoluted decay profile. Insert (A): Plot of the Residuals versus Channel Number. Insert (B): Plot of the Autocorrelation versus Channel Number. Channel width = 0.180 ns.

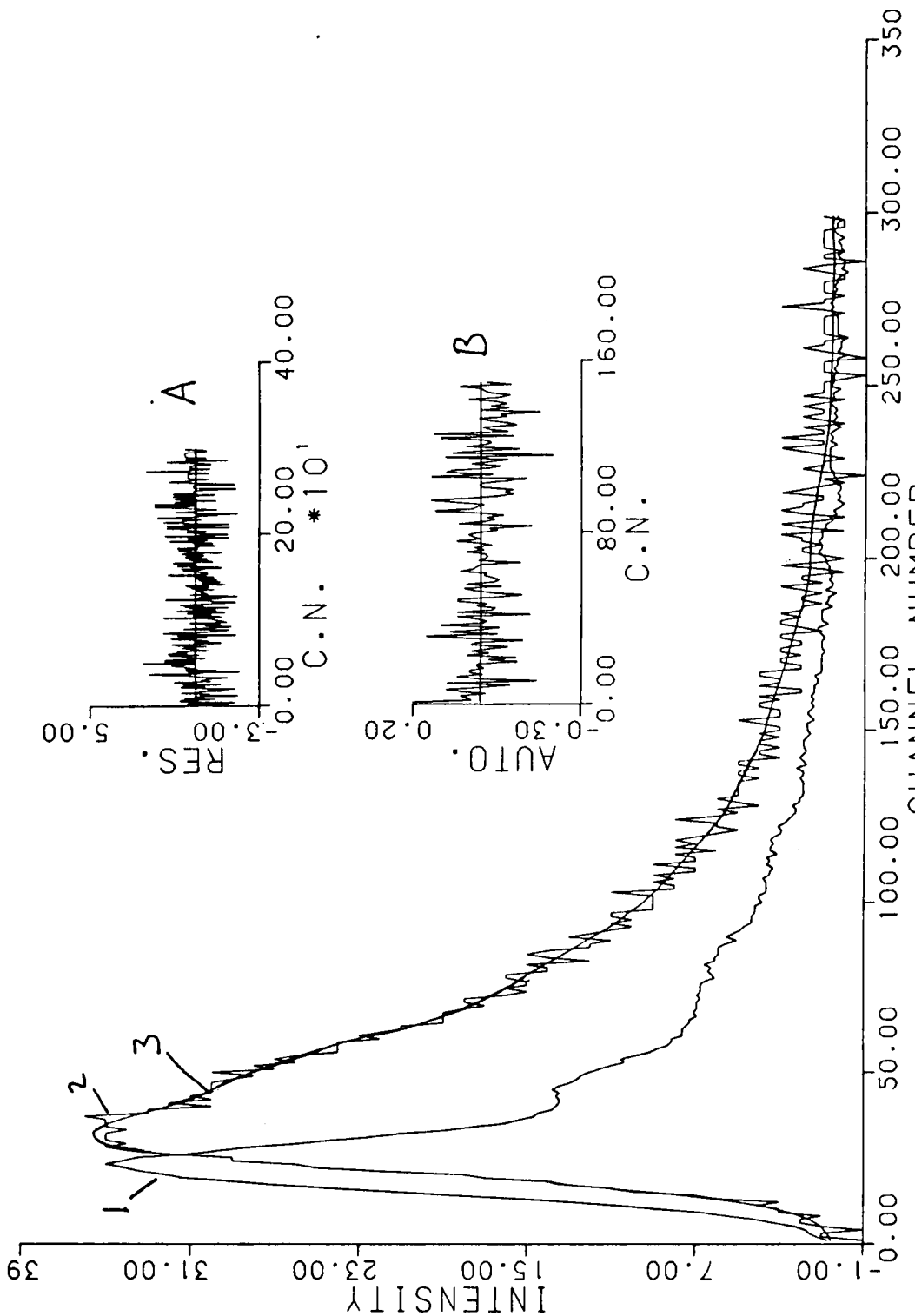

Fig. III.3.

between 0 and 12 ns relative to the peak of the exciting light pulse. The time-resolved spectra are shown in Fig. III.4.

Acrylamide quenching studies yielded a very high K_{sv} for tryptophan ($16.2M^{-1}$), in agreement with the results of Eftink and Ghiron (1976a). The Stern-Volmer plot used to determine the K_{sv} for tryptophan is shown in Fig. III.5.

Next, studies were done to resolve the optical properties of melittin. Melittin was introduced into different environments which included Tris buffer, various concentrations of inorganic phosphate and NaCl, and two different model phospholipid membranes. The analysis of the wavelength-dependent ns fluorescence decay profiles can be found in Figs. III.6 through III.35 with a summary of the fluorescence decay time values in Table III.1.

Time-resolved fluorescence measurements were made by fixing the time-window ($\sim$ 75 ps) of the boxcar averager relative to the peak of the lamp profile and then scanning the emission spectrum of the sample with a Bausch and Lomb monochromator. The various spectra can be seen in Figs. III.36 through III.43. Melittin in 0.01 M Tris buffer exhibited a spectral maximum of 350 nm with a very small time-dependent emission shift as in the case of free tryptophan. When melittin was introduced into 0.15 M inorganic phosphate, however, the peak of the spectrum blue-shifted to approximately 335 nm with a red shift in the time-resolved spectra of approximately 4 nm between -2.4 and 10 ns. Similar results were obtained with 0.5 M inorganic phosphate with a further shift to the blue of the emission maximum. After binding melittin to

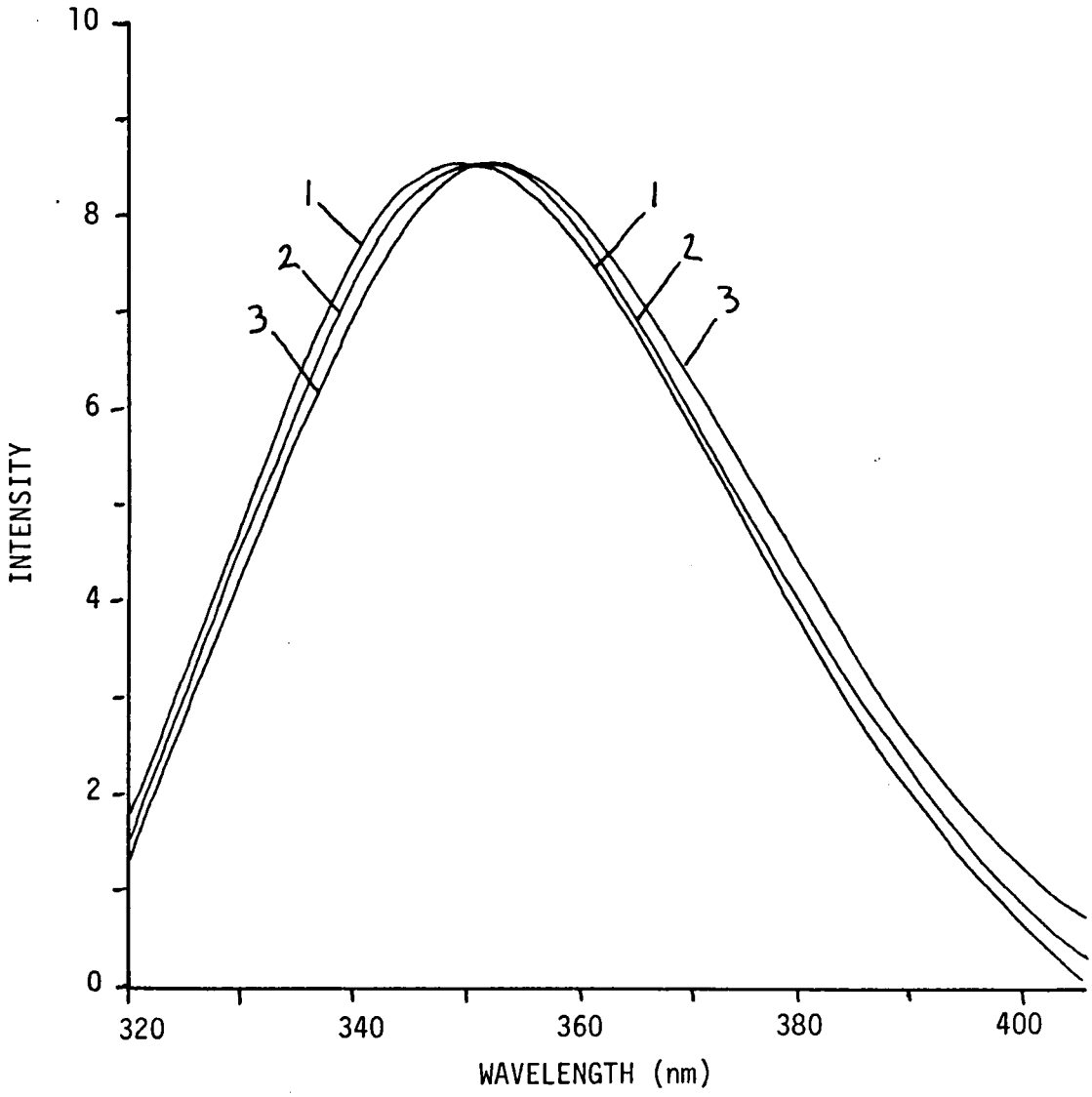

Fig. III.4. Time-resolved spectra of tryptophan in Tris buffer. Time values are relative to the peak of the lamp. (1) = -2 ns; (2) = 0 ns; (3) = 12 ns.

Fig. III.5. Stern-Volmer plot of acrylamide quenching analysis of tryptophan in Tris buffer. Dotted line represents the Stern-Volmer plot Fo/F vs. [Q]. Solid line represents the modified Stern-Volmer plot (Fo/F)e-V[Q] vs. [Q].

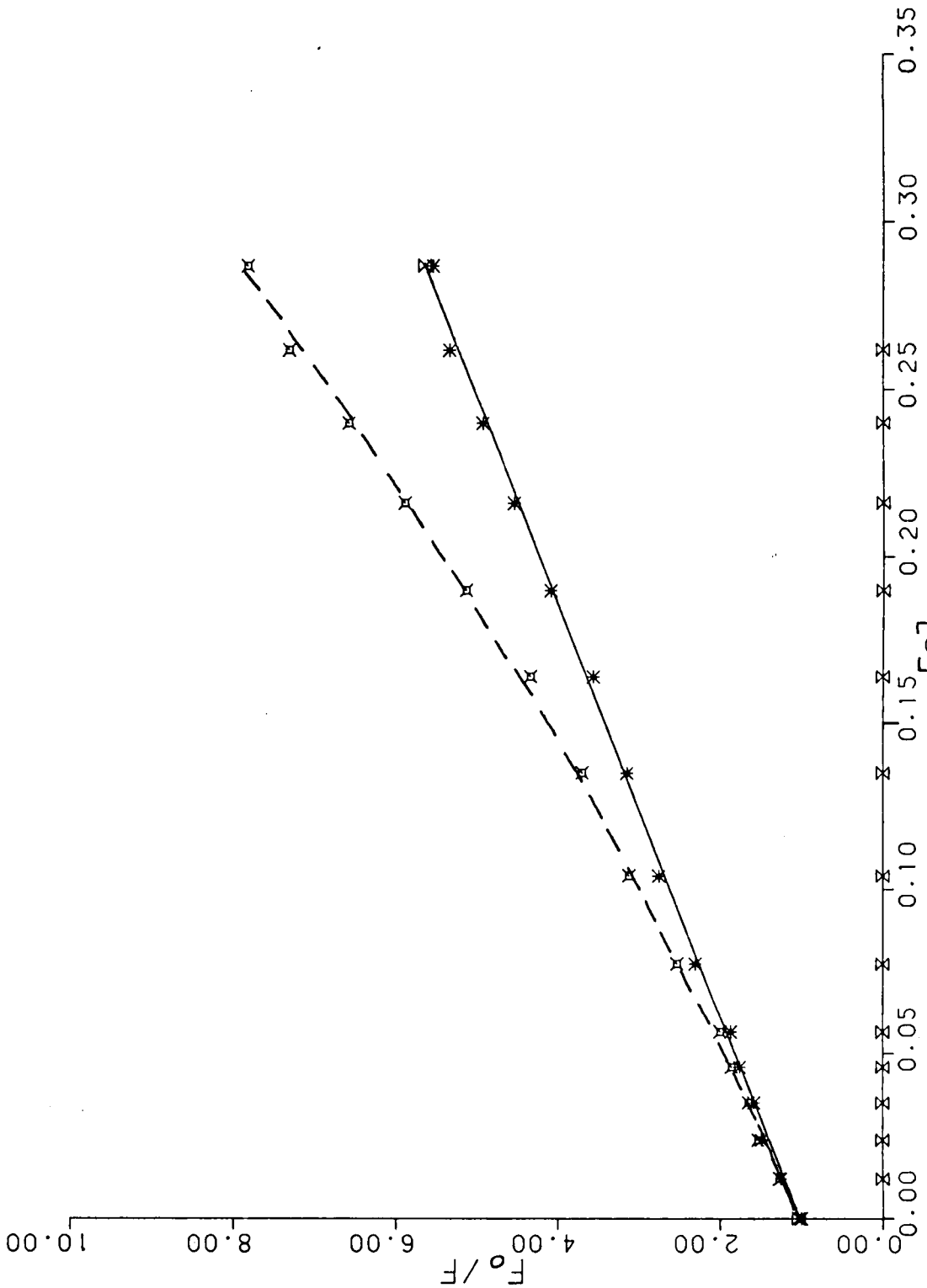

Fig. III.5.

Fig. III.6. Fluorescence decay profile of melittin in Tris buffer (emission wavelength = 330 nm). Curve (1) represents the lamp profile. Curve (2) represents the experimental fluorescence decay profile while curve (3) is the convoluted decay profile. Insert (A): Plot of the Residuals versus Channel Number. Insert (B): Plot of the Autocorrelation versus Channel Number. Channel width = 0.158 ns.

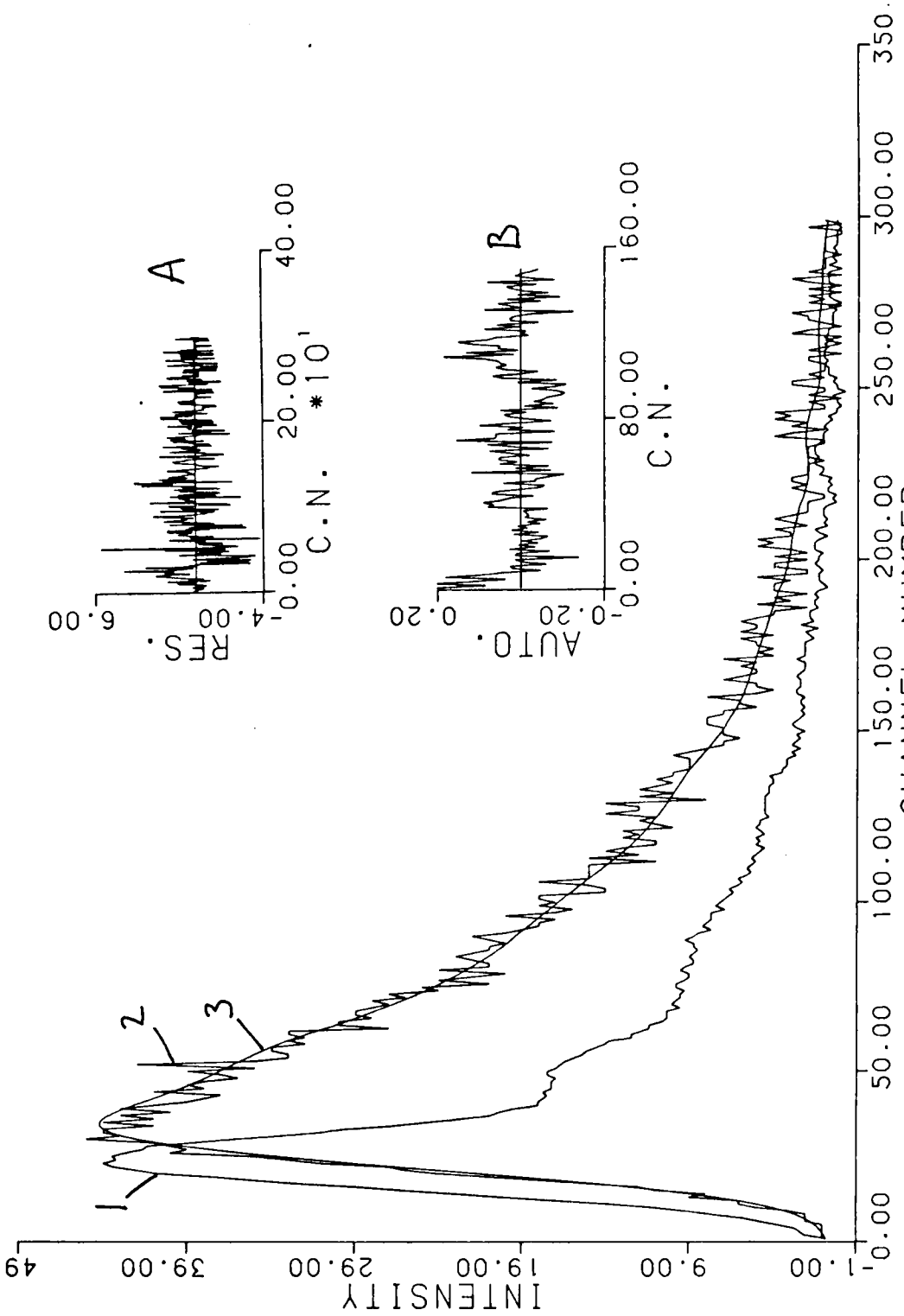
INTENSITY
1.00
9.00
19.00
29.00
39.00
49
CHANNEL NUMBER
0.00
50.00
100.00
150.00
200.00
250.00
300.00
350.
1
2
3
A
RES.
6.00
-4.00
0.00
20.00
40.00
C.N.
*10'
B
AUTO.
0.20
-0.20
0.00
80.00
160.00
C.N.

Fig. III.6.

Fig. III.7. Fluorescence decay profile of melittin in Tris buffer (emission wavelength = 360 nm). Curve (1) represents the lamp profile. Curve (2) represents the experimental fluorescence decay profile while curve (3) is the convoluted decay profile. Insert (A): Plot of the Residuals versus Channel Number. Insert (B): Plot of the Autocorrelation versus Channel Number. Channel width = 0.158 ns.

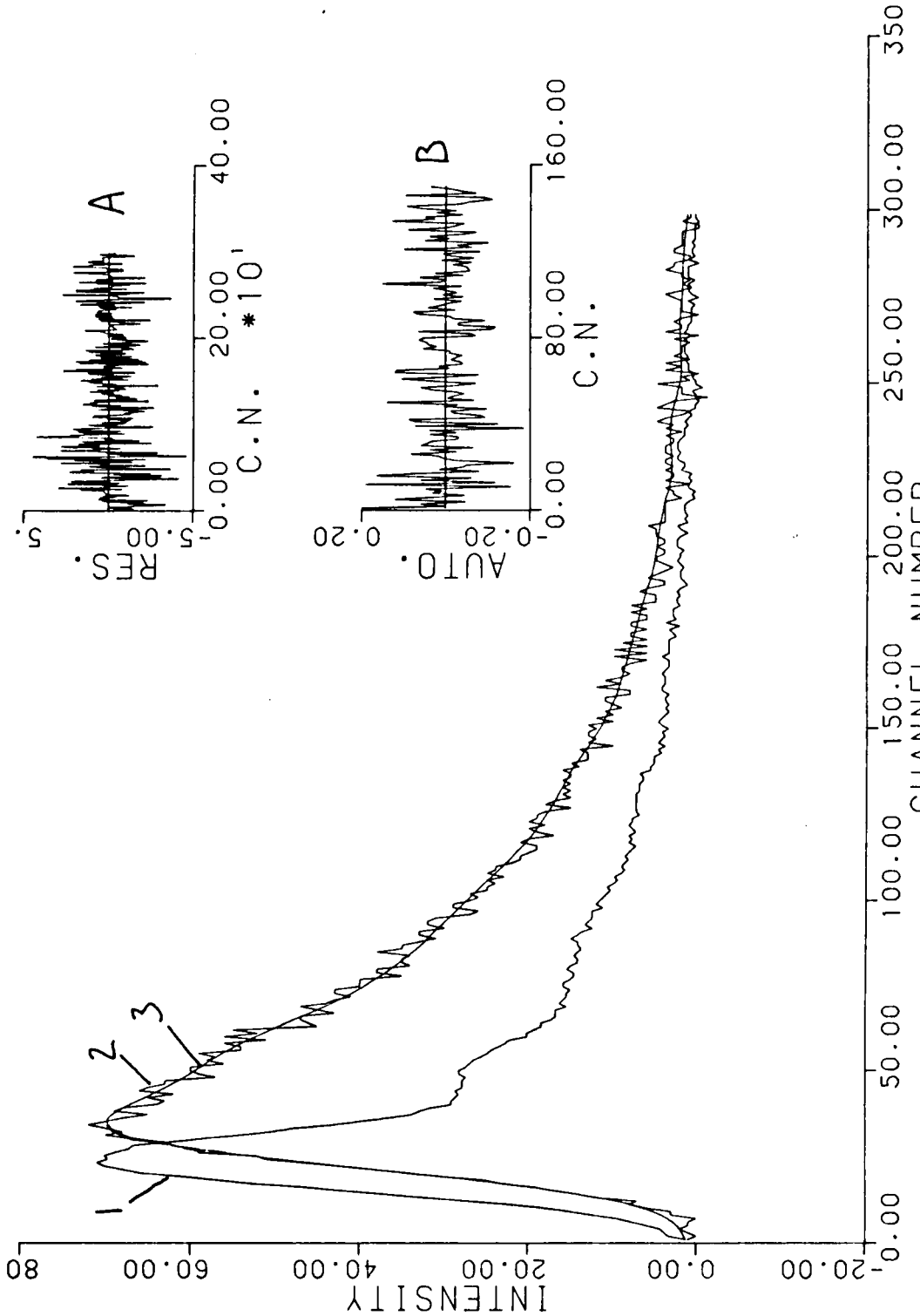
INTENSITY
80.00
60.00
40.00
20.00
0.00
-20.00
0.00
50.00
100.00
150.00
200.00
250.00
300.00
350
CHANNEL NUMBER
1
2
3
A
RES.
5.00
-5.00
0.00
20.00
40.00
C.N.
*10¹
B
AUTO.
0.20
-0.20
0.00
80.00
160.00
C.N.

Fig. III.7.

Fig. III.8. Fluorescence decay profile of melittin in Tris buffer (emission wavelength = 390 nm). Curve (1) represents the lamp profile. Curve (2) represents the experimental fluorescence decay profile while curve (3) is the convoluted decay profile. Insert (A): Plot of the Residuals versus Channel Number. Insert (B): Plot of the Autocorrelation versus Channel Number. Channel width = 0.158 ns.

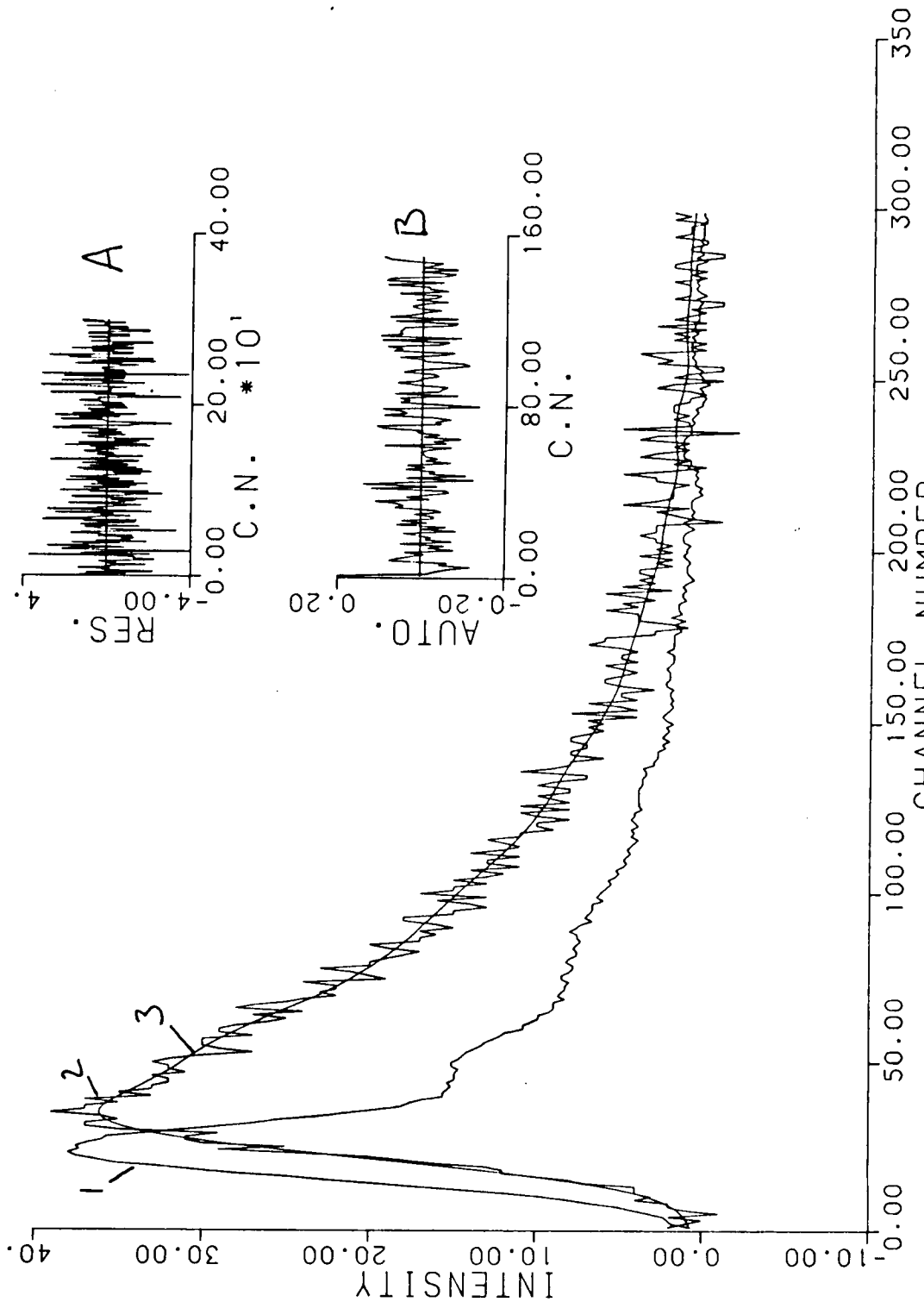
A
B
RES.
AUTO.
C.N. *10¹
C.N.
INTENSITY
CHANNEL NUMBER
1
2
3
-10.00
0.00
10.00
20.00
30.00
40.00
0.00
50.00
100.00
150.00
200.00
250.00
300.00
350
-4.00
4.00
0.00
20.00
40.00
-0.20
0.20
80.00
160.00

Fig. III.8.

Fig. III.9. Fluorescence decay profile of melittin + 0.15 M K_2HPO_4 (emission wavelength = 330 nm). Curve (1) represents the lamp profile. Curve (2) represents the experimental fluorescence decay profile while curve (3) is the convoluted decay profile. Insert (A): Plot of the Residuals versus Channel Number. Insert (B): Plot of the Autocorrelation versus Channel Number. Channel width = 0.154 ns.

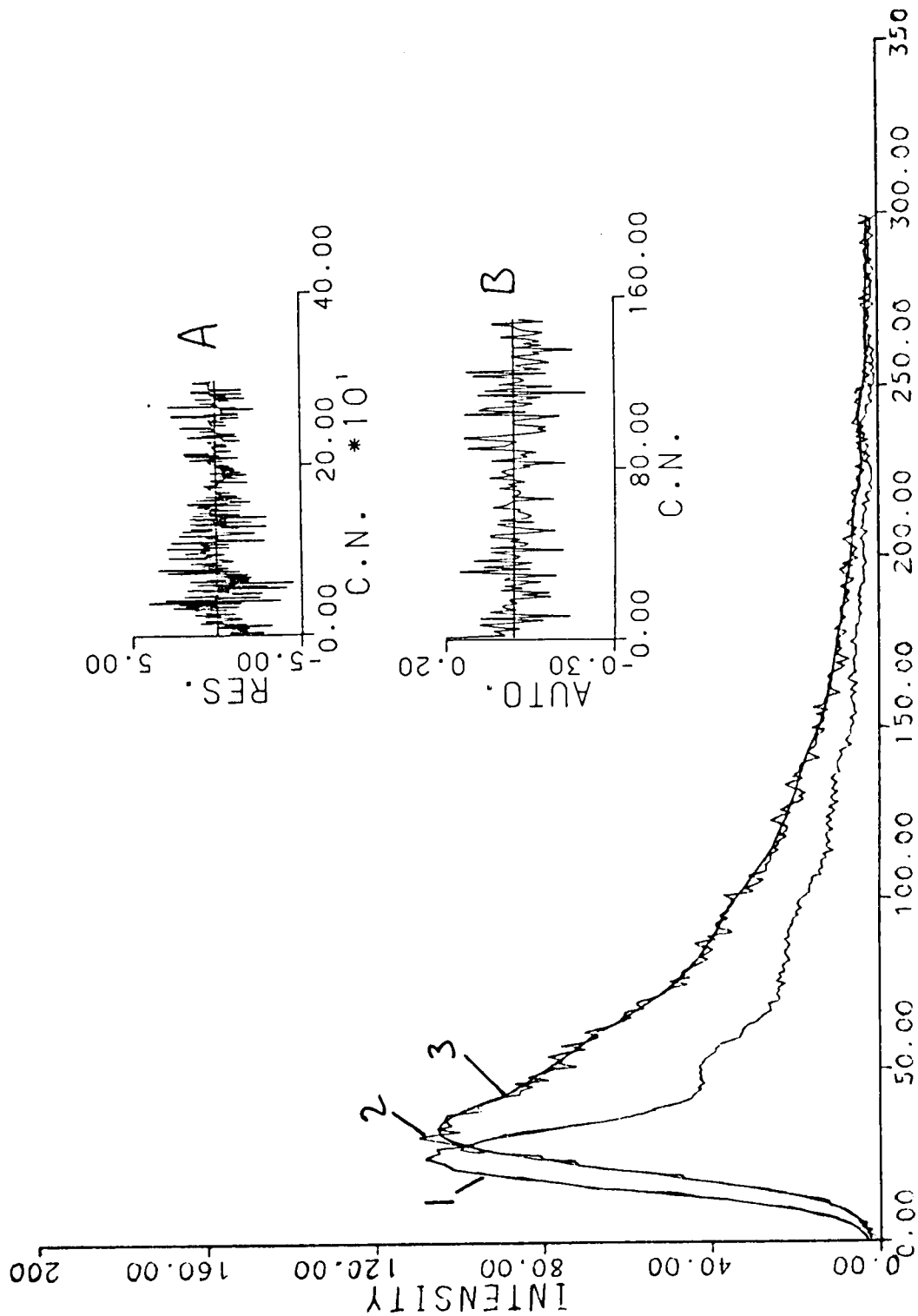
INTENSITY
0.00
40.00
80.00
120.00
160.00
200
0.00
50.00
100.00
150.00
200.00
250.00
300.00
350
CHANNEL NUMBER
1
2
3
A
RES.
5.00
-5.00
0.00
20.00
40.00
C.N. *10¹
B
AUTO.
0.20
-0.30
0.00
80.00
160.00
C.N.

Fig. III.9.

Fig. III.10. Fluorescence decay profile of melittin + 0.15 M K_2HPO_4 (emission wavelength = 340 nm). Curve (1) represents the lamp profile. Curve (2) represents the experimental fluorescence decay profile while curve (3) is the convoluted decay profile. Insert (A): Plot of the Residuals versus Channel Number. Insert (B): Plot of the Autocorrelation versus Channel Number. Channel width = 0.186 ns.

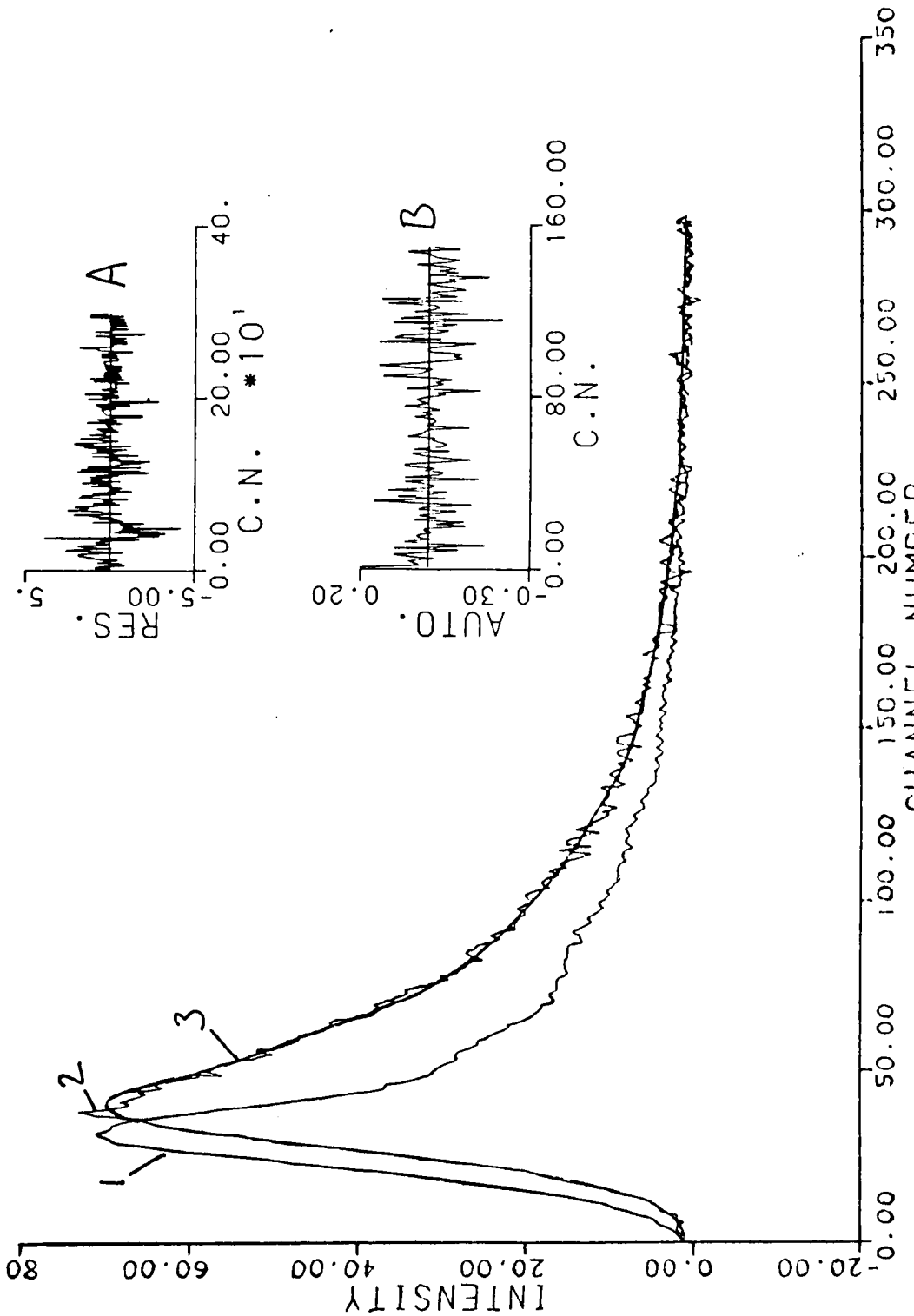
INTENSITY
80.00
60.00
40.00
20.00
0.00
-20.00
0.00
50.00
100.00
150.00
200.00
250.00
300.00
350
CHANNEL NUMBER
1
2
3
A
RES.
5.
-5.00
0.00
20.00
40.
C.N. *10'
B
AUTO.
0.20
0.30
-0.00
80.00
160.00
C.N.

Fig. III.10.

Fig. III.11. Fluorescence decay profile of melittin + 0.15 M K_2HPO_4 (emission wavelength = 360 nm). Curve (1) represents the lamp profile. Curve (2) represents the experimental fluorescence decay profile while curve (3) is the convoluted decay profile. Insert (A): Plot of the Residuals versus Channel Number. Insert (B): Plot of the Autocorrelation versus Channel Number. Channel width = 0.154 ns.

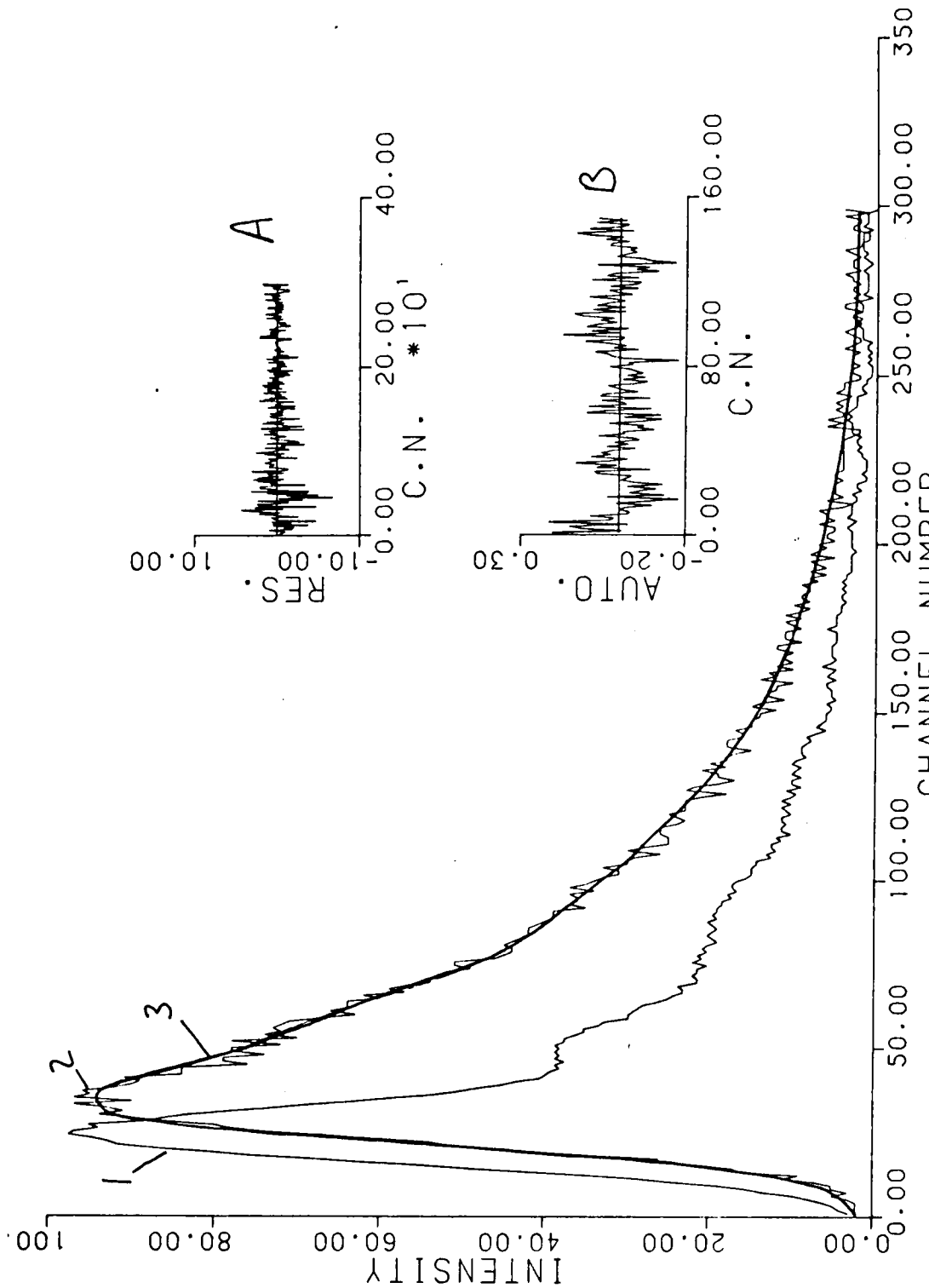
INTENSITY
0.00
20.00
40.00
60.00
80.00
100.
0.00
50.00
100.00
150.00
200.00
250.00
300.00
350
CHANNEL NUMBER
1
2
3
A
RES.
10.00
-10.00
0.00
20.00
40.00
C.N.
*10'
B
AUTO.
0.30
-0.20
0.00
80.00
160.00
C.N.

Fig. III.11.

Fig. III.12. Fluorescence decay profile of melittin + 0.15 M K_2HPO_4 (emission wavelength = 390 nm). Curve (1) represents the lamp profile. Curve (2) represents the experimental fluorescence decay profile while curve (3) is the convoluted decay profile. Insert (A): Plot of the Residuals versus Channel Number. Insert (B): Plot of the Autocorrelation versus Channel Number. Channel width = 0.154 ns.

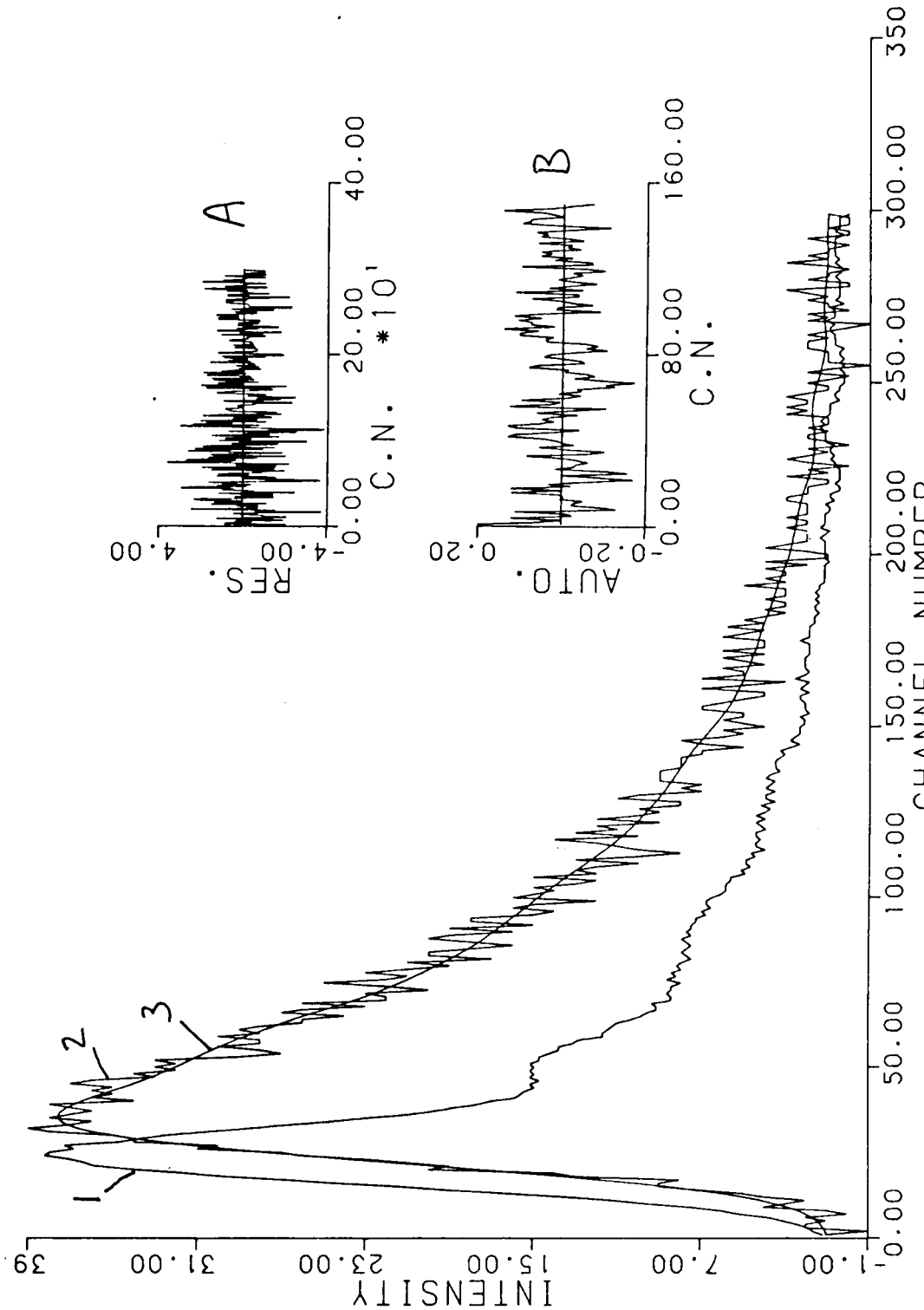
INTENSITY
1.00
7.00
15.00
23.00
31.00
39
0.00
50.00
100.00
150.00
200.00
250.00
300.00
350
CHANNEL NUMBER
1
2
3
A
RES.
4.00
-4.00
0.00
20.00
40.00
C.N.
*10'
B
AUTO.
0.20
-0.20
0.00
80.00
160.00
C.N.

Fig. III.12.

Fig. III.13. Fluorescence decay profile of melittin + 0.5 M K_2HPO_4 (emission wavelength = 330 nm). Curve (1) represents the lamp profile. Curve (2) represents the experimental fluorescence decay profile while curve (3) is the convoluted decay profile. Insert (A): Plot of the Residuals versus Channel Number. Insert (B): Plot of the Autocorrelation versus Channel Number. Channel width = 0.173 ns.

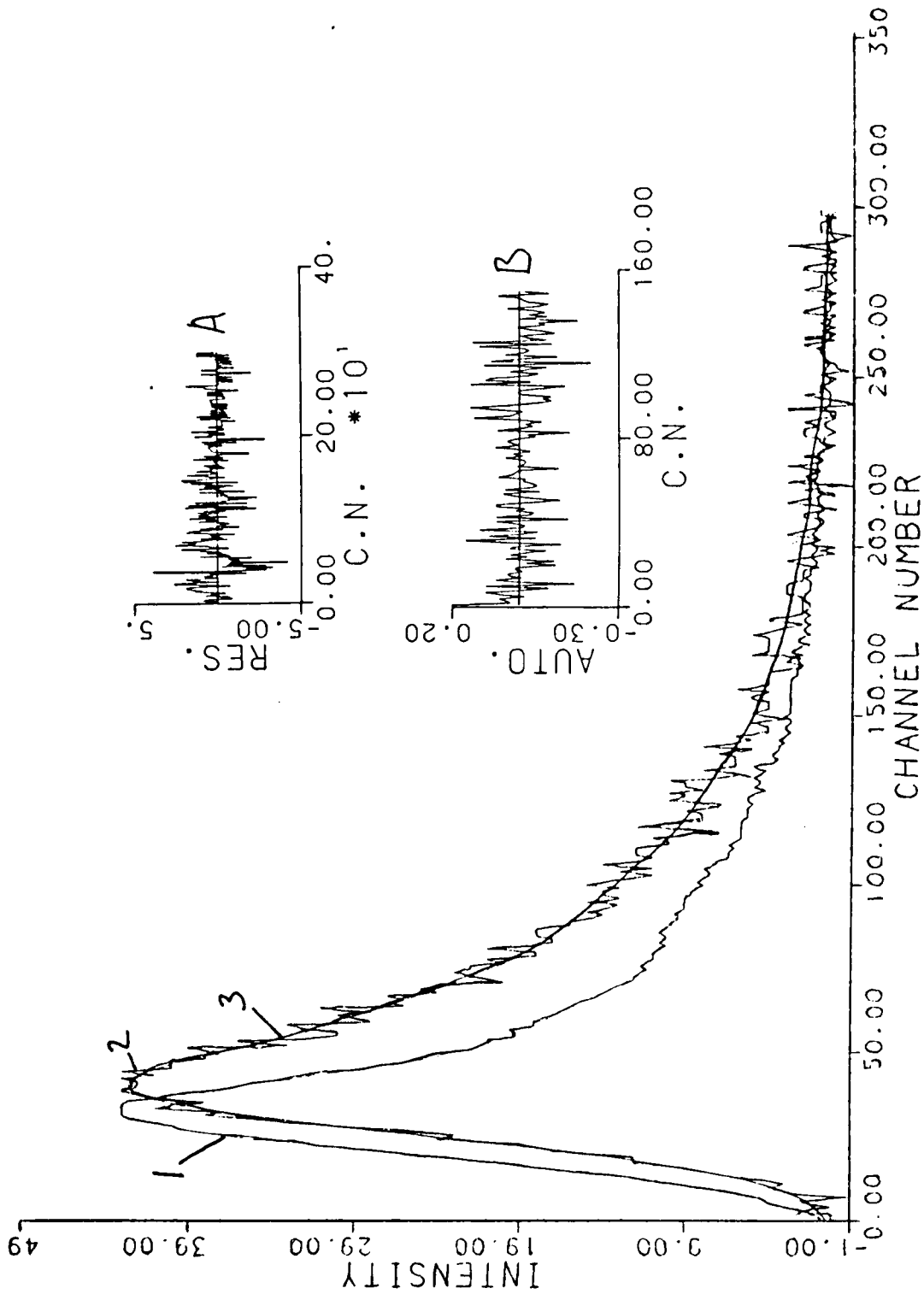
INTENSITY
49
39.00
29.00
19.00
9.00
-1.00
0.00
50.00
100.00
150.00
200.00
250.00
300.00
350
CHANNEL NUMBER
1
2
3
A
RES.
5.
5.00
-5.00
0.00
20.00
40.
C.N.
*10'
B
AUTO.
0.20
0.30
-0.30
0.00
80.00
160.00
C.N.

Fig. III.13.

Fig. III.14. Fluorescence decay profile of melittin + 0.5 M K_2HPO_4 (emission wavelength = 340 nm). Curve (1) represents the lamp profile. Curve (2) represents the experimental fluorescence decay profile while curve (3) is the convoluted decay profile. Insert (A): Plot of the Residuals versus Channel Number. Insert (B): Plot of the Autocorrelation versus Channel Number. Channel width = 0.129 ns.

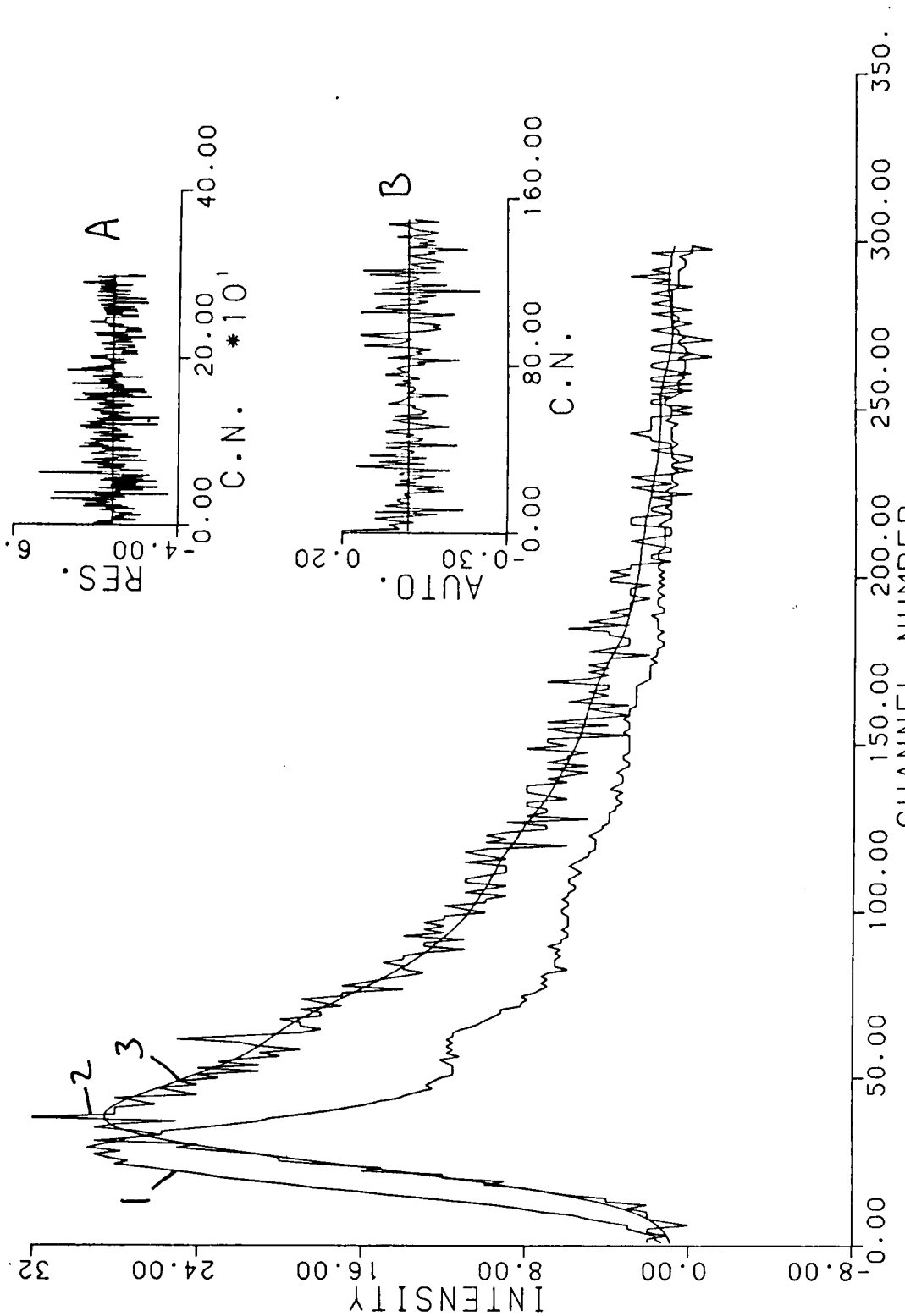
INTENSITY
32
24.00
16.00
8.00
0.00
-8.00
0.00
50.00
100.00
150.00
200.00
250.00
300.00
350.
CHANNEL NUMBER
1
2
3
A
RES.
6.
-4.00
0.00
20.00
40.00
C.N. *10¹
B
AUTO.
0.20
-0.30
0.00
80.00
160.00
C.N.

Fig. III.14.

Fig. III.15. Fluorescence decay profile of melittin + 0.5 M K_2HPO_4 (emission wavelength = 360 nm). Curve (1) represents the lamp profile. Curve (2) represents the experimental fluorescence decay profile while curve (3) is the convoluted decay profile. Insert (A): Plot of the Residuals versus Channel Number. Insert (B): Plot of the Autocorrelation versus Channel Number. Channel width = 0.129 ns.

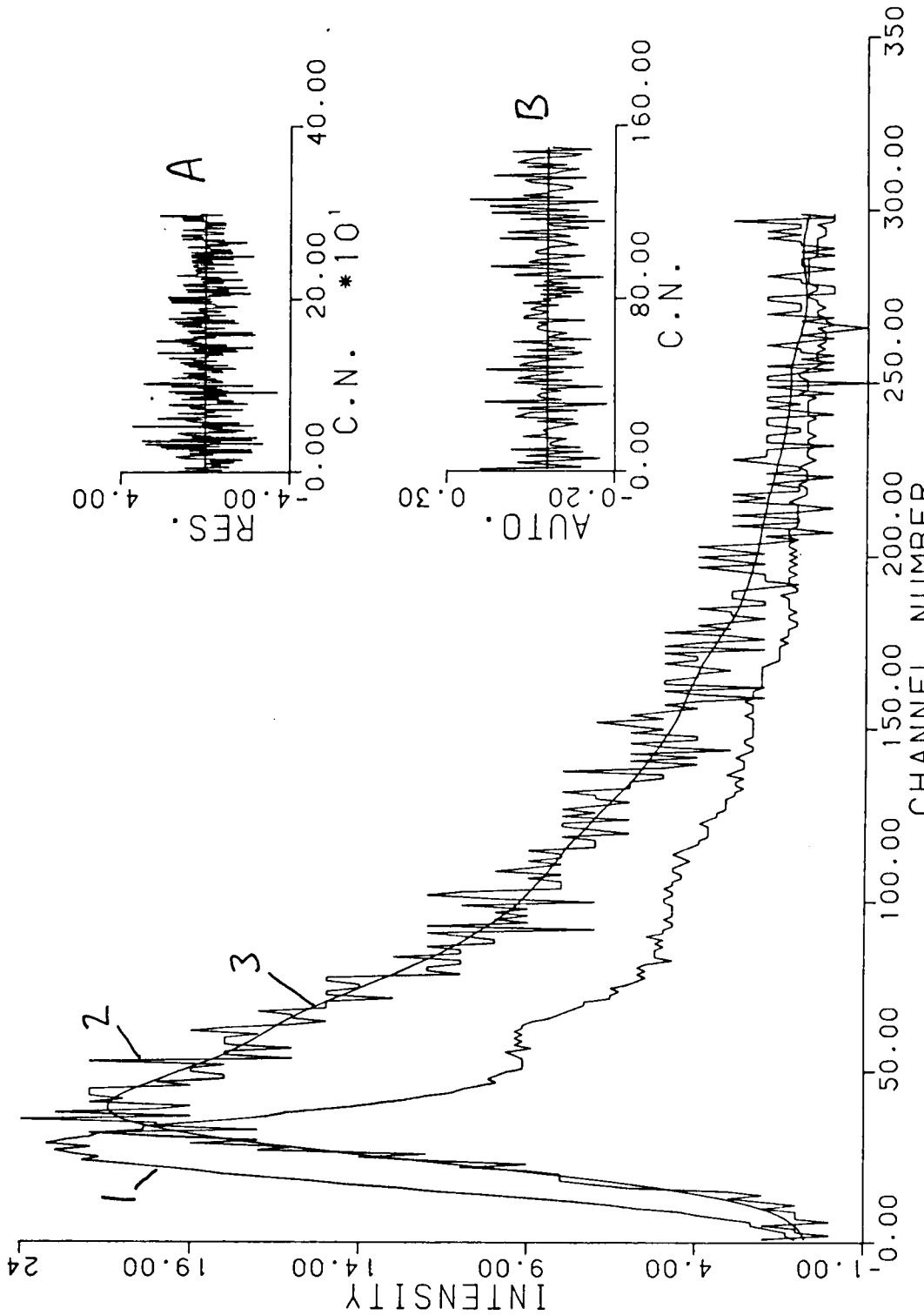
INTENSITY
24
19.00
14.00
9.00
4.00
-1.00
0.00
50.00
100.00
150.00
200.00
250.00
300.00
350
CHANNEL NUMBER
1
2
3
A
RES.
4.00
-4.00
0.00
20.00
40.00
C.N. *10¹
B
AUTO.
0.30
-0.20
0.00
80.00
160.00
C.N.

Fig. III.15.

Fig. III.16. Fluorescence decay profile of melittin + 0.5 M K_2HPO_4 (emission wavelength = 390 nm). Curve (1) represents the lamp profile. Curve (2) represents the experimental fluorescence decay profile while curve (3) is the convoluted decay profile. Insert (A): Plot of the Residuals versus Channel Number. Insert (B): Plot of the Autocorrelation versus Channel Number. Channel width = 0.129 ns.

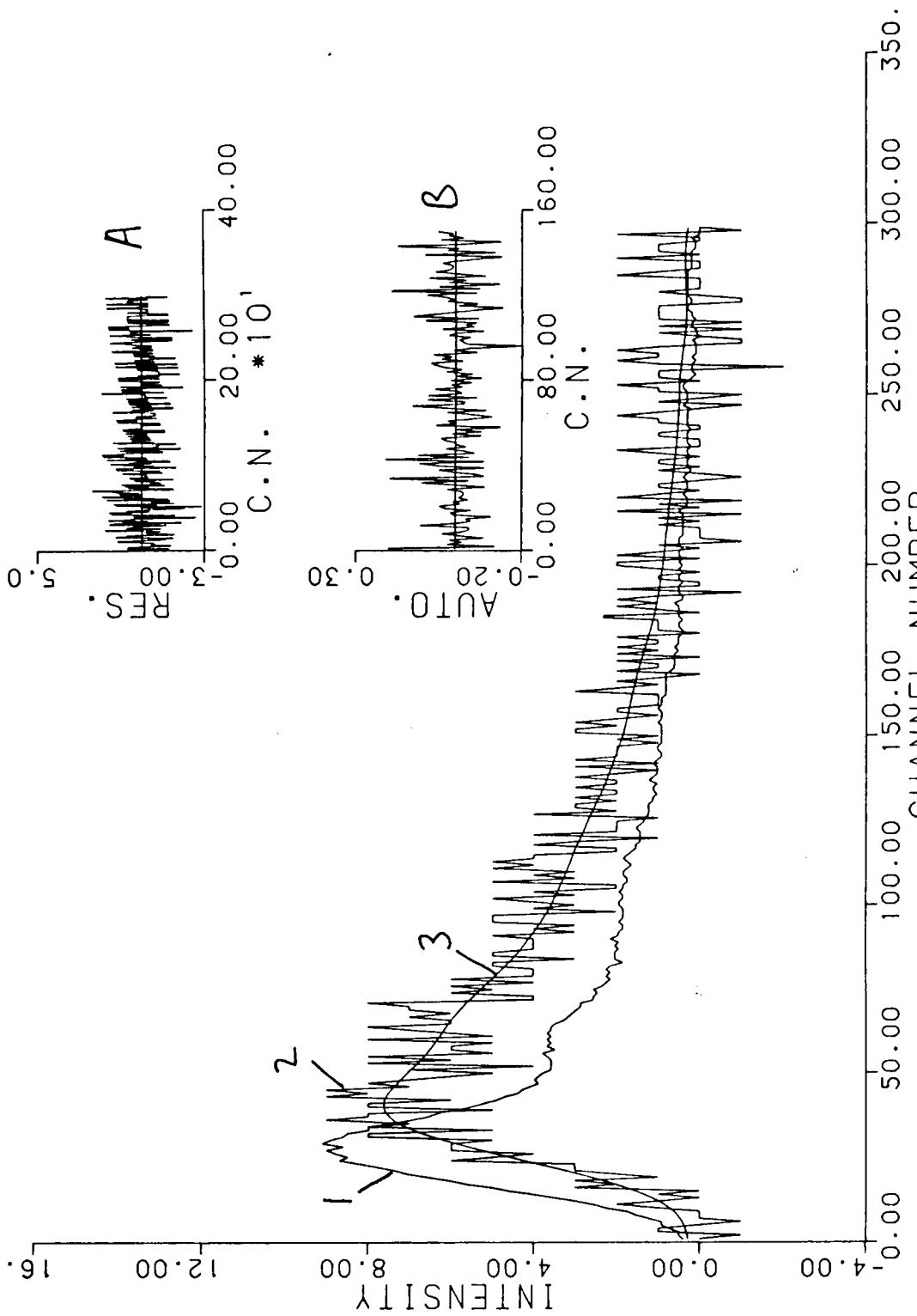
INTENSITY
16.
12.00
8.00
4.00
0.00
-4.00
0.00
50.00
100.00
150.00
200.00
250.00
300.00
350.
CHANNEL NUMBER
1
2
3
A
RES.
5.0
-3.00
0.00
20.00
40.00
C.N. *10¹
B
AUTO.
0.30
-0.20
0.00
80.00
160.00
C.N.

Fig. III.16.

Fig. III.17. Fluorescence decay profile of melittin + 0.15 M NaCl (emission wavelength = 330 nm). Curve (1) represents the lamp profile. Curve (2) represents the experimental fluorescence decay profile while curve (3) is the convoluted decay profile. Insert (A): Plot of the Residuals versus Channel Number. Insert (B): Plot of the Autocorrelation versus Channel Number. Channel width = 0.188 ns.

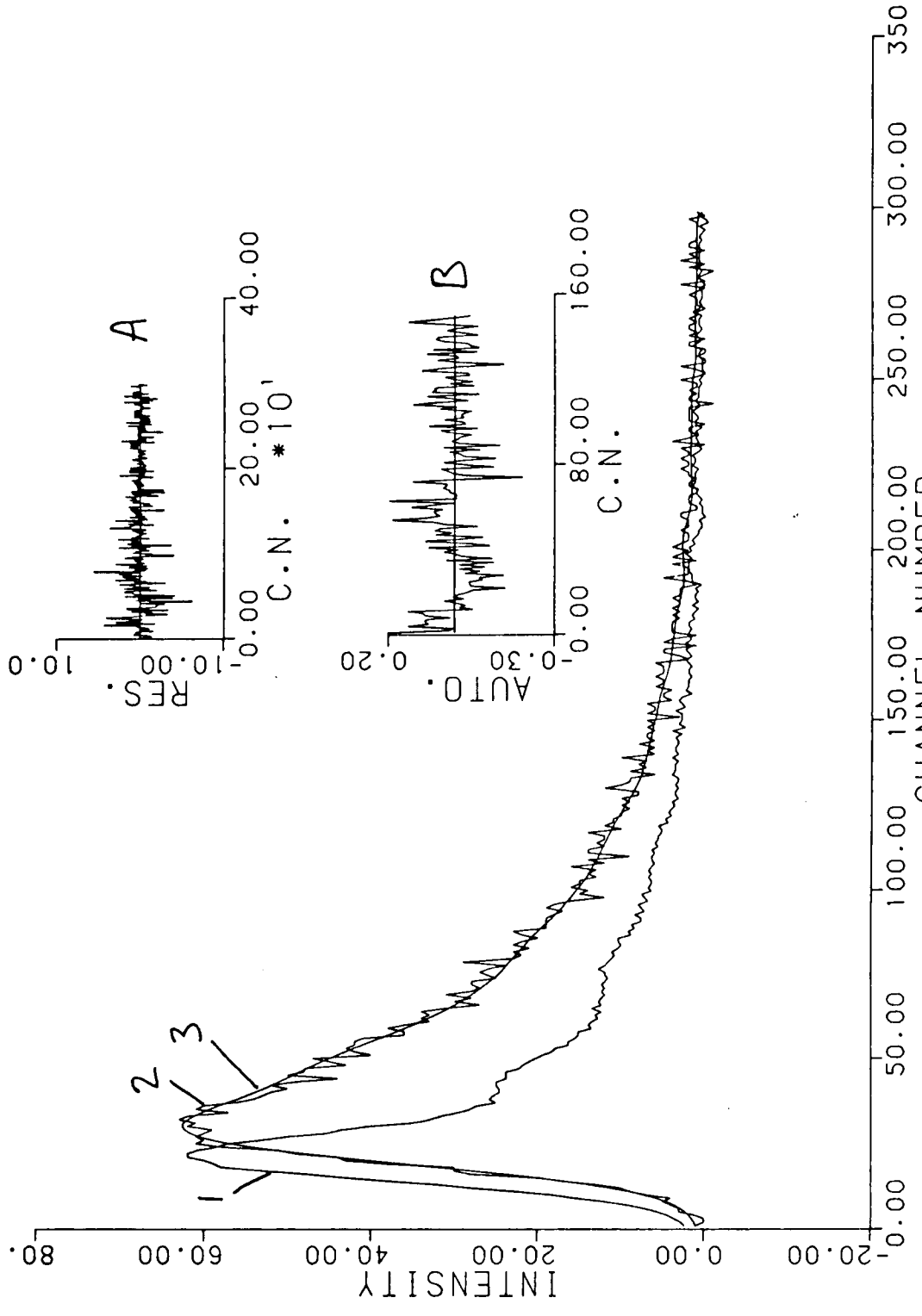
INTENSITY
80.00
60.00
40.00
20.00
0.00
-20.00
0.00
50.00
100.00
150.00
200.00
250.00
300.00
350
CHANNEL NUMBER
1
2
3
A
RES.
10.00
0.00
-10.00
C.N.
*10'
0.00
20.00
40.00
B
AUTO.
0.20
0.00
-0.30
C.N.
0.00
80.00
160.00

Fig. III.17.

Fig. III.18. Fluorescence decay profile of melittin + 0.15 M NaCl (emission wavelength = 360 nm). Curve (1) represents the lamp profile. Curve (2) represents the experimental fluorescence decay profile while curve (3) is the convoluted decay profile. Insert (A): Plot of the Residuals versus Channel Number. Insert (B): Plot of the Autocorrelation versus Channel Number. Channel width = 0.188 ns.

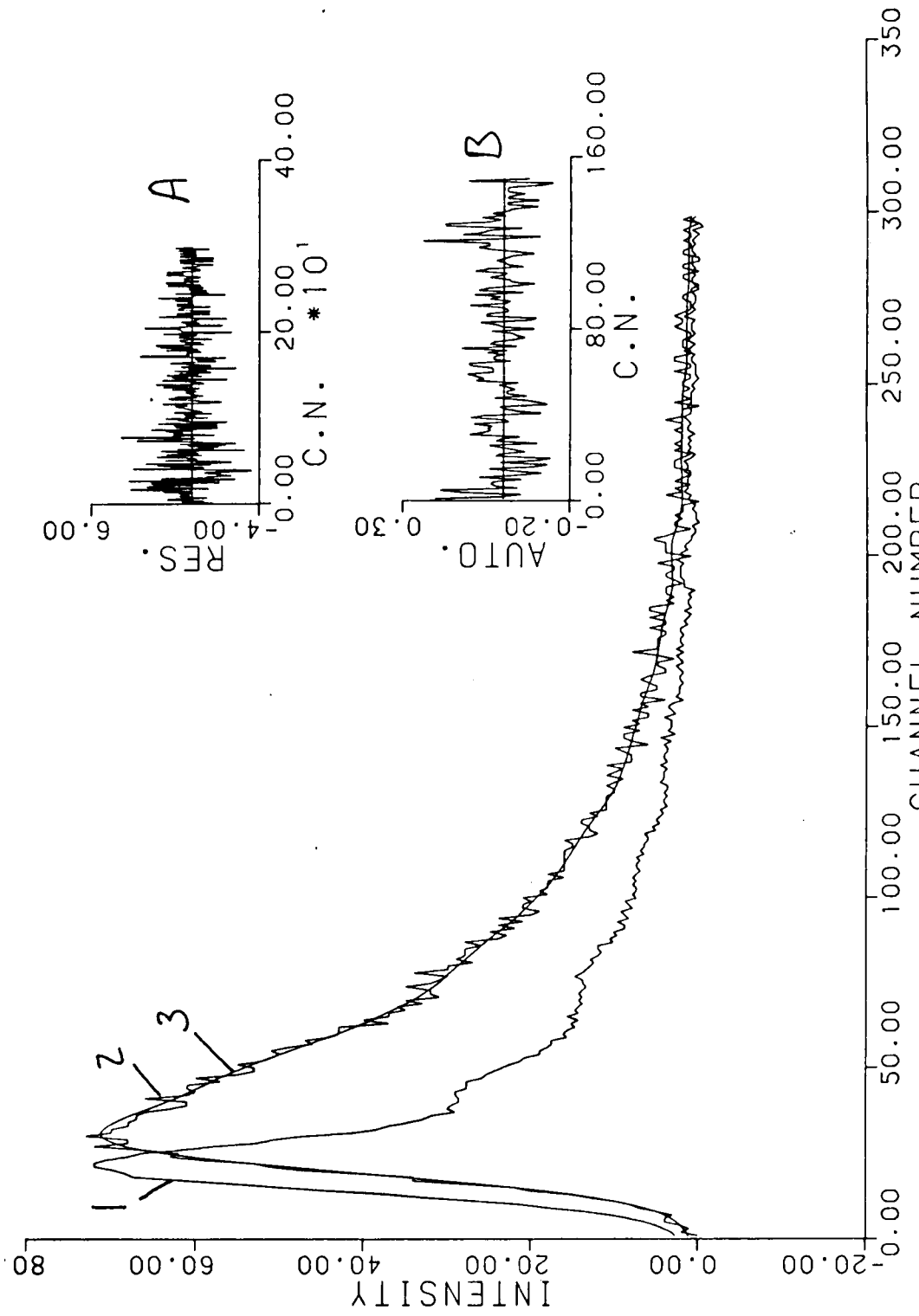
INTENSITY
80.00
60.00
40.00
20.00
0.00
-20.00
0.00
50.00
100.00
150.00
200.00
250.00
300.00
350.
CHANNEL NUMBER
1
2
3
A
RES.
6.00
-4.00
0.00
20.00
40.00
C.N. *10¹
B
AUTO.
0.30
-0.20
0.00
80.00
160.00
C.N.

Fig. III.18.

Fig. III.19. Fluorescence decay profile of melittin + 0.15 M NaCl (emission wavelength = 390 nm). Curve (1) represents the lamp profile. Curve (2) represents the experimental fluorescence decay profile while curve (3) is the convoluted decay profile. Insert (A): Plot of the Residuals versus Channel Number. Insert (B): Plot of the Autocorrelation versus Channel Number. Channel width = 0.188 ns.

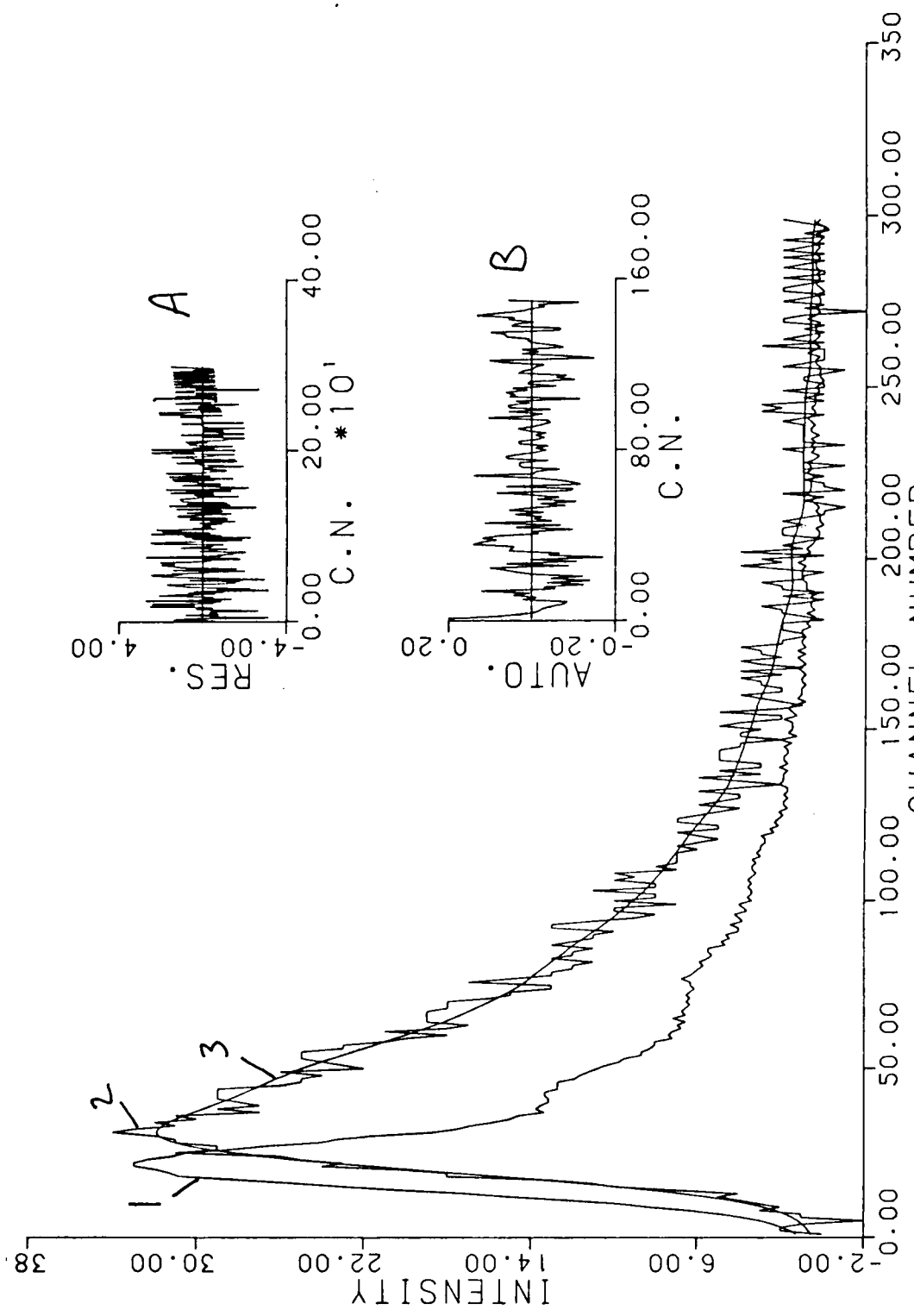
INTENSITY
38.00
30.00
22.00
14.00
6.00
-2.00
0.00
50.00
100.00
150.00
200.00
250.00
300.00
350
CHANNEL NUMBER
1
2
3
A
RES.
4.00
-4.00
0.00
20.00
40.00
C.N. *10¹
B
AUTO.
0.20
-0.20
0.00
80.00
160.00
C.N.

Fig. III.19.

Fig. III.20. Fluorescence decay profile of melittin + 1.0 M NaCl (emission wavelength = 330 nm). Curve (1) represents the lamp profile. Curve (2) represents the experimental fluorescence decay profile while curve (3) is the convoluted decay profile. Insert (A): Plot of the Residuals versus Channel Number. Insert (B): Plot of the Autocorrelation versus Channel Number. Channel width = 0.126 ns.

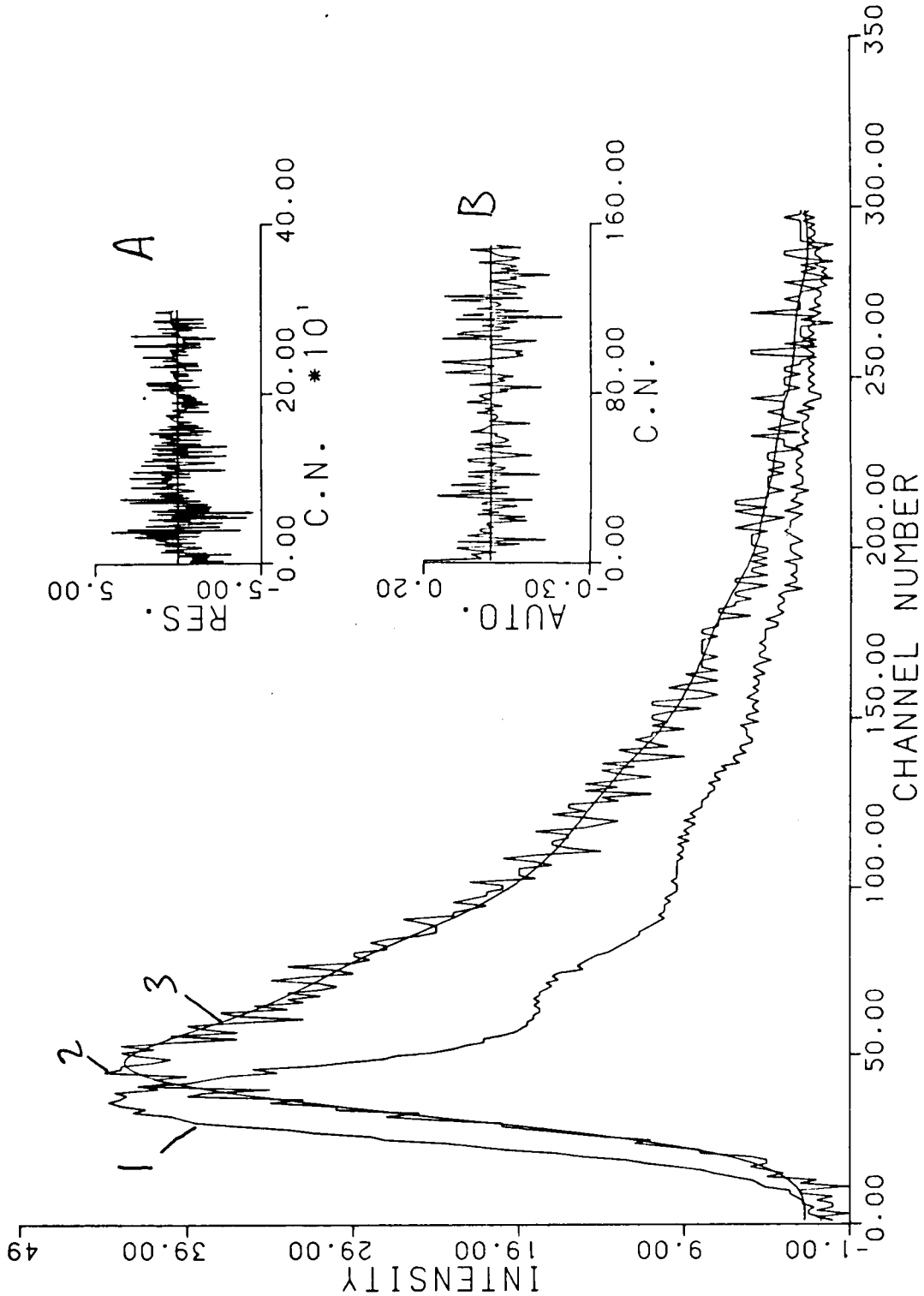
INTENSITY
-1.00
9.00
19.00
29.00
39.00
49
0.00
50.00
100.00
150.00
200.00
250.00
300.00
350
CHANNEL NUMBER
1
2
3
A
RES.
5.00
-5.00
0.00
20.00
40.00
C.N.
*10'
B
AUTO.
0.20
-0.30
0.00
80.00
160.00
C.N.

Fig. III.20.

Fig. III.21. Fluorescence decay profile of melittin + 1.0 M NaCl (emission wavelength = 340 nm). Curve (1) represents the lamp profile. Curve (2) represents the experimental fluorescence decay profile while curve (3) is the convoluted decay profile. Insert (A): Plot of the Residuals versus Channel Number. Insert (B): Plot of the Autocorrelation versus Channel Number. Channel width = 0.167 ns.

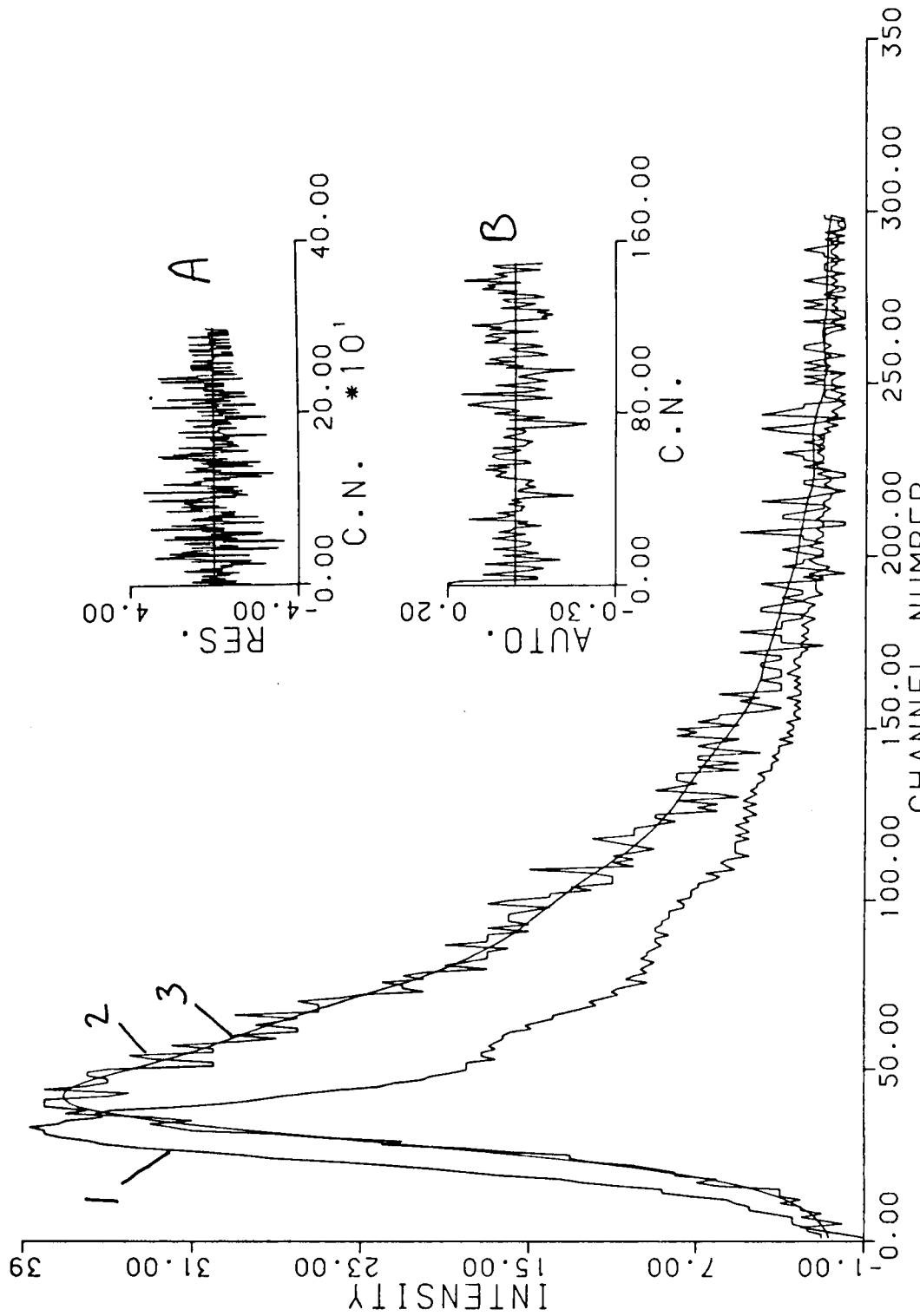
INTENSITY
1.00
7.00
15.00
23.00
31.00
39
0.00
50.00
100.00
150.00
200.00
250.00
300.00
350
CHANNEL NUMBER
1
2
3
A
RES.
-4.00
4.00
0.00
20.00
40.00
C.N. *10¹
B
AUTO.
-0.30
0.20
0.00
80.00
160.00
C.N.

Fig. III.21.

Fig. III.22. Fluorescence decay profile of melittin + 1.0 M NaCl (emission wavelength = 360 nm). Curve (1) represents the lamp profile. Curve (2) represents the experimental fluorescence decay profile while curve (3) is the convoluted decay profile. Insert (A): Plot of the Residuals versus Channel Number. Insert (B): Plot of the Autocorrelation versus Channel Number. Channel width = 0.126 ns.

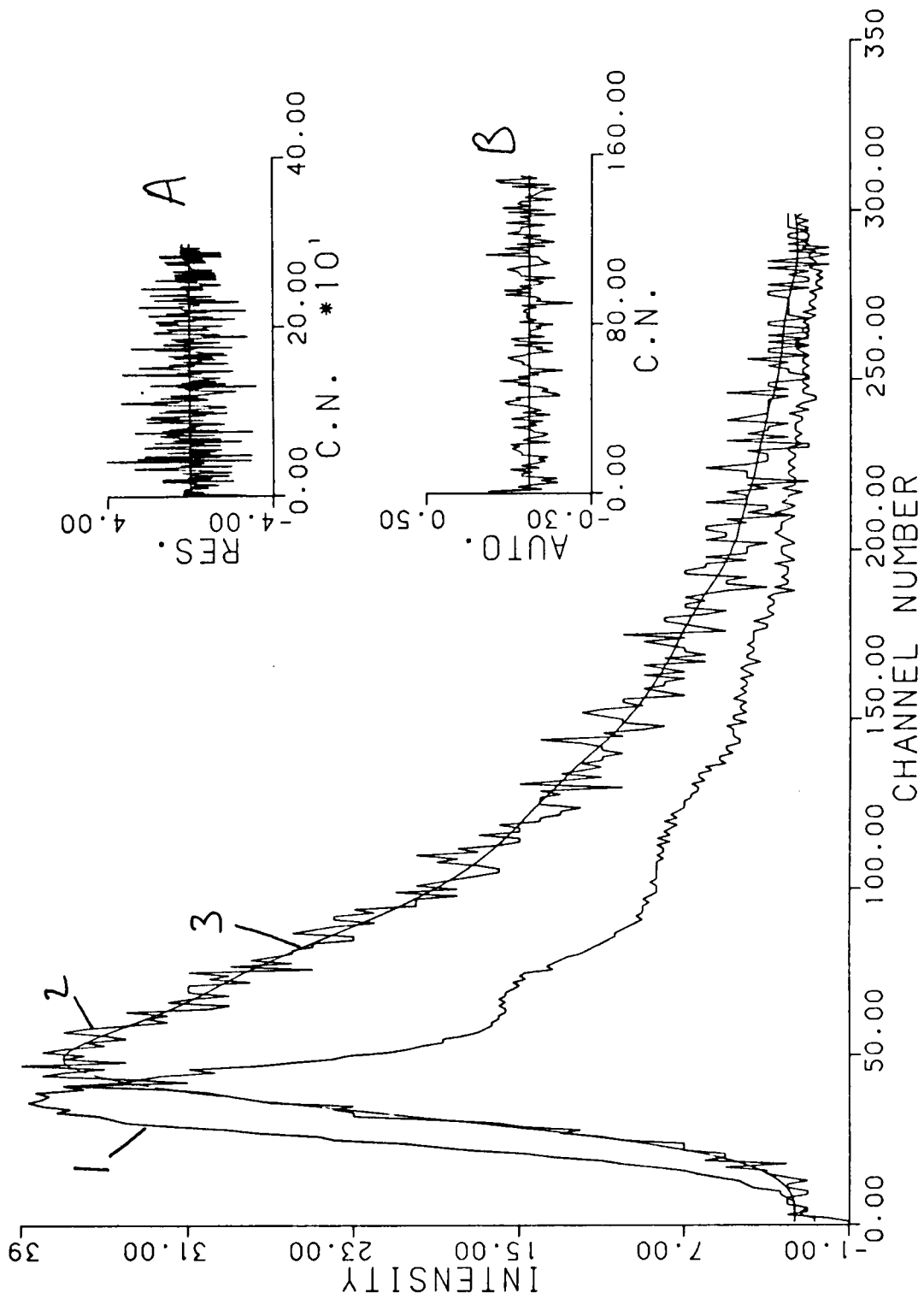
INTENSITY
-1.00
7.00
15.00
23.00
31.00
39
0.00
50.00
100.00
150.00
200.00
250.00
300.00
350
CHANNEL NUMBER
1
2
3
A
RES.
-4.00
4.00
-0.00
20.00
40.00
C.N. *10¹
B
AUTO.
-0.30
0.50
0.00
80.00
160.00
C.N.

Fig. III.22.

Fig. III.23. Fluorescence decay profile of melittin + 1.0 M NaCl (emission wavelength = 390 nm). Curve (1) represents the lamp profile. Curve (2) represents the experimental fluorescence decay profile while curve (3) is the convoluted decay profile. Insert (A): Plot of the Residuals versus Channel Number. Insert (B): Plot of the Autocorrelation versus Channel Number. Channel width = 0.126 ns.

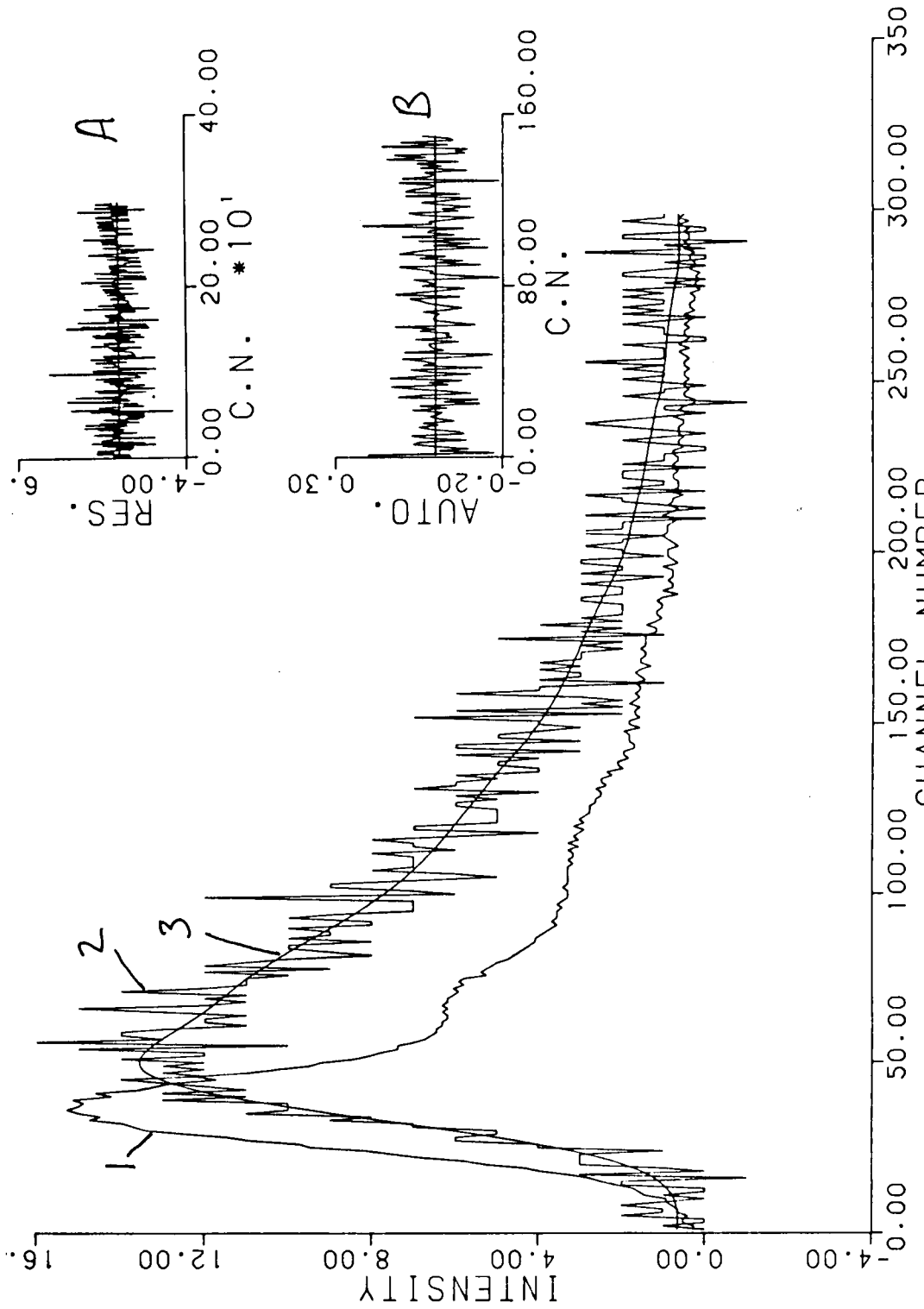
INTENSITY
16.00
12.00
8.00
4.00
0.00
-4.00
CHANNEL NUMBER
0.00
50.00
100.00
150.00
200.00
250.00
300.00
350
1
2
3
A
RES.
6.00
-4.00
C.N. *10¹
0.00
20.00
40.00
B
AUTO.
0.30
-0.20
C.N.
0.00
80.00
160.00

Fig. III.23.

Fig. III.24. Fluorescence decay profile of melittin in egg lecithin (emission wavelength = 340 nm). Curve (1) represents the lamp profile. Curve (2) represents the experimental fluorescence decay profile while curve (3) is the convoluted decay profile. Insert (A): Plot of the Residuals versus Channel Number. Insert (B): Plot of the Autocorrelation versus Channel Number. Channel width = 0.166 ns.

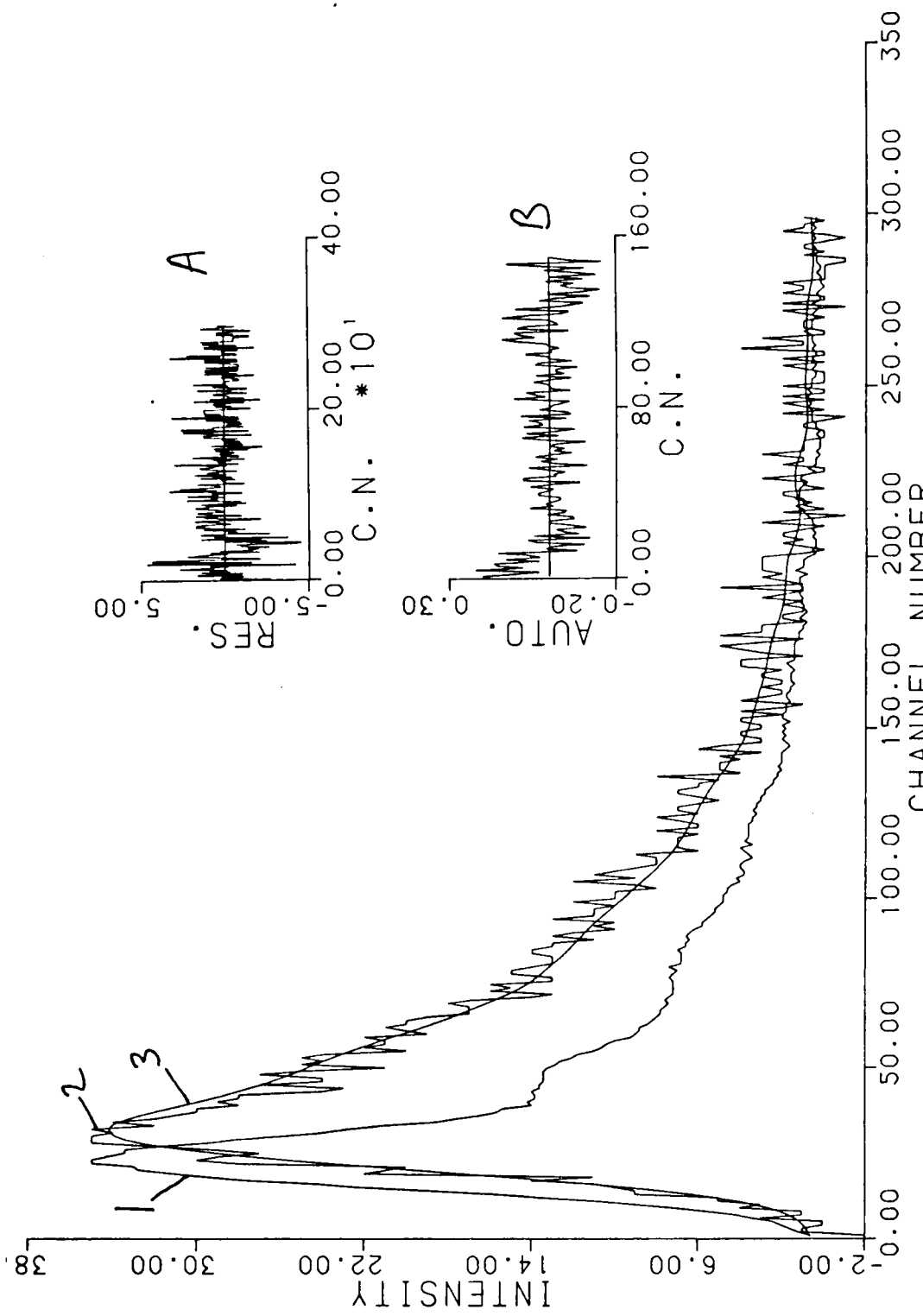
INTENSITY
38.00
30.00
22.00
14.00
6.00
-2.00
0.00
50.00
100.00
150.00
200.00
250.00
300.00
350
CHANNEL NUMBER
1
2
3
A
RES.
5.00
-5.00
0.00
20.00
40.00
C.N.
*10¹
B
AUTO.
0.30
-0.20
0.00
80.00
160.00
C.N.

Fig. III.24.

Fig. III.25. Fluorescence decay profile of melittin in egg lecithin (emission wavelength = 360 nm). Curve (1) represents the lamp profile. Curve (2) represents the experimental fluorescence decay profile while curve (3) is the convoluted decay profile. Insert (A): Plot of the Residuals versus Channel Number. Insert (B): Plot of the Autocorrelation versus Channel Number. Channel width = 0.166 ns.

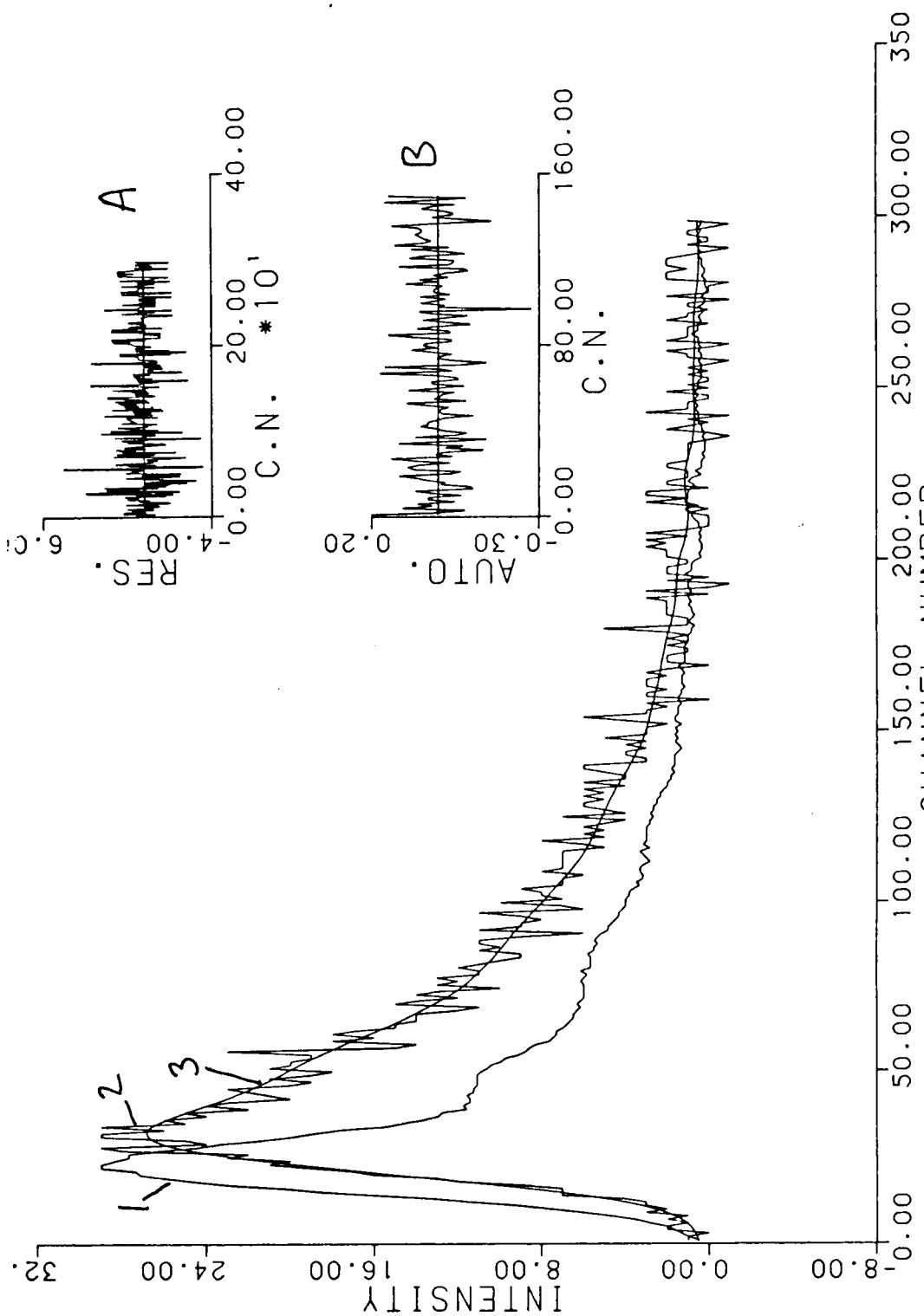
INTENSITY
32.
24.00
16.00
8.00
0.00
-8.00
0.00
50.00
100.00
150.00
200.00
250.00
300.00
350
CHANNEL NUMBER
1
2
3
A
RES.
6.0
-4.00
0.00
20.00
40.00
C.N. *10¹
B
AUTO.
0.20
-0.30
0.00
80.00
160.00
C.N.

Fig. III.25.

Fig. III.26. Fluorescence decay profile of melittin in egg lecithin (emission wavelength = 390 nm). Curve (1) represents the lamp profile. Curve (2) represents the experimental fluorescence decay profile while curve (3) is the convoluted decay profile. Insert (A): Plot of the Residuals versus Channel Number. Insert (B): Plot of the Autocorrelation versus Channel Number. Channel width = 0.166 ns.

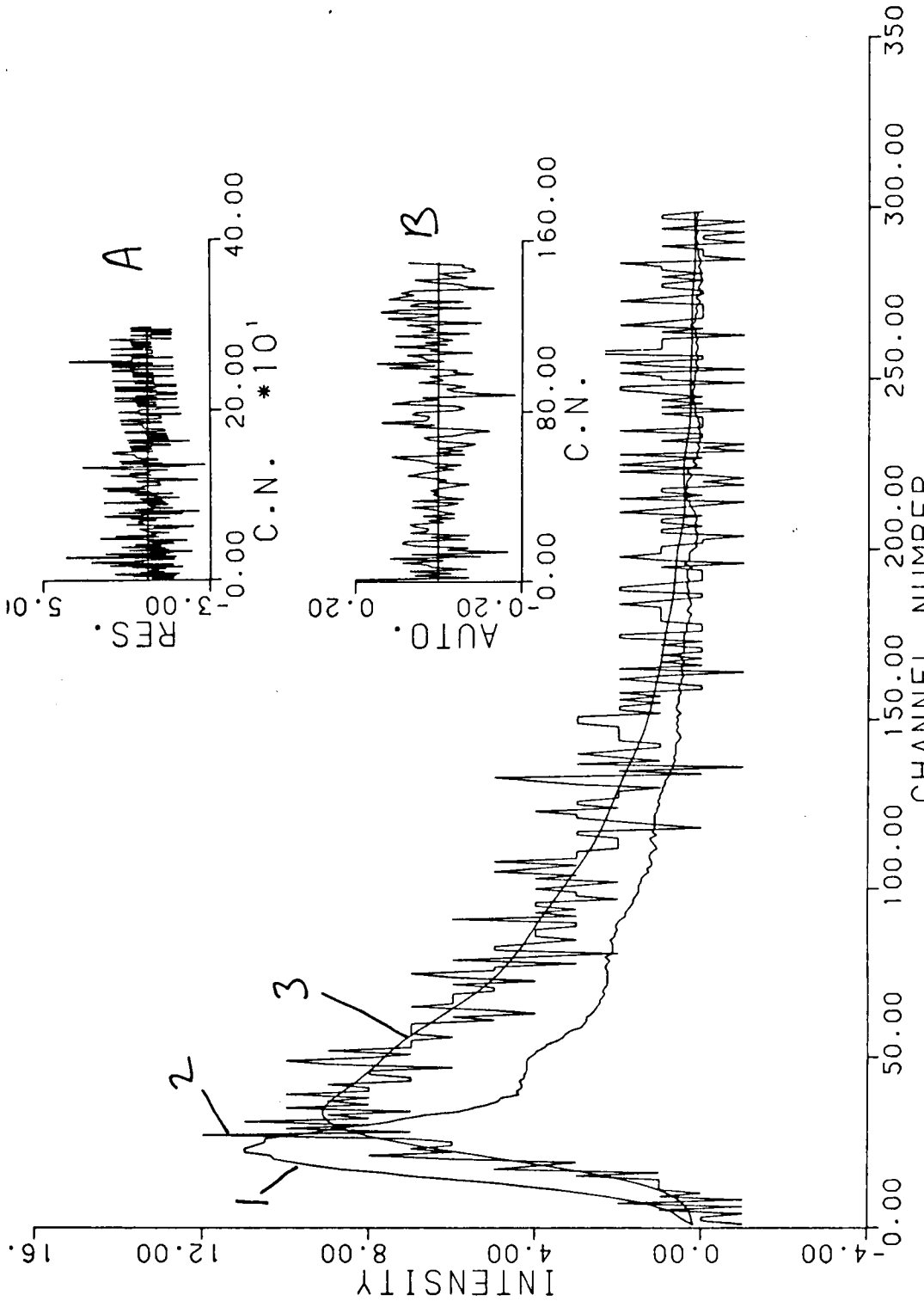
INTENSITY
16.00
12.00
8.00
4.00
0.00
-4.00
0.00
50.00
100.00
150.00
200.00
250.00
300.00
350
CHANNEL NUMBER
1
2
3
A
RES.
5.00
-3.00
0.00
20.00
40.00
C.N.
*10¹
B
AUTO.
0.20
-0.20
0.00
80.00
160.00
C.N.

Fig. III.26.

Fig. III.27. Fluorescence decay profile of melittin in distearoyllecithin (emission wavelength = 340 nm). Curve (1) represents the lamp profile. Curve (2) represents the experimental fluorescence decay profile while curve (3) is the convoluted decay profile. Insert (A): Plot of the Residuals versus Channel Number. Insert (B): Plot of the Autocorrelation versus Channel Number. Channel width = 0.186 ns.

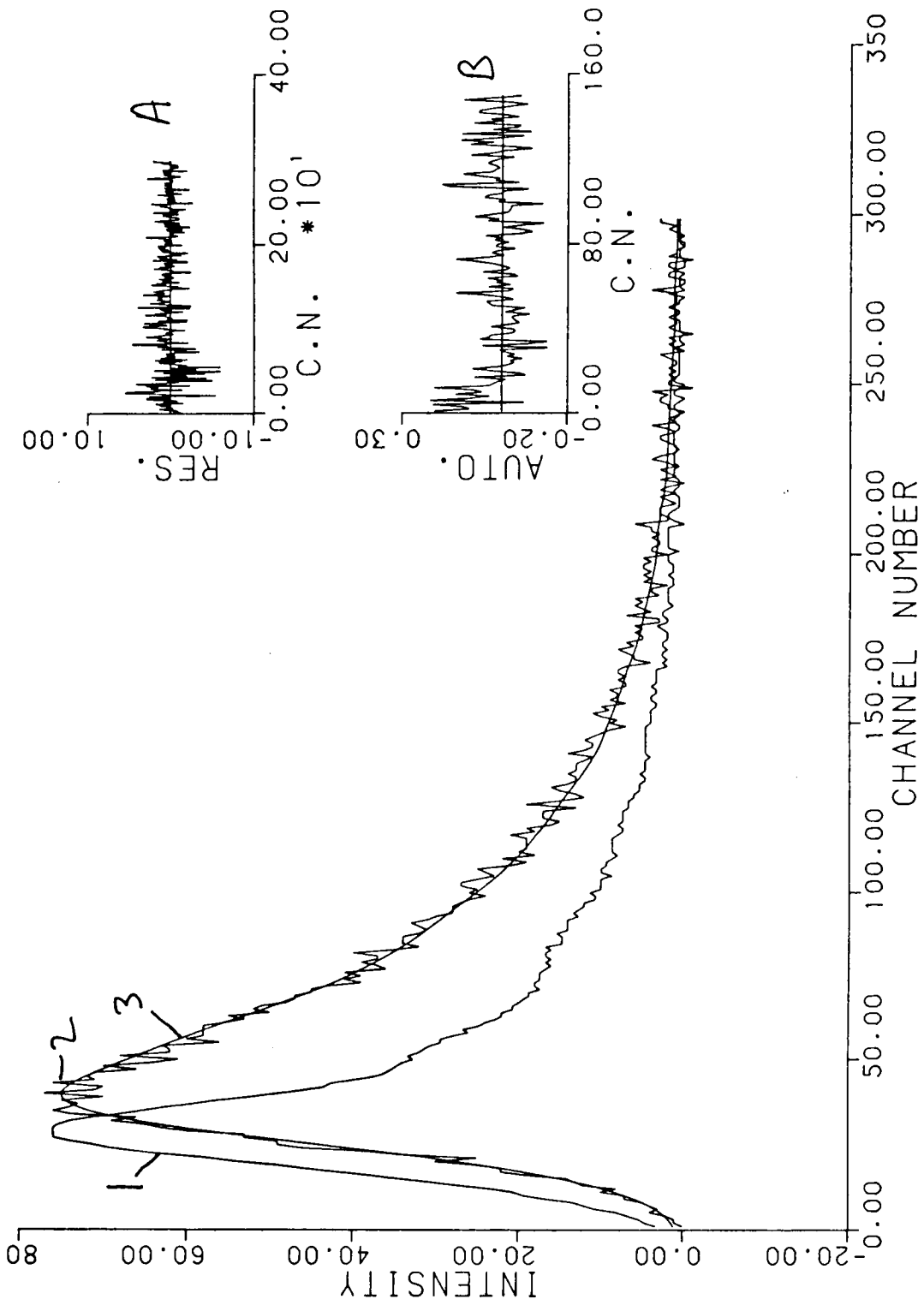
INTENSITY
80
60.00
40.00
20.00
0.00
-20.00
0.00
50.00
100.00
150.00
200.00
250.00
300.00
350
CHANNEL NUMBER
1
2
3
A
RES.
10.00
-10.00
0.00
20.00
40.00
C.N.
*10'
B
AUTO.
0.30
-0.20
0.00
80.00
160.0
C.N.

Fig. III.27.

Fig. III.28. Fluorescence decay profile of melittin in distearoyllecithin (emission wavelength = 360 nm). Curve (1) represents the lamp profile. Curve (2) represents the experimental fluorescence decay profile while curve (3) is the convoluted decay profile. Insert (A): Plot of the Residuals versus Channel Number. Insert (B): Plot of the Autocorrelation versus Channel Number. Channel width = 0.186 ns.

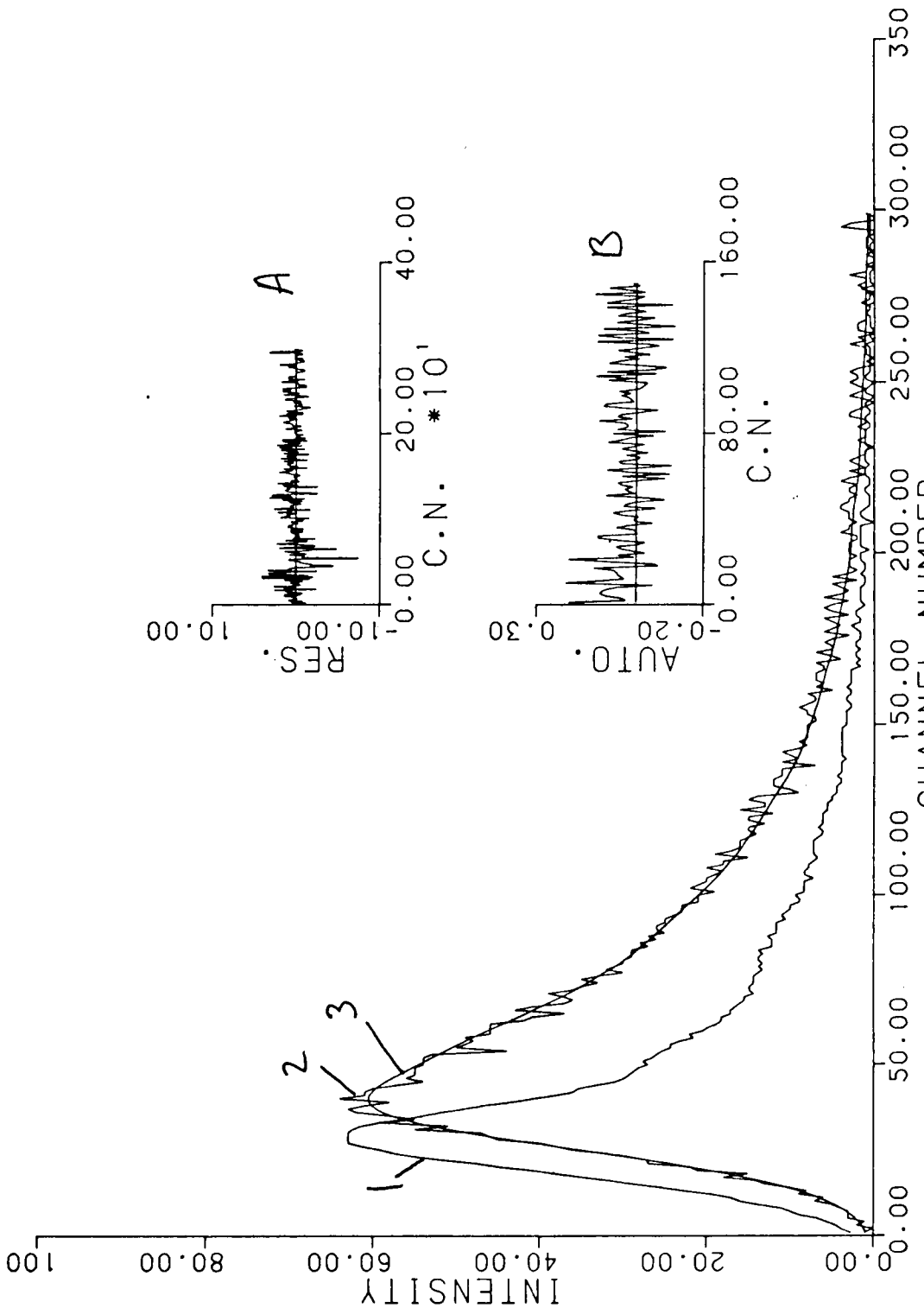
INTENSITY
0.00
20.00
40.00
60.00
80.00
100
0.00
50.00
100.00
150.00
200.00
250.00
300.00
350
CHANNEL NUMBER
1
2
3
A
RES.
-10.00
10.00
0.00
20.00
40.00
C.N.
*10'
B
AUTO.
-0.20
0.30
0.00
80.00
160.00
C.N.

Fig. III.28.

Fig. III.29. Fluorescence decay profile of melittin in distearoyllecithin (emission wavelength = 390 nm). Curve (1) represents the lamp profile. Curve (2) represents the experimental fluorescence decay profile while curve (3) is the convoluted decay profile. Insert (A): Plot of the Residuals versus Channel Number. Insert)B): Plot of the Autocorrelation versus Channel Number. Channel width = 0.186 ns.

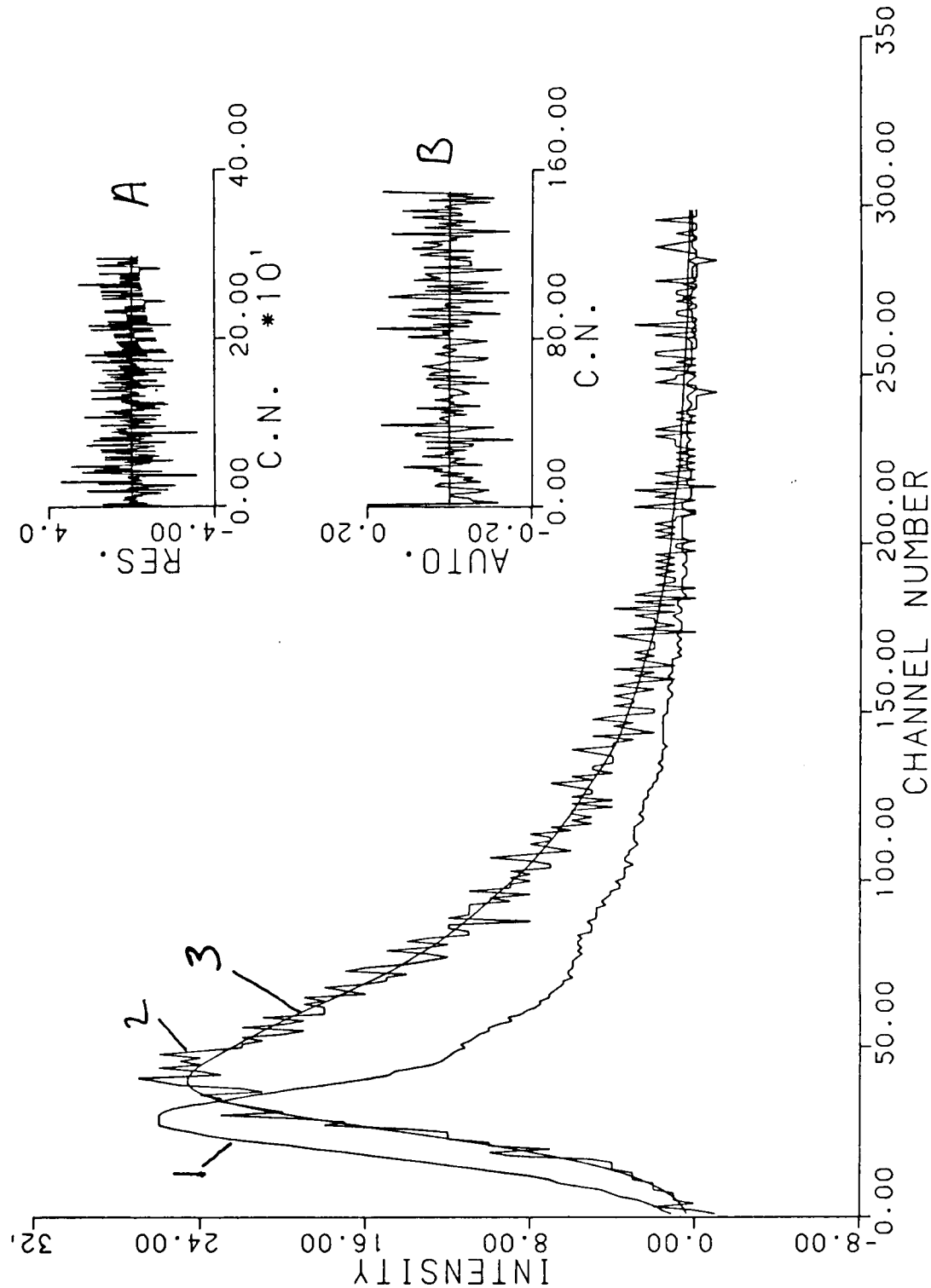
INTENSITY
32.
24.00
16.00
8.00
0.00
-8.00
0.00
50.00
100.00
150.00
200.00
250.00
300.00
350
CHANNEL NUMBER
1
2
3
A
RES.
4.0
-4.00
0.00
20.00
40.00
C.N. *10'
B
AUTO.
0.20
-0.20
0.00
80.00
160.00
C.N.

Fig. III.29.

Fig. III.30. Fluorescence decay profile of melittin in distearoyllecithin at 61°C (emission wavelength = 340 nm). Curve (1) represents the lamp profile. Curve (2) represents the experimental fluorescence decay profile while curve (3) is the convoluted decay profile. Insert (A): Plot of the Residuals versus Channel Number. Insert (B): Plot of the Autocorrelation versus Channel Number. Channel width = 0.160 ns.

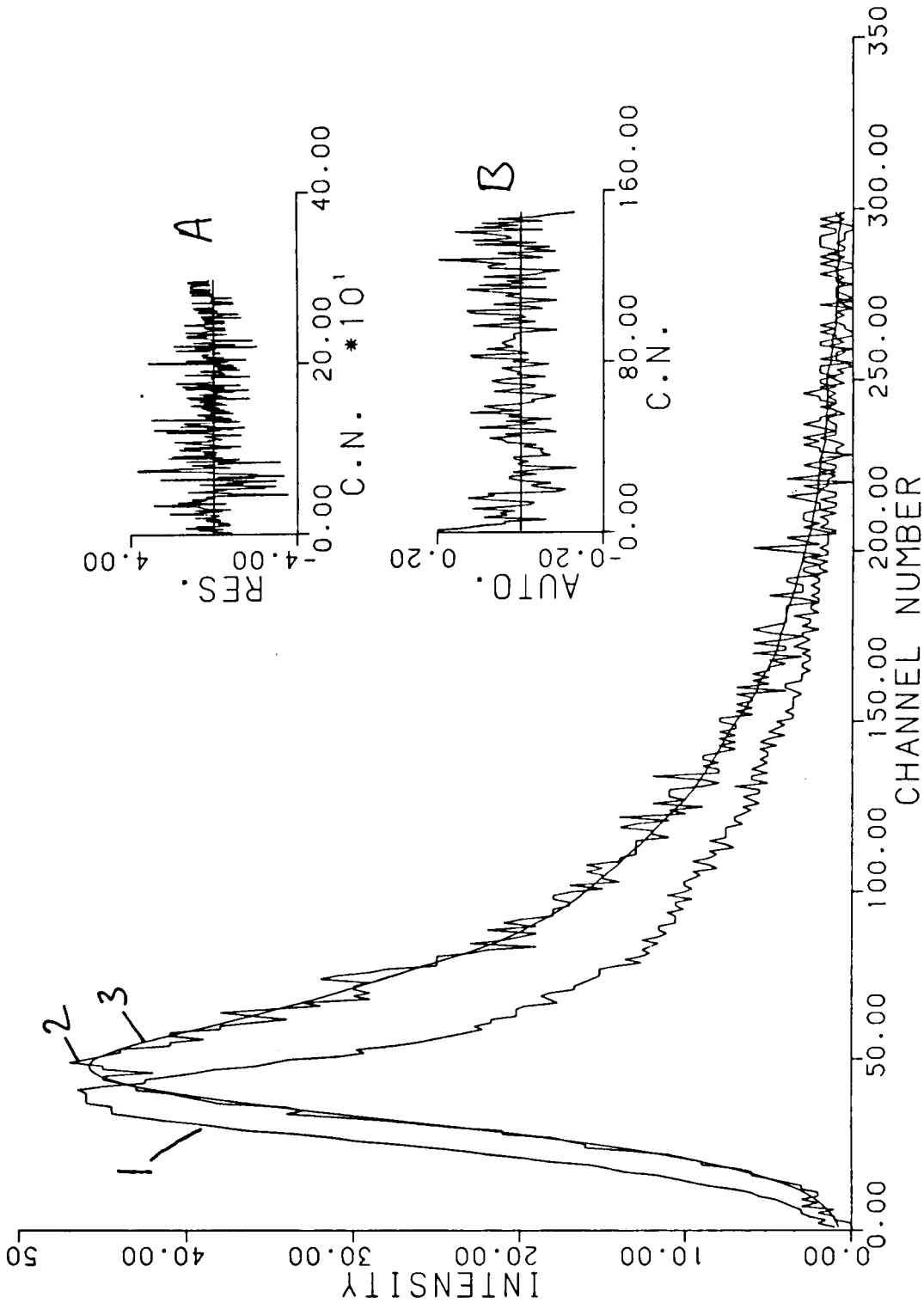
INTENSITY
0.00
10.00
20.00
30.00
40.00
50
0.00
50.00
100.00
150.00
200.00
250.00
300.00
350
CHANNEL NUMBER
1
2
3
A
RES.
4.00
-4.00
0.00
20.00
40.00
C.N.
*10¹
B
AUTO.
0.20
-0.20
0.00
80.00
160.00
C.N.

Fig. III.30.

Fig. III.31. Fluorescence decay profile of melittin in distearoyllecithin at 61°C (emission wavelength = 360 nm). Curve (1) represents the lamp profile. Curve (2) represents the experimental fluorescence decay profile while curve (3) is the convoluted decay profile. Insert (A): Plot of the Residuals versus Channel Number. Insert (B): Plot of the Autocorrelation versus Channel Number. Channel width = 0.160 ns.

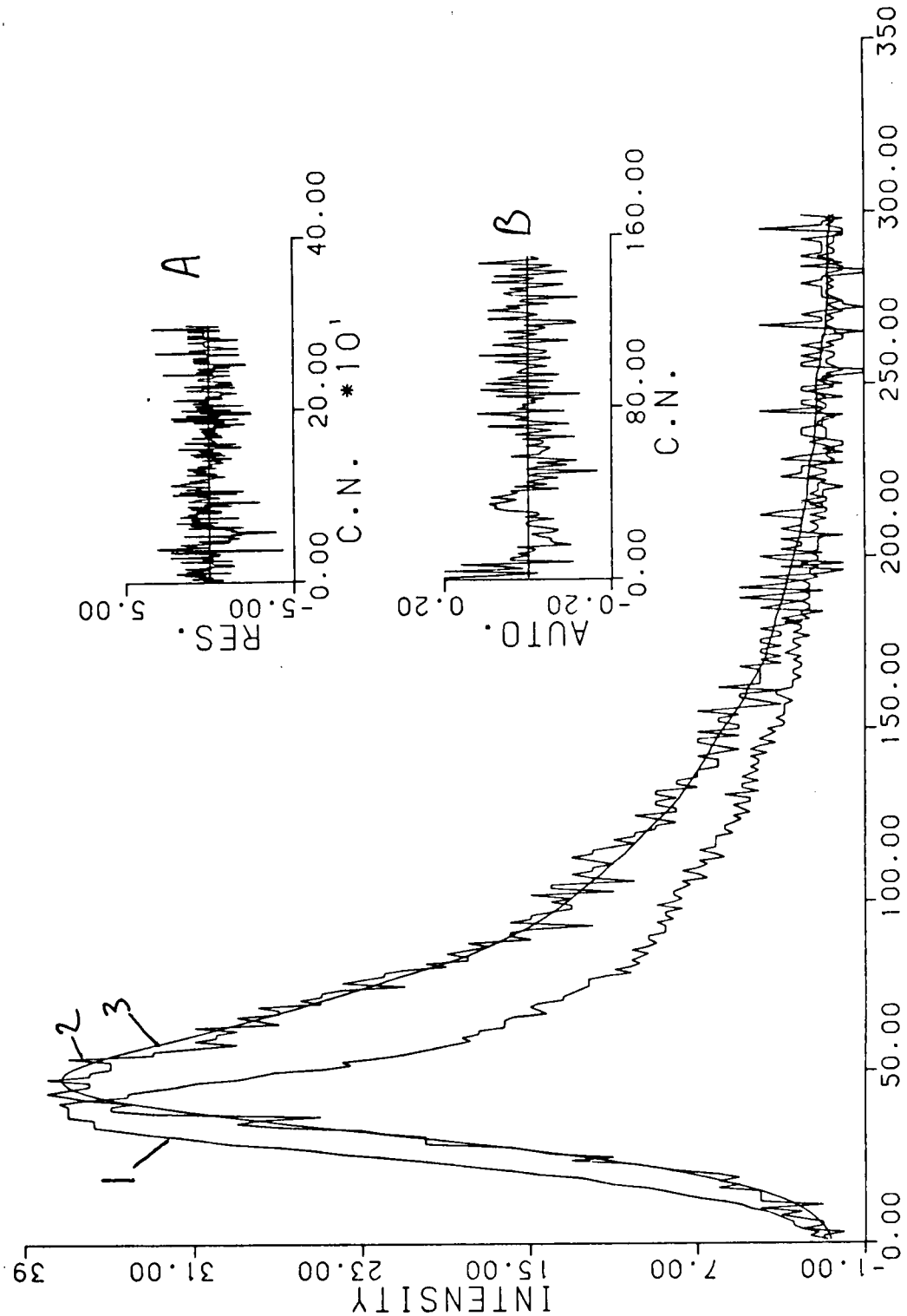
INTENSITY
39.00
31.00
23.00
15.00
7.00
-1.00
0.00
50.00
100.00
150.00
200.00
250.00
300.00
350
CHANNEL NUMBER
1
2
3
A
RES.
5.00
-5.00
0.00
20.00
40.00
C.N.
*10'
B
AUTO.
0.20
-0.20
0.00
80.00
160.00
C.N.

Fig. III.31.

Fig. III.32. Fluorescence decay profile of melittin in distearoyllecithin at 61°C (emission wavelength = 390 nm). Curve (1) represents the lamp profile. Curve (2) represents the experimental fluorescence decay profile while curve (3) is the convoluted decay profile. Insert (A): Plot of the Residuals versus Channel Number. Insert (B): Plot of the Autocorrelation versus Channel Number. Channel width = 0.160 ns.

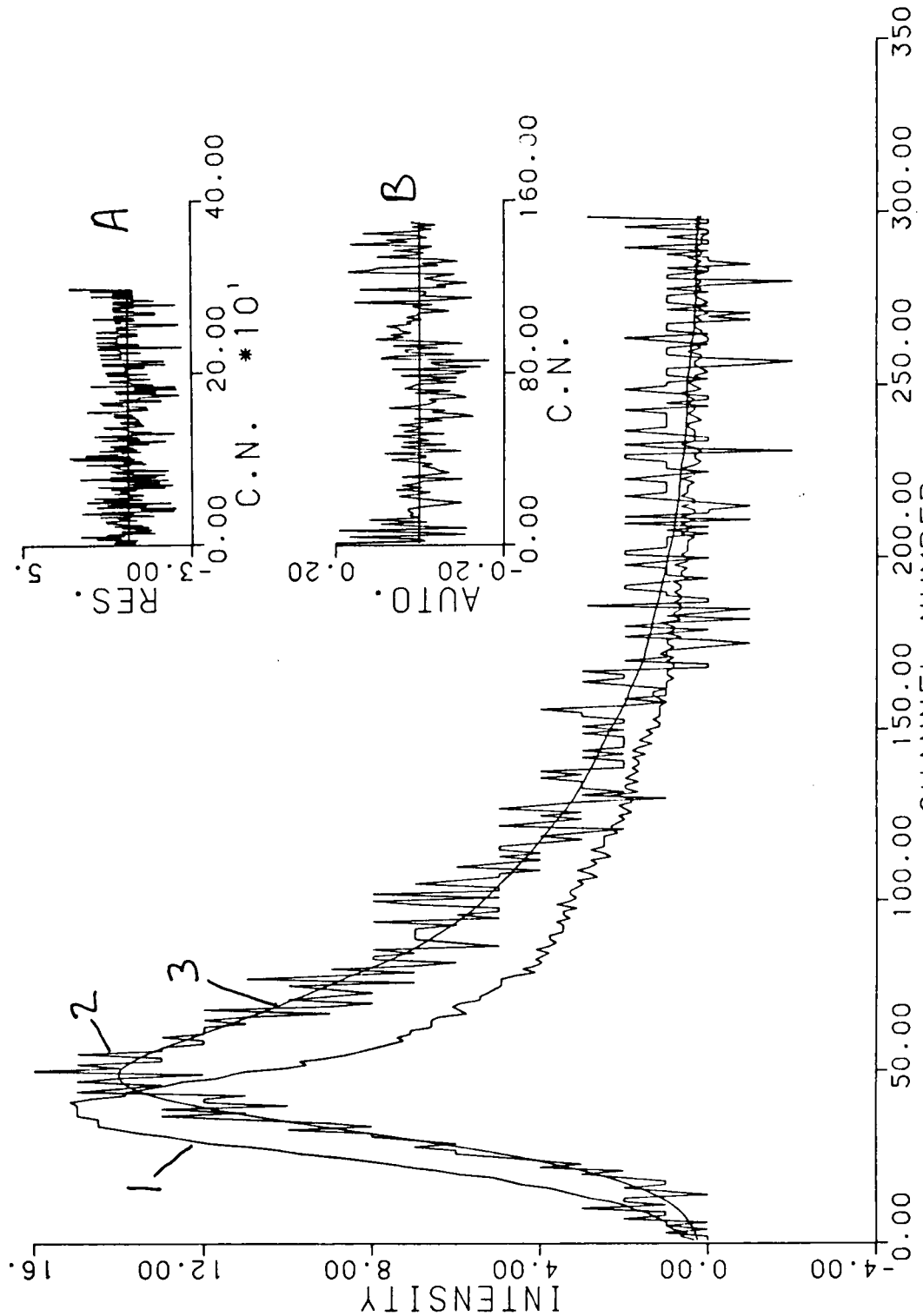
INTENSITY
16.00
12.00
8.00
4.00
0.00
-4.00
0.00
50.00
100.00
150.00
200.00
250.00
300.00
350
CHANNEL NUMBER
1
2
3
A
RES.
-3.00
0.00
20.00
40.00
C.N. *10'
B
AUTO.
-0.20
0.20
0.00
80.00
160.00
C.N.

Fig. III.32.

Fig. III.33. Fluorescence decay profile of melittin in Tris buffer at 61°C (emission wavelength = 330 nm). Curve (1) represents the lamp profile. Curve (2) represents the experimental fluorescence decay profile while curve (3) is the convoluted decay profile. Insert (A): Plot of the Residuals versus Channel Number. Insert (B): Plot of the Autocorrelation versus Channel Number. Channel width = 0.150 ns.

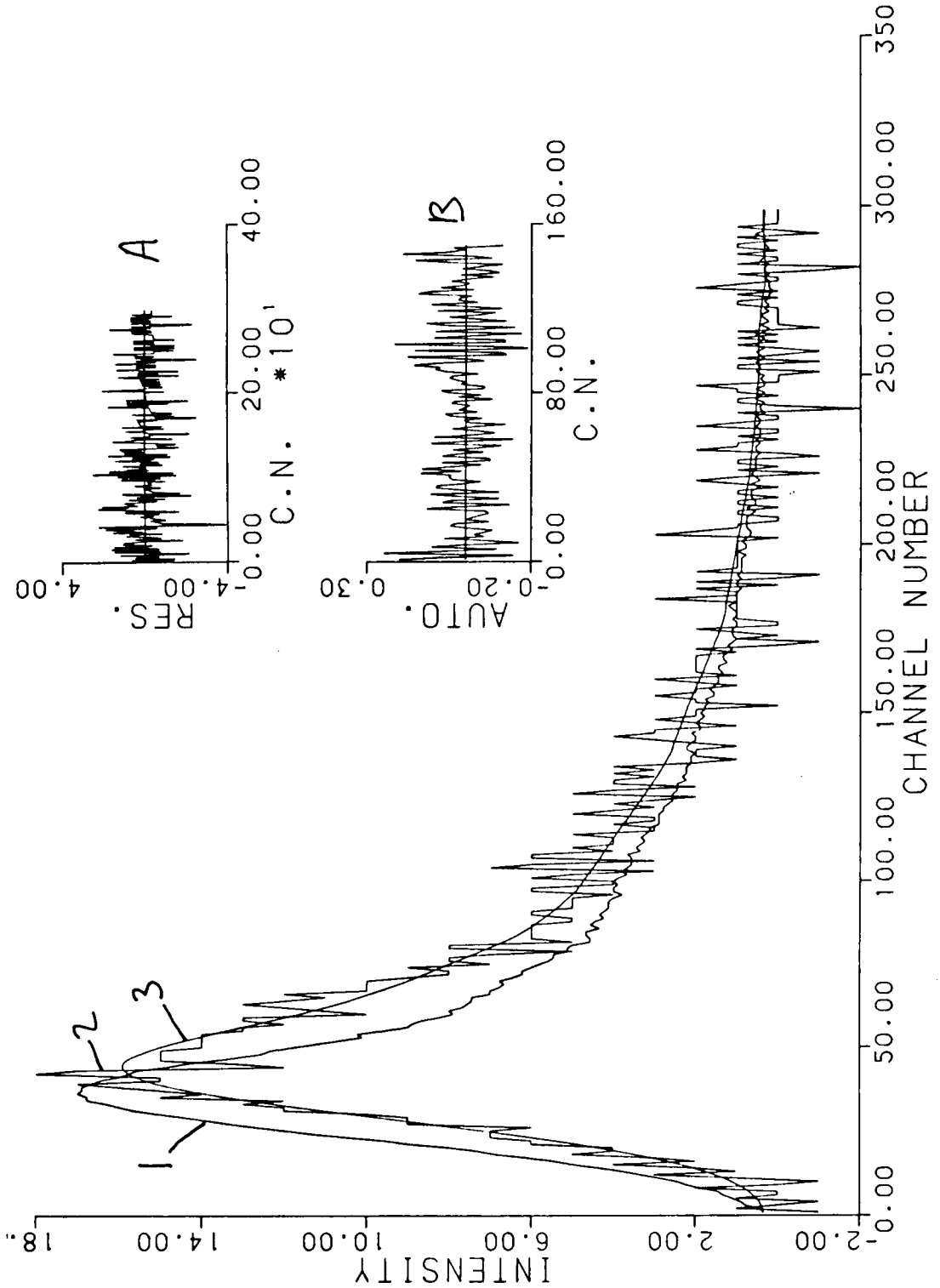
INTENSITY
18.00
14.00
10.00
6.00
2.00
-2.00
0.00
50.00
100.00
150.00
200.00
250.00
300.00
350
CHANNEL NUMBER
1
2
3
A
RES.
4.00
-4.00
0.00
20.00
40.00
C.N.
*10¹
B
AUTO.
0.30
-0.20
0.00
80.00
160.00
C.N.

Fig. III.33.

Fig. III.34. Fluorescence decay profile of melittin in Tris buffer at 61°C (emission wavelength = 360 nm). Curve (1) represents the lamp profile. Curve (2) represents the experimental fluorescence decay profile while curve (3) is the convoluted decay profile.
Insert (A): Plot of the Residuals versus Channel Number.
Insert (B): Plot of the Autocorrelation versus Channel Number.
Channel width = 0.169 ns.

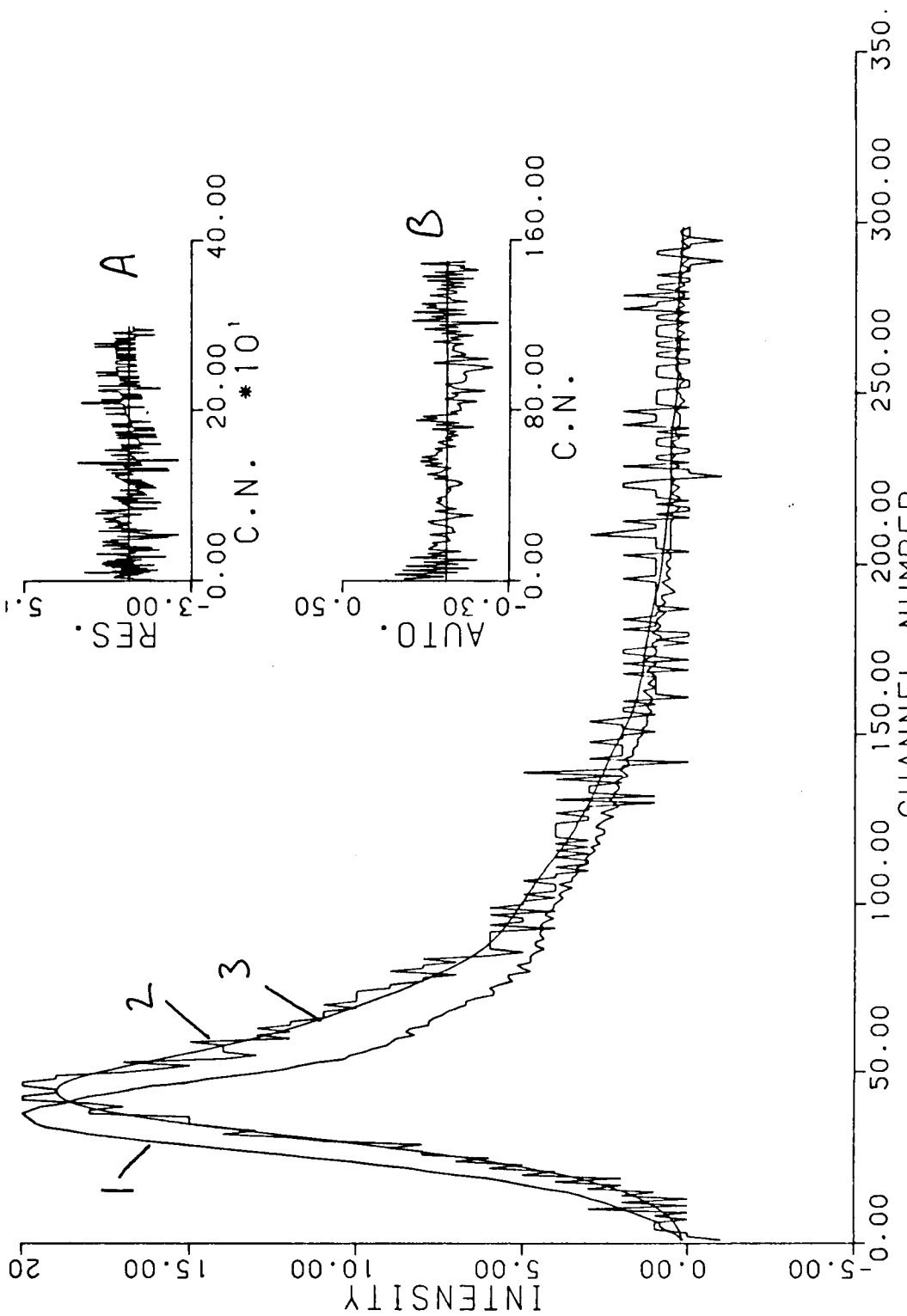
INTENSITY
20
15.00
10.00
5.00
0.00
-5.00
0.00
50.00
100.00
150.00
200.00
250.00
300.00
350.
CHANNEL NUMBER
1
2
3
A
RES.
5.
-3.00
0.00
20.00
40.00
C.N.
*10¹
B
AUTO.
0.50
-0.30
0.00
80.00
160.00
C.N.

Fig. III.34.

Fig. III.35. Fluorescence decay profile of melittin in Tris buffer at 61°C (emission wavelength = 390 nm). Curve (1) represents the lamp profile. Curve (2) represents the experimental fluorescence decay profile while curve (3) is the convoluted decay profile. Insert (A): Plot of the Residuals versus Channel Number. Insert (B): Plot of the Autocorrelation versus Channel Number. Channel width = 0.150 ns.

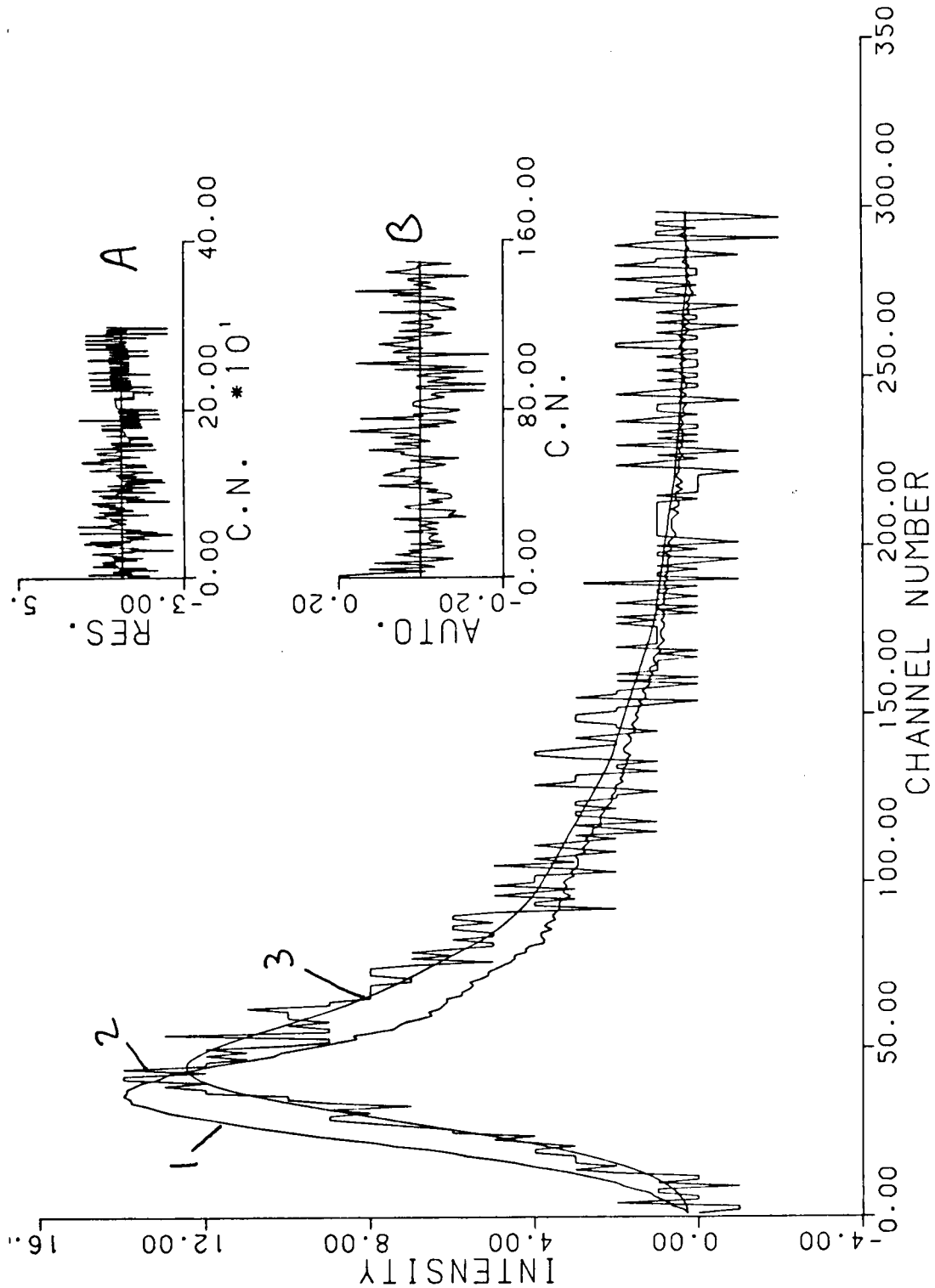
INTENSITY
16.00
12.00
8.00
4.00
0.00
-4.00
0.00
50.00
100.00
150.00
200.00
250.00
300.00
350
CHANNEL NUMBER
1
2
3
A
RES.
5.
-3.00
0.00
20.00
40.00
C.N.
*10¹
B
AUTO.
0.20
-0.20
0.00
80.00
160.00
C.N.

Fig. III.35.

Table III.1

Nanosecond Fluorescence Parameters for Wavelength-Dependence Analysis

Substance	Emission Wavelength (nm) 320 τ_o (ns)	τ_c (ns)	A_o/A_c	340 τ_o (ns)	360 τ_o (ns)	390 τ_o (ns)
Melittin (free)	3.0	-	0.15	-	3.1	3.2
Melittin + 0.15 M K_2HPO_4	2.5	0.6	1.48	2.3	2.6	3.0
Melittin + 0.5 M K_2HPO_4	2.8	0.9	0.58	2.1	2.5	2.8
Melittin + 0.15 M NaCl	2.6	-	0.24	-	3.0	3.1
Melittin + 1.0 M NaCl	2.2	-	0.24	2.4	2.6	3.0
Melittin in Egg Lecithin	-	-	-	2.2	2.4	3.1
Melittin in D.S.L.	-	-	-	3.2	3.4	3.6
Melittin in D.S.L. (61°C)	-	-	-	2.1	2.3	2.6
Melittin (free) (61°C)	1.4	-	0.09	-	1.4	1.4

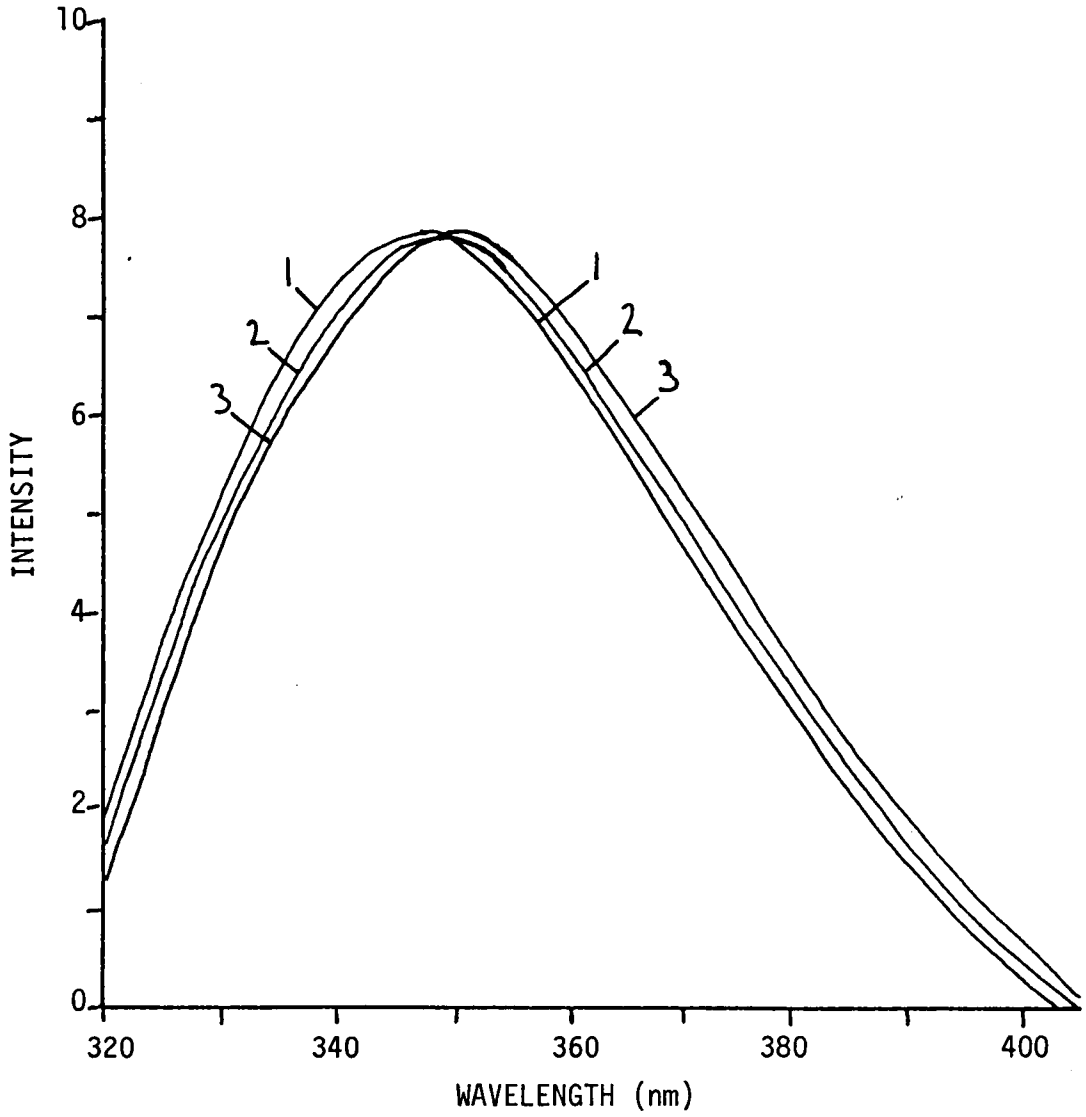

Fig. III.36. Time-resolved spectra of melittin in Tris buffer. Time values are relative to the peak of the lamp. (1) = -2 ns; (2) = 0 ns; (3) = 12 ns.

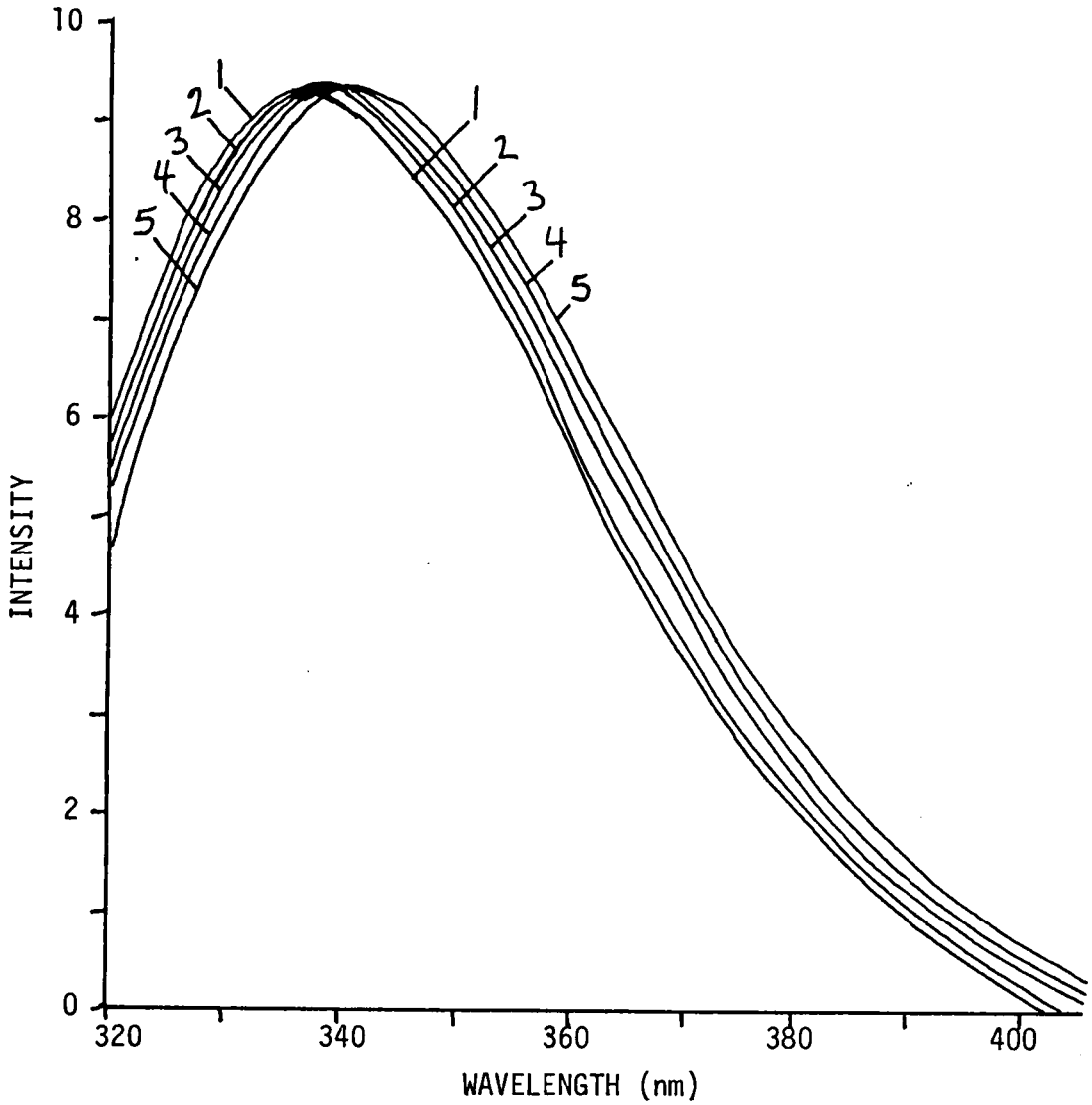

Fig. III.37. Time-resolved spectra of melittin + 0.15 M K_2HPO_4. Time values are relative to the peak of the lamp. (1) = -2.4 ns; (2) = -1.0 ns; (3) = +1 ns; (4) = +3 ns; (5) = +10 ns.

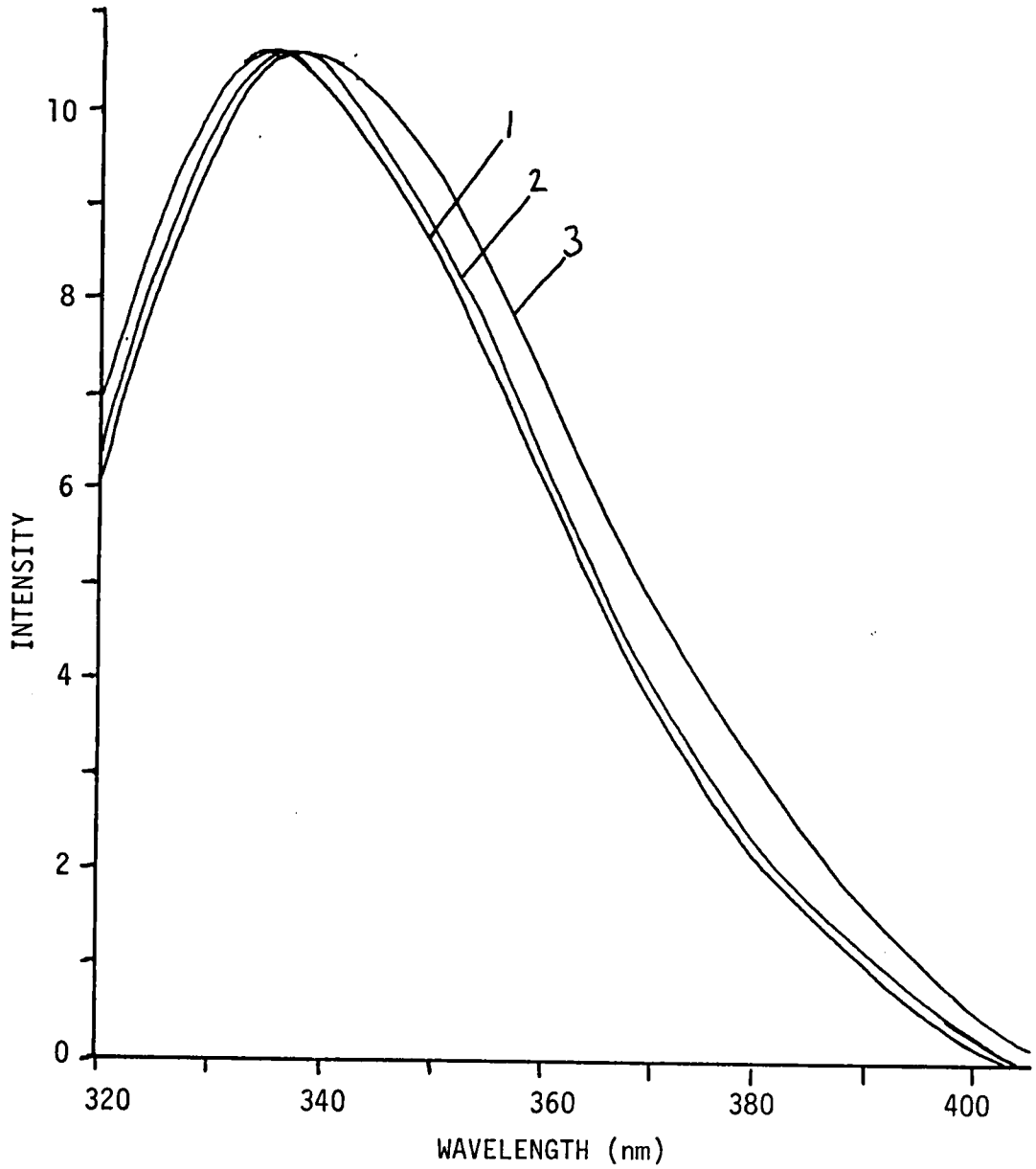

Fig. III.38. Time-resolved spectra of melittin + 0.5 M K_2HPO_4. Time values are relative to the peak of the lamp. (1) = -2 ns; (2) = +1 ns; (3) = +12 ns.

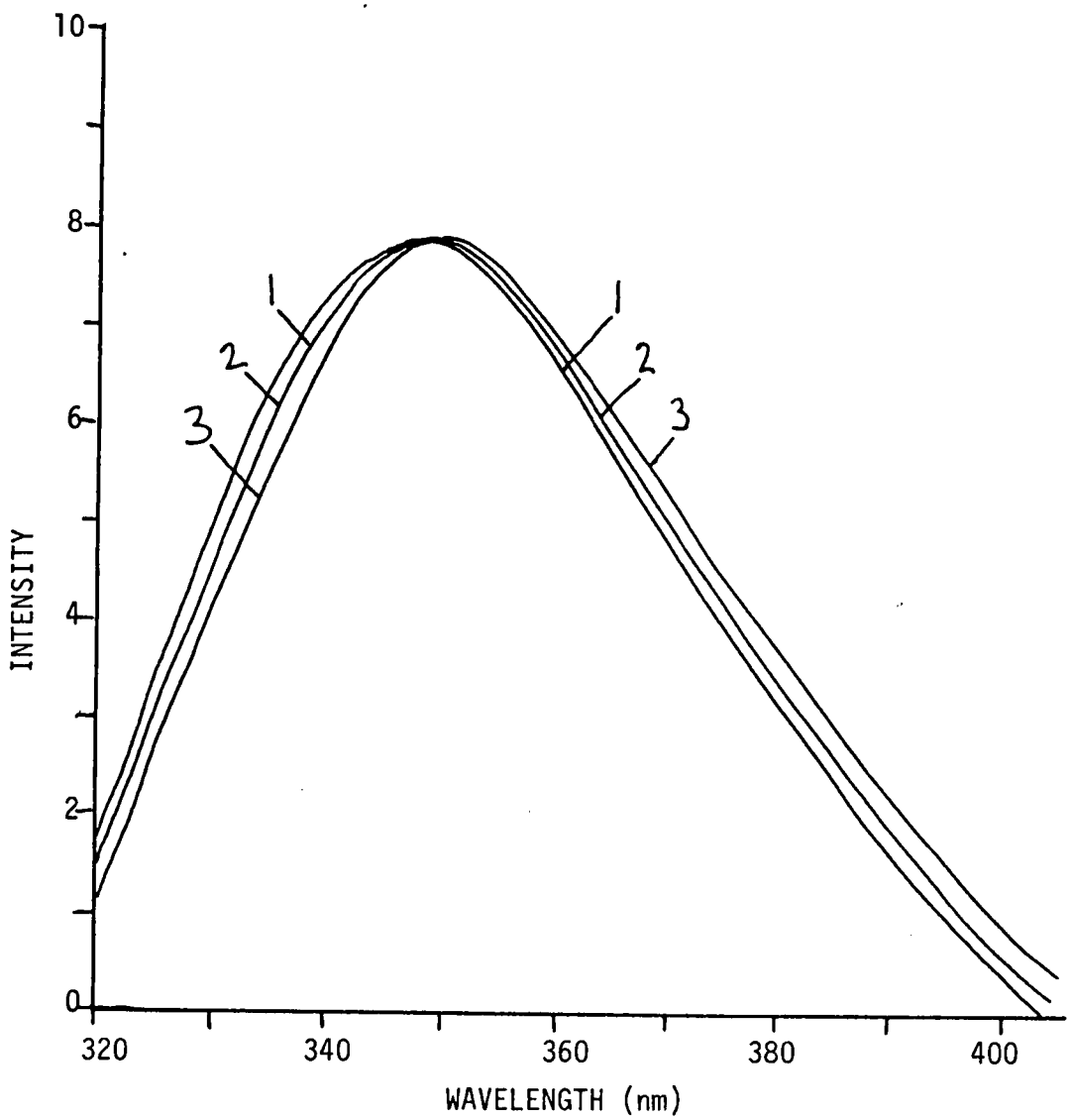

Fig. III.39. Time-resolved spectra of melittin + 0.15 M NaCl. Time values are relative to the peak of the lamp. (1) = -2 ns; (2) = 0 ns; (3) = 15 ns.

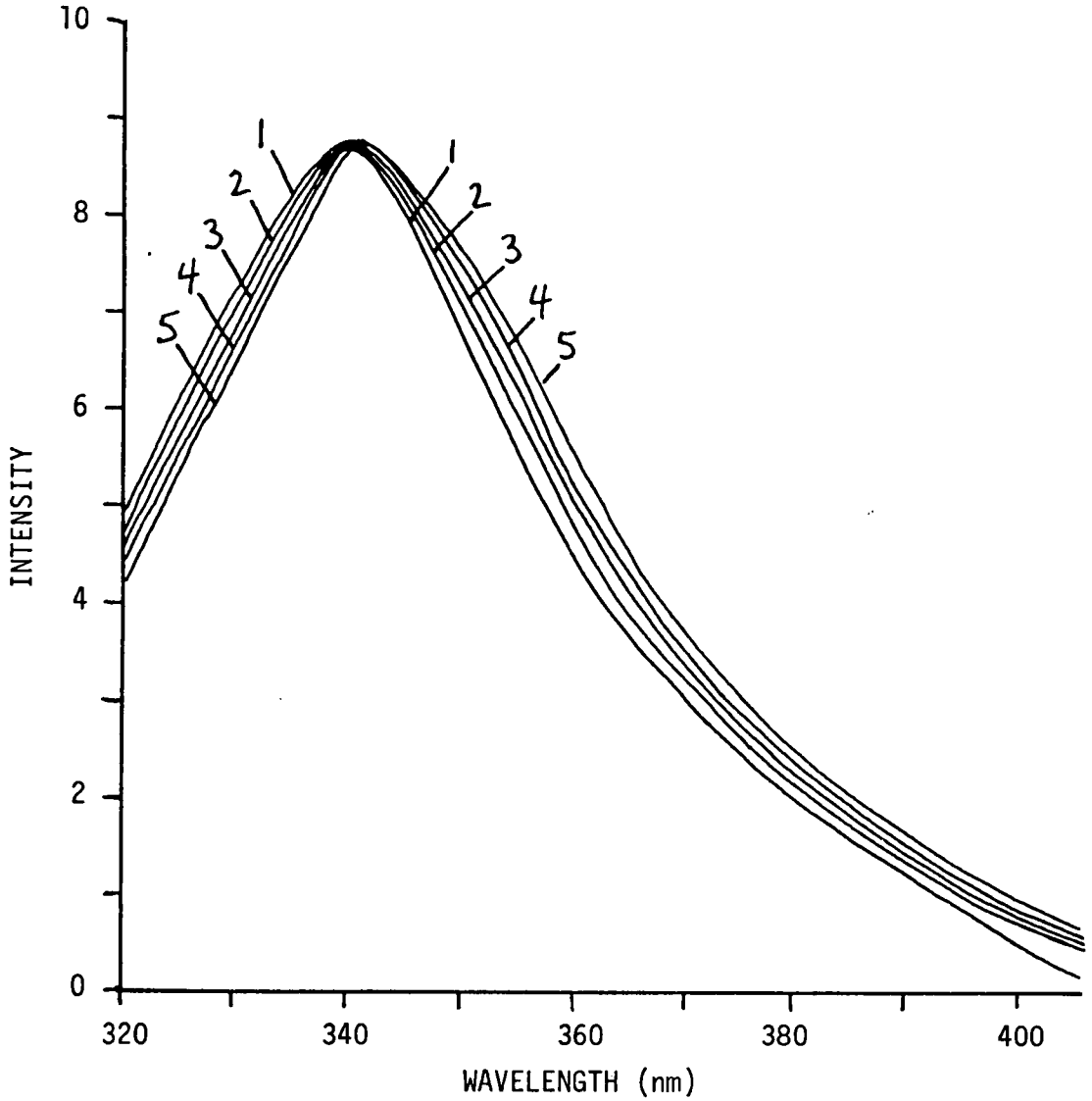

Fig. III.40. Time-resolved spectra of melittin + 1.0 M NaCl. Time values are relative to the peak of the lamp. (1) = -2 ns; (2) = -1 ns; (3) = +1 ns; (4) = +3 ns; (5) = +10 ns.

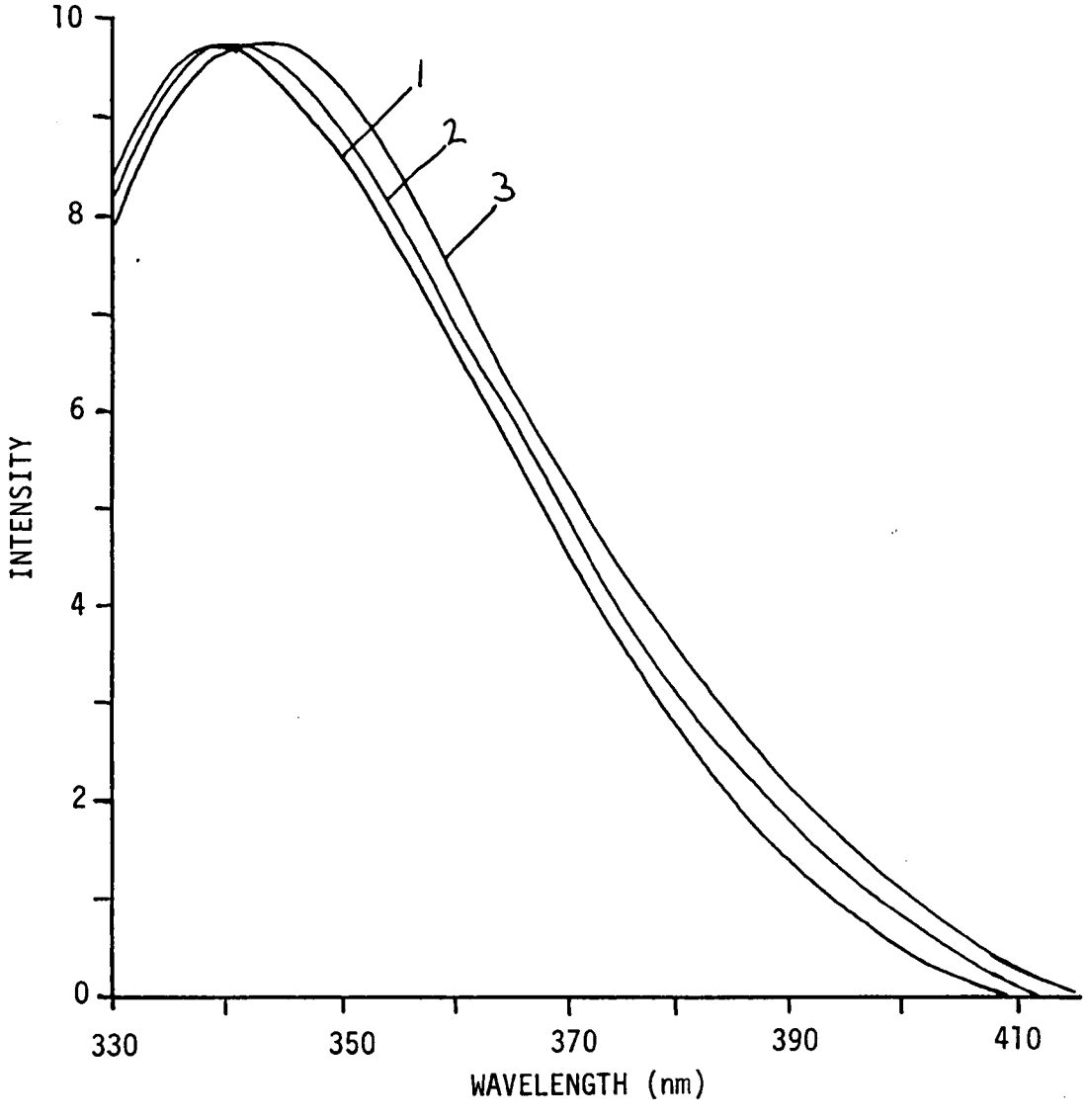

Fig. III.41. Time-resolved spectra of melittin in egg lecithin. Time values are relative to the peak of the lamp. (1) = -2.2 ns; (2) = -1 ns; (3) = +3 ns.

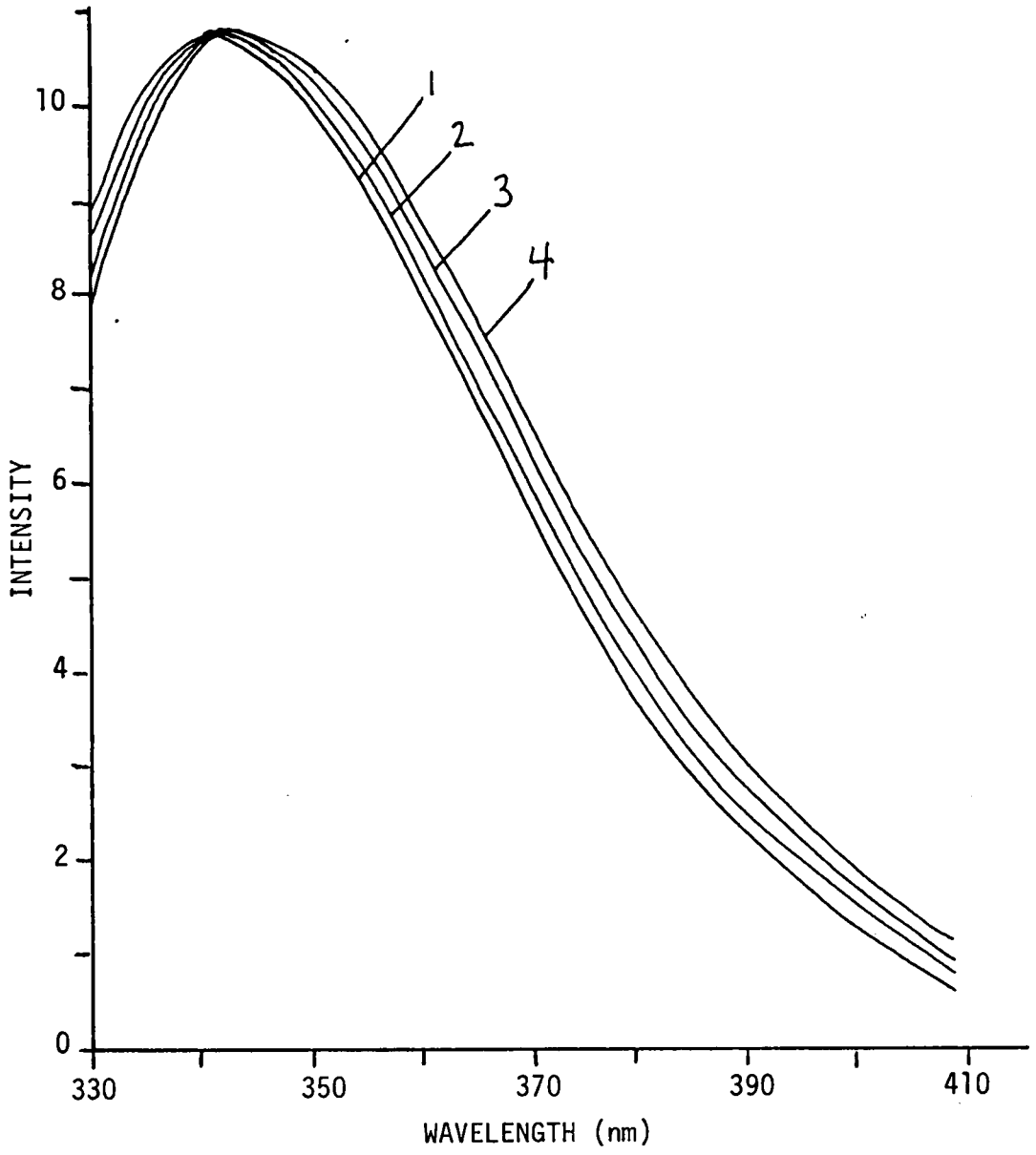

Fig. III. 42. Time-resolved spectra of melittin in distearoyllecithin. Time values are relative to the peak of the lamp. (1) = -2 ns; (2) = 0 ns; (3) = 3 ns; (4) = 12 ns.

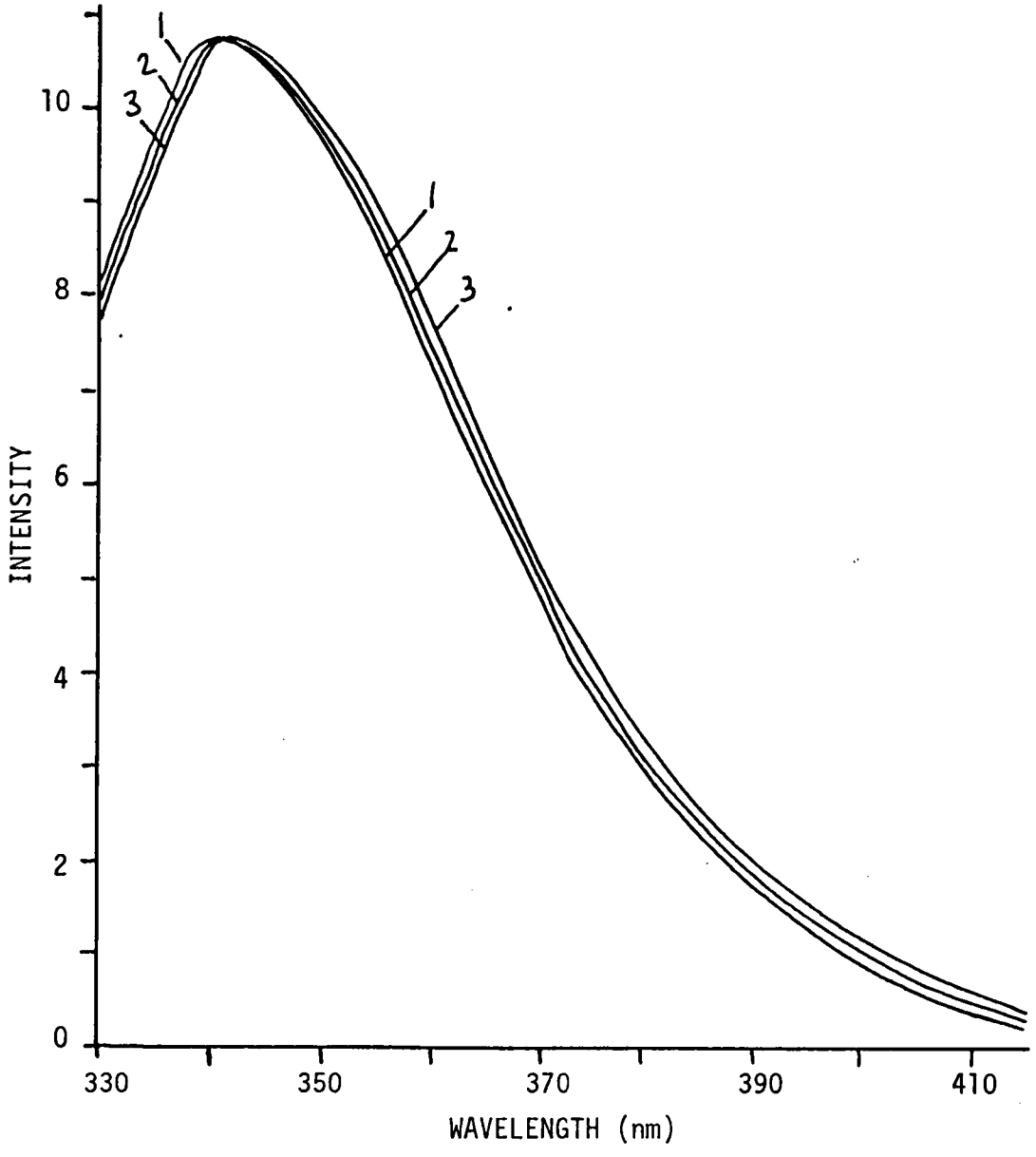

Fig. III.43. Time-resolved spectra of melittin in distearoyllecithin at 61°C. Time values are relative to the peak of the lamp. (1) = -2 ns; (2) = -1 ns; (3) = +12 ns.

egg lecithin, the fluorescence spectral maximum blue-shifted to approximately 340 nm with a red shift of 3 nm occurring between -2.2 and 3 ns. Time resolved studies also showed a major blue-shift (to 342 nm) of the spectral maximum in the case of melittin in the presence of 1.0 M NaCl. A red-shift of 4 nm occurred between -2 and 10 ns when melittin was introduced to a 1.0 M NaCl environment. A very minor shift (1 nm) to the blue was observed when melittin was in the presence of 0.15 M NaCl. Time-resolved studies done on melittin bound to distearoyllecithin at room temperature indicated a shift of the peak of the fluorescence spectrum to 343 nm with a red shift of 3 nm taking place between -2 and 12 ns. When distearoyllecithin was raised to 61°C (above its phase transition temperature of 51°C), the maximum of the spectrum blue-shifted to 345 nm exhibiting very minimal red-shifts with respect to time (Fig. III.43). Melittin in 0.01 M Tris buffer was also studied at 61°C (data not shown) and the time-resolved spectrum was identical to melittin in Tris buffer at room temperature.

Nanosecond depolarization studies were undertaken in order to investigate the internal mobility of melittin in different environments. From depolarization studies, one can determine r(t) (emission anisotropy) and ϕ (rotational correlation time). The deconvoluted data can be found in Figs. III.44 through III.51. The actual emission anisotropy data can be seen in Figs. III.52 through III.59. Also, a summary of the depolarization parameters can be found in Table III.2.

Acrylamide quenching studies provided information on the nature of binding between melittin and model membranes. By doing a Stern-Volmer

Fig. III.44. Depolarization data ($I_V(t)$-$I_H(t)$) of melittin in Tris buffer. Curve (1) represents the lamp profile. Curve (2) represents the experimental fluorescence ($I_V(t)$-$I_H(t)$) decay profile while curve (3) is the convoluted decay profile. Insert (A): Plot of the Residuals versus Channel Number. Insert (B): Plot of the Autocorrelation versus Channel Number. Channel width = 0.138 ns.

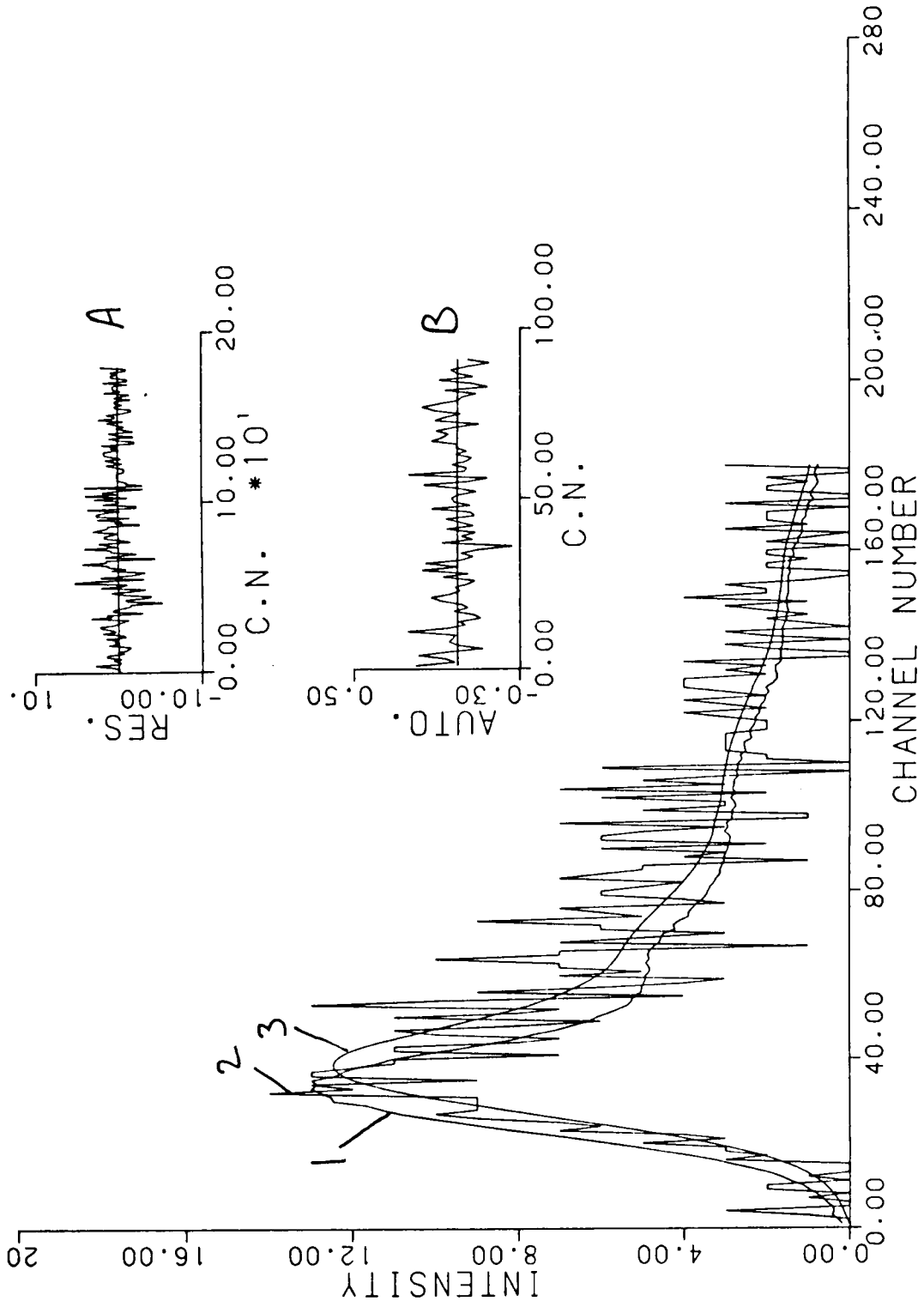
INTENSITY
0.00
4.00
8.00
12.00
16.00
20
CHANNEL NUMBER
0.00
40.00
80.00
120.00
160.00
200.00
240.00
280
1
2
3
A
RES.
10.
-10.00
0.00
10.00
20.00
C.N.
*10¹
B
AUTO.
0.50
-0.30
0.00
50.00
100.00
C.N.

Fig. III.44.

Fig. III.45. Depolarization data ($I_V(t)$-$I_H(t)$) of melittin + 0.15 M K_2HPO_4. Curve (1) represents the lamp profile. Curve (2) represents the experimental fluorescence ($I_V(t)$-$I_H(t)$) decay profile while curve (3) is the convoluted decay profile. Insert (A): Plot of the Residuals versus Channel Number. Insert (B): Plot of the Autocorrelation versus Channel Number. Channel width = 0.171 ns.

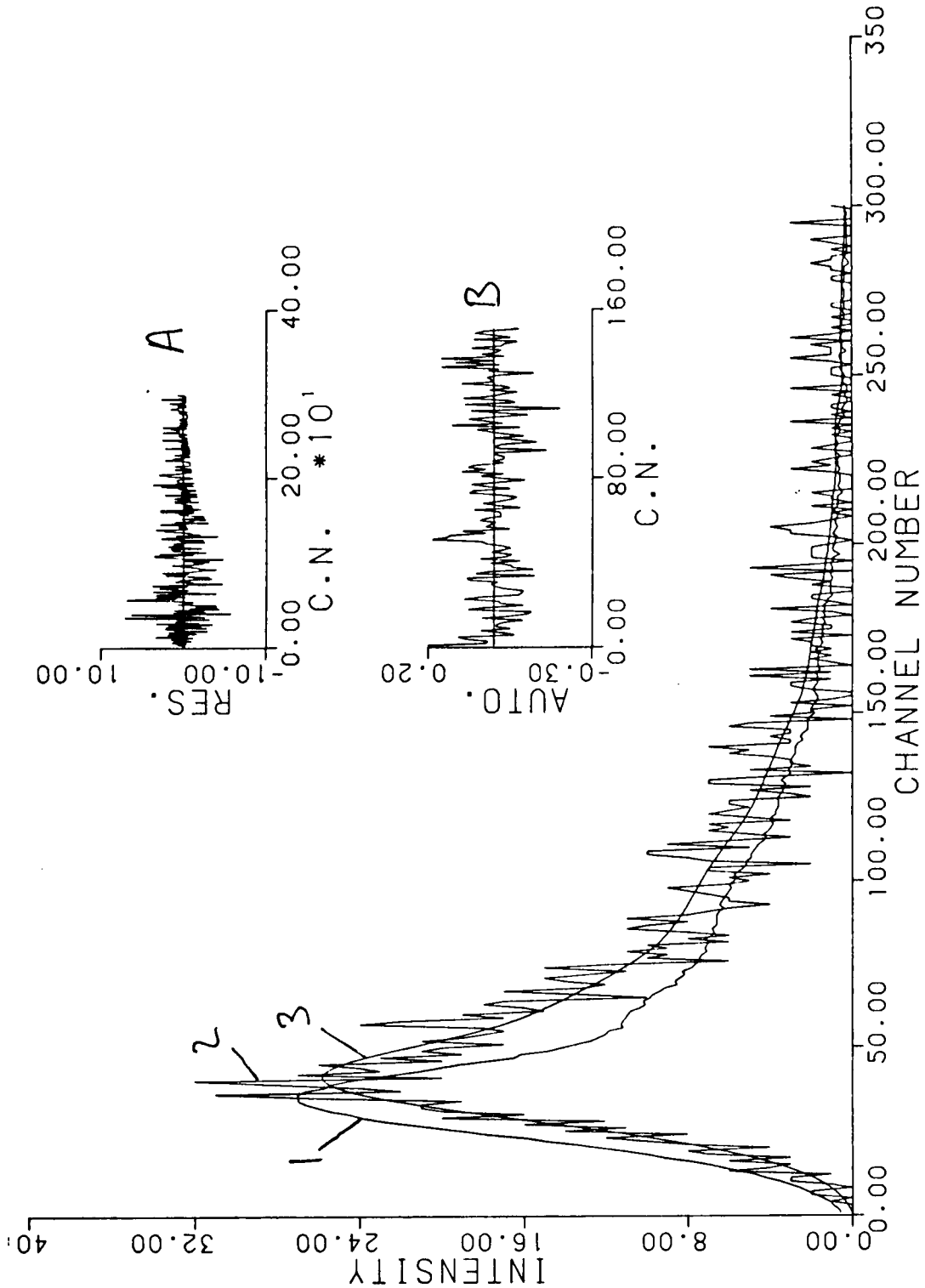
INTENSITY
0.00
8.00
16.00
24.00
32.00
40
0.00
50.00
100.00
150.00
200.00
250.00
300.00
350
CHANNEL NUMBER
1
2
3
A
RES.
-10.00
10.00
0.00
20.00
40.00
C.N.
*10¹
B
AUTO.
-0.30
0.20
0.00
80.00
160.00
C.N.

Fig. III.45.

Fig. III.46. Depolarization data ($I_V(t)$-$I_H(t)$) of melittin + 0.5 M K_2HPO_4. Curve (1) represents the lamp profile. Curve (2) represents the experimental fluorescence ($I_V(t)$-$I_H(t)$) decay profile while curve (3) is the convoluted decay profile. Insert (A): Plot of the Residuals versus Channel Number. Insert (B): Plot of the Autocorrelation versus Channel Number. Channel width = 0.168 ns.

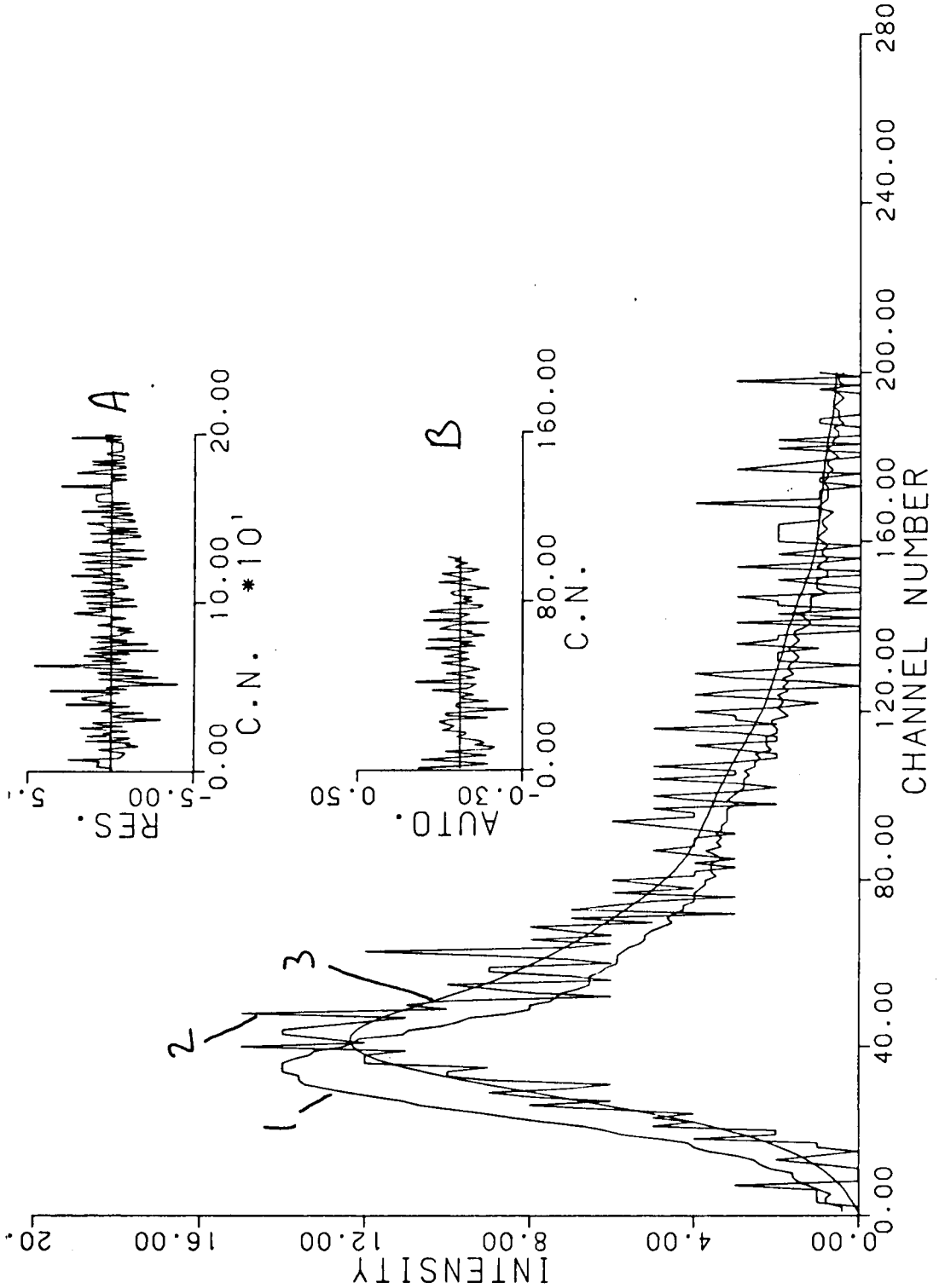
INTENSITY
0.00
4.00
8.00
12.00
16.00
20.
0.00
40.00
80.00
120.00
160.00
200.00
240.00
280
CHANNEL NUMBER
1
2
3
A
RES.
-5.00
5.
0.00
10.00
20.00
C.N.
*10'
B
AUTO.
-0.30
0.50
0.00
80.00
160.00
C.N.

Fig. III.46.

Fig. III.47. Depolarization data ($I_V(t)$-IH(t)) of melittin + 0.15 M NaCl. Curve (1) represents the lamp profile. Curve (2) represents the experimental fluorescence ($I_V(t)$-$I_H(t)$) decay profile while curve (3) is the convoluted decay profile. Insert (A): Plot of the Residuals versus Channel Number. Insert (B): Plot of the Autocorrelation versus Channel Number. Channel width = 0.193 ns.

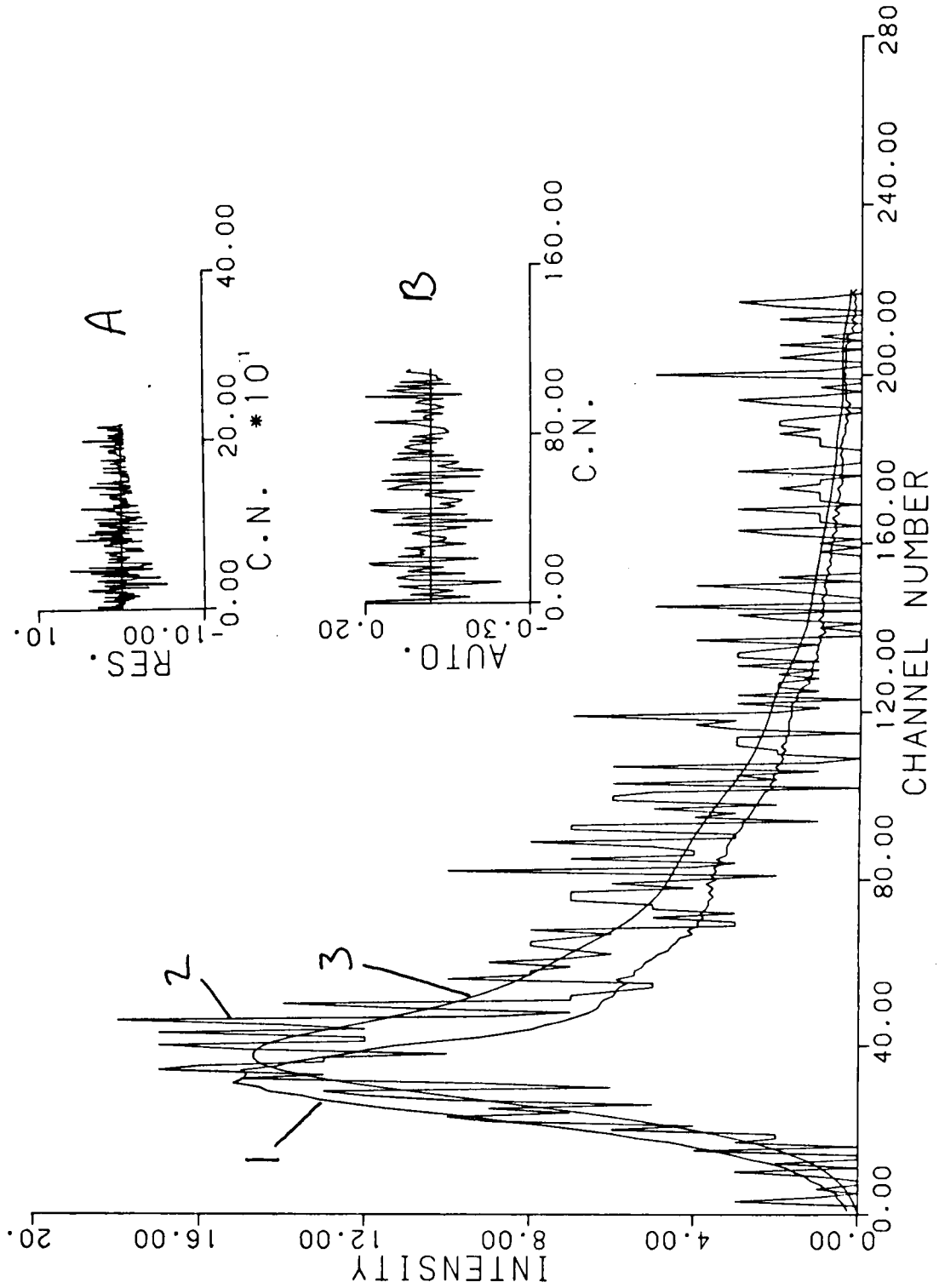
INTENSITY
0.00
4.00
8.00
12.00
16.00
20.
CHANNEL NUMBER
0.00
40.00
80.00
120.00
160.00
200.00
240.00
280
1
2
3
A
RES.
10.00
10.
0.00
20.00
40.00
C.N. *10⁻¹
B
AUTO.
-0.30
0.20
0.00
80.00
160.00
C.N.

Fig. III.47.

Fig. III.48. Depolarization data ($I_V(t)-I_H(t)$) of melittin + 1.0 M NaCl. Curve (1) represents the lamp profile. Curve (2) represents the experimental fluorescence ($I_V(t)-I_H(t)$) decay profile while curve (3) is the convoluted decay profile. Insert (A): Plot of the Residuals versus Channel Number. Insert (B): Plot of the Autocorrelation versus Channel Number. Channel width = 0.167 ns.

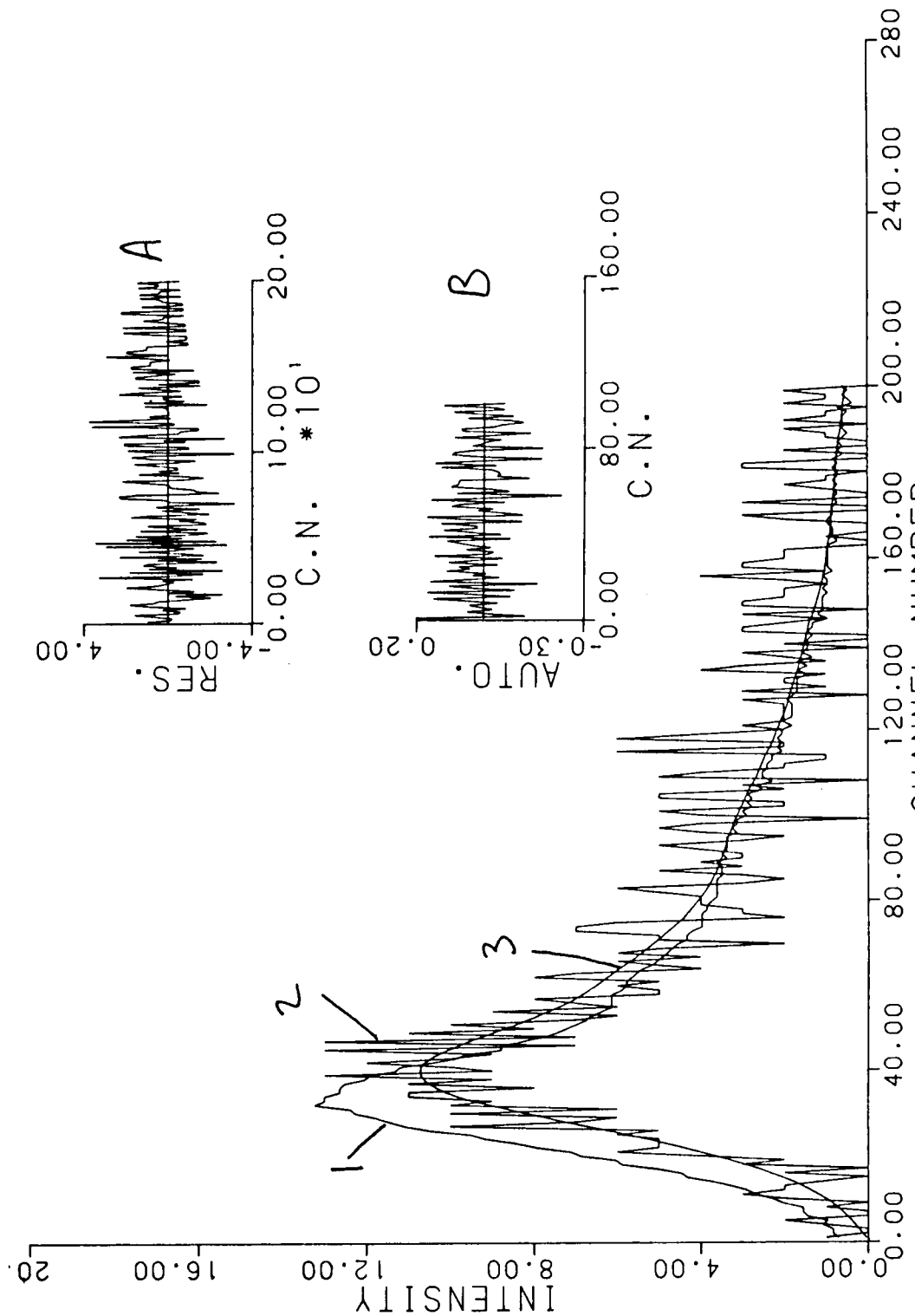
INTENSITY
0.00
4.00
8.00
12.00
16.00
20
0.00
40.00
80.00
120.00
160.00
200.00
240.00
280
CHANNEL NUMBER
1
2
3
A
RES.
4.00
-4.00
0.00
10.00
20.00
C.N. *10¹
B
AUTO.
0.20
-0.30
0.00
80.00
160.00
C.N.

Fig. III.48.

Fig. III.49. Depolarization data ($I_V(t)-I_H(t)$) of melittin in egg lecithin. Curve (1) represents the lamp profile. Curve (2) represents the experimental fluorescence $I_V(t)-I_H(t)$ decay profile while curve (3) is the convoluted decay profile. Insert (A): Plot of the Residuals versus Channel Number. Insert (B): Plot of the Autocorrelation versus Channel Number. Channel width = 0.190 ns.

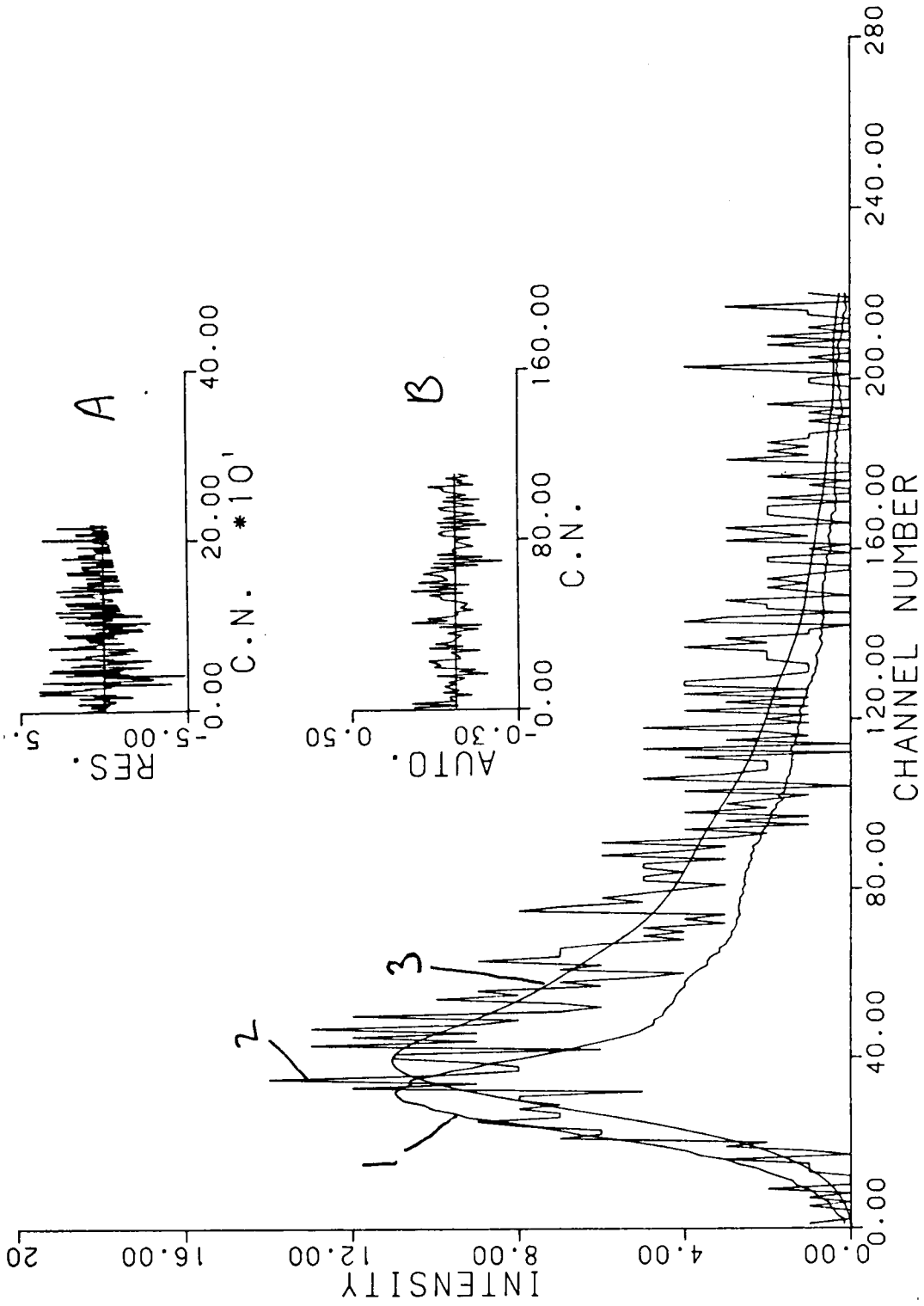
INTENSITY
0.00
4.00
8.00
12.00
16.00
20
0.00
40.00
80.00
120.00
160.00
200.00
240.00
280
CHANNEL NUMBER
1
2
3
A
RES.
5.00
-5.00
0.00
20.00
40.00
C.N.
*10'
B
AUTO.
0.50
-0.30
0.00
80.00
160.00
C.N.

Fig. III.49.

Fig. III.50. Depolarization data ($I_V(t)$-$I_H(t)$) of melittin in distearoyllecithin. Curve (1) represents the lamp profile. Curve (2) represents the experimental fluorescence ($I_V(t)$-$I_H(t)$) decay profile while curve (3) is the convoluted decay profile. Insert (A): Plot of the Residuals versus Channel Number. Insert (B): Plot of the Autocorrelation versus Channel Number. Channel width = 0.159 ns.

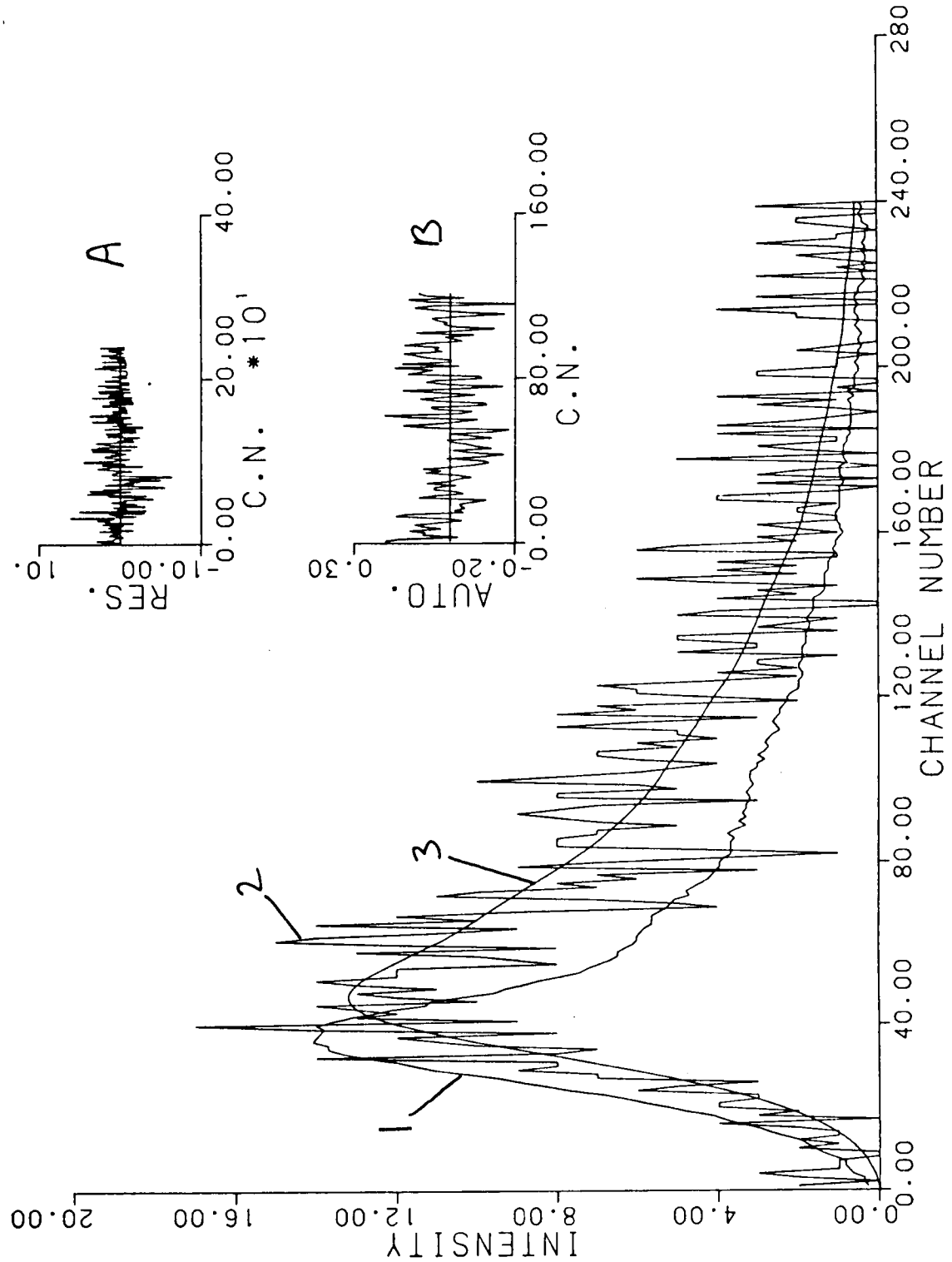
A
B
RES.
AUTO.
C.N. *10¹
C.N.
INTENSITY
CHANNEL NUMBER
1
2
3
0.00
4.00
8.00
12.00
16.00
20.00
40.00
80.00
120.00
160.00
200.00
240.00
280
-10.00
10.
-0.00
20.00
40.00
-0.20
0.30
-0.00
80.00
160.00

Fig. III.50.

Fig. III.51. Depolarization data ($I_V(t)$-$I_H(t)$) of melittin in distearoyllecithin at 61°C. Curve (1) represents the lamp profile. Curve (2) represents the experimental fluorescence ($I_V(t)$-$I_H(t)$) decay profile while curve (3) is the convoluted decay profile. Insert (A): Plot of the Residuals versus Channel Number. Insert (B): Plot of the Autocorrelation versus Channel Number. Channel width = 0.186 ns.

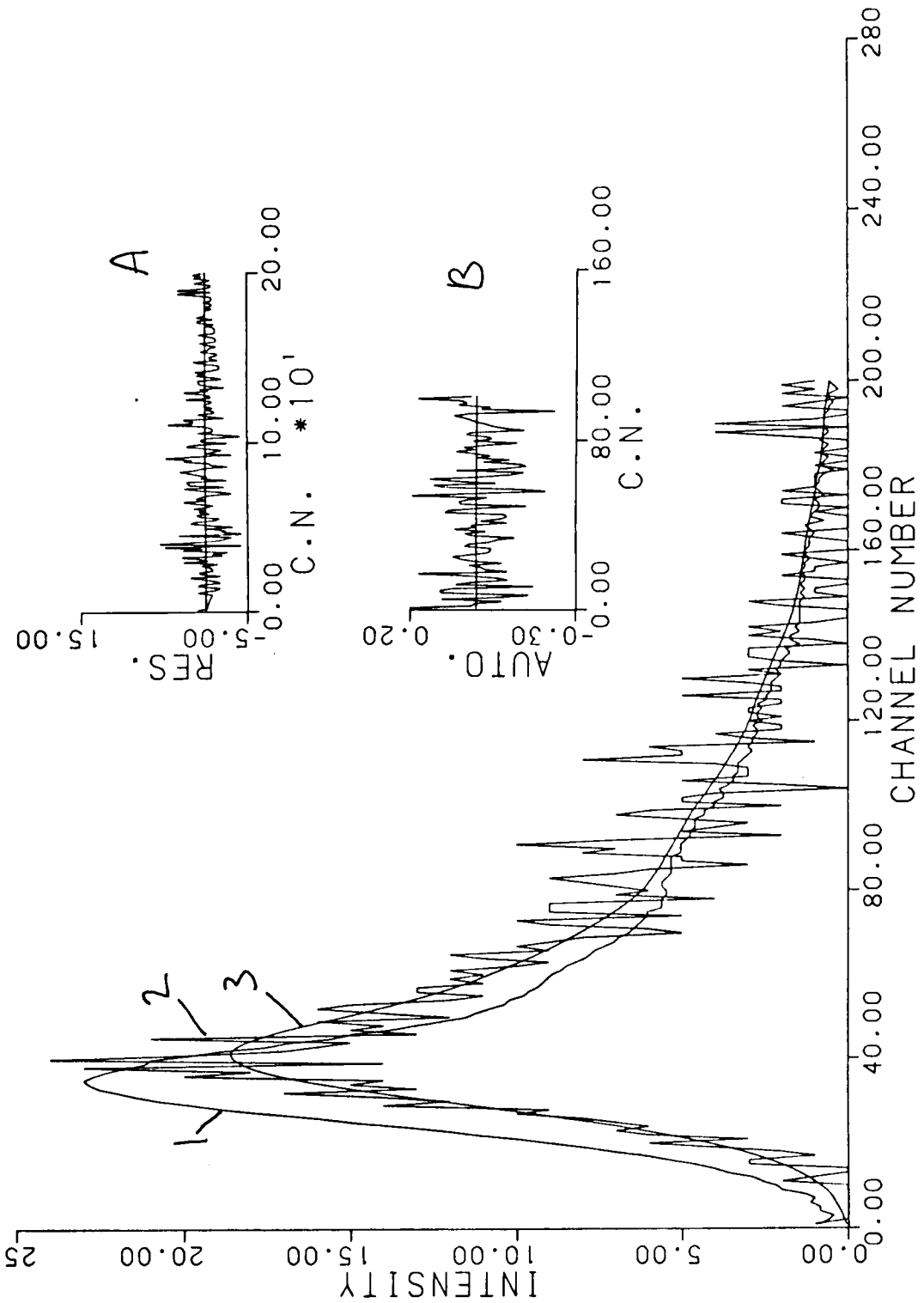
INTENSITY
0.00
5.00
10.00
15.00
20.00
25
CHANNEL NUMBER
0.00
40.00
80.00
120.00
160.00
200.00
240.00
280
1
2
3
A
RES.
-5.00
15.00
0.00
10.00
20.00
C.N.
*10¹
B
AUTO.
-0.30
0.20
0.00
80.00
160.00
C.N.

Fig. III.51.

Fig. III.52. Actual emission anisotropy (r(t)) plotted against channel number for melittin in Tris buffer (see text for more detail). Channel width = 0.138 ns.

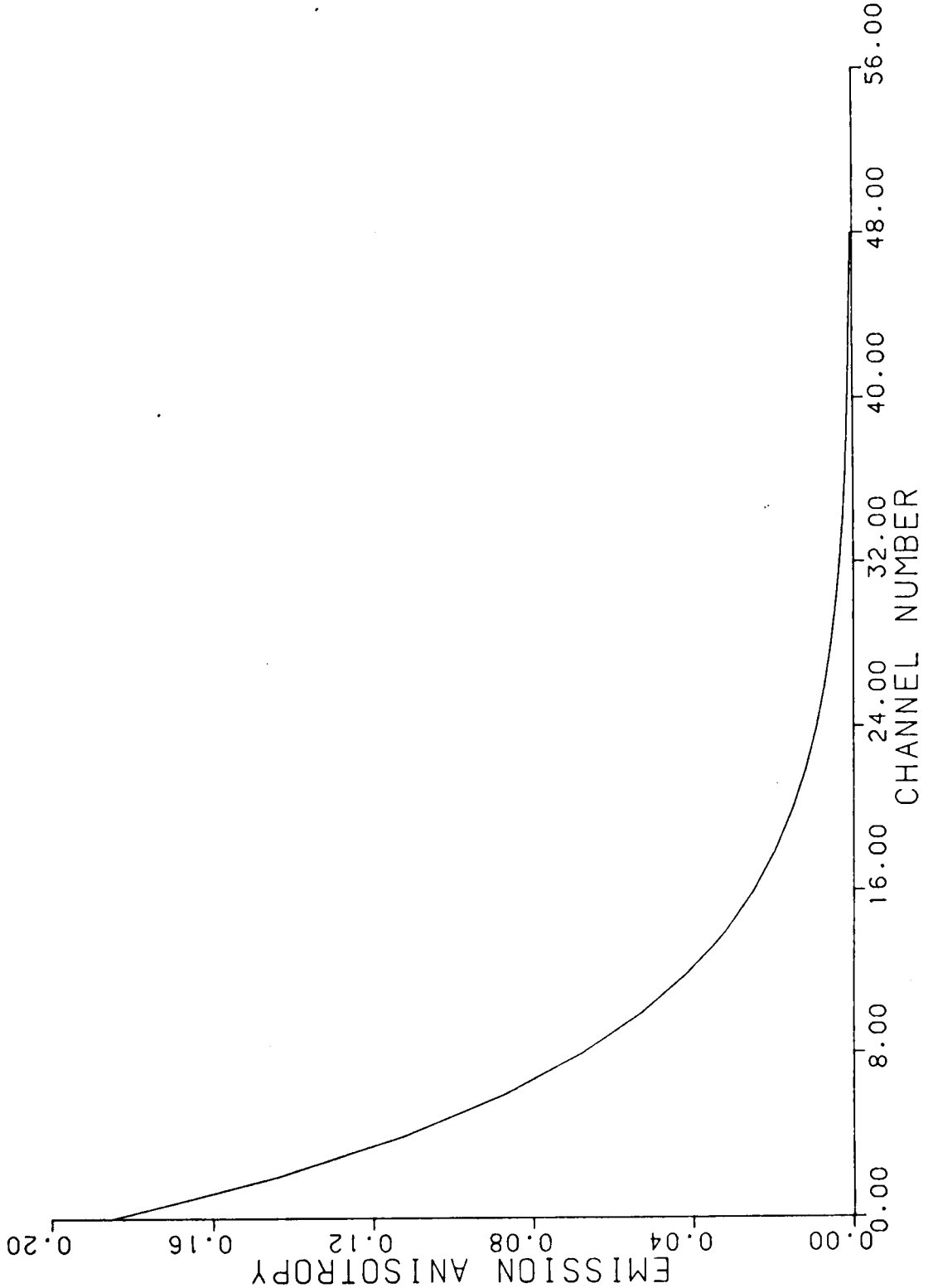
EMISSION ANISOTROPY
0.00
0.04
0.08
0.12
0.16
0.20
0.00
8.00
16.00
24.00
32.00
40.00
48.00
56.00
CHANNEL NUMBER

Fig. III.52.

Fig. III.53. Actual emission anisotropy (r(t)) plotted against channel number for melittin + 0.15 M K_2HPO_4 (see text for more detail). Channel width = 0.171 ns.

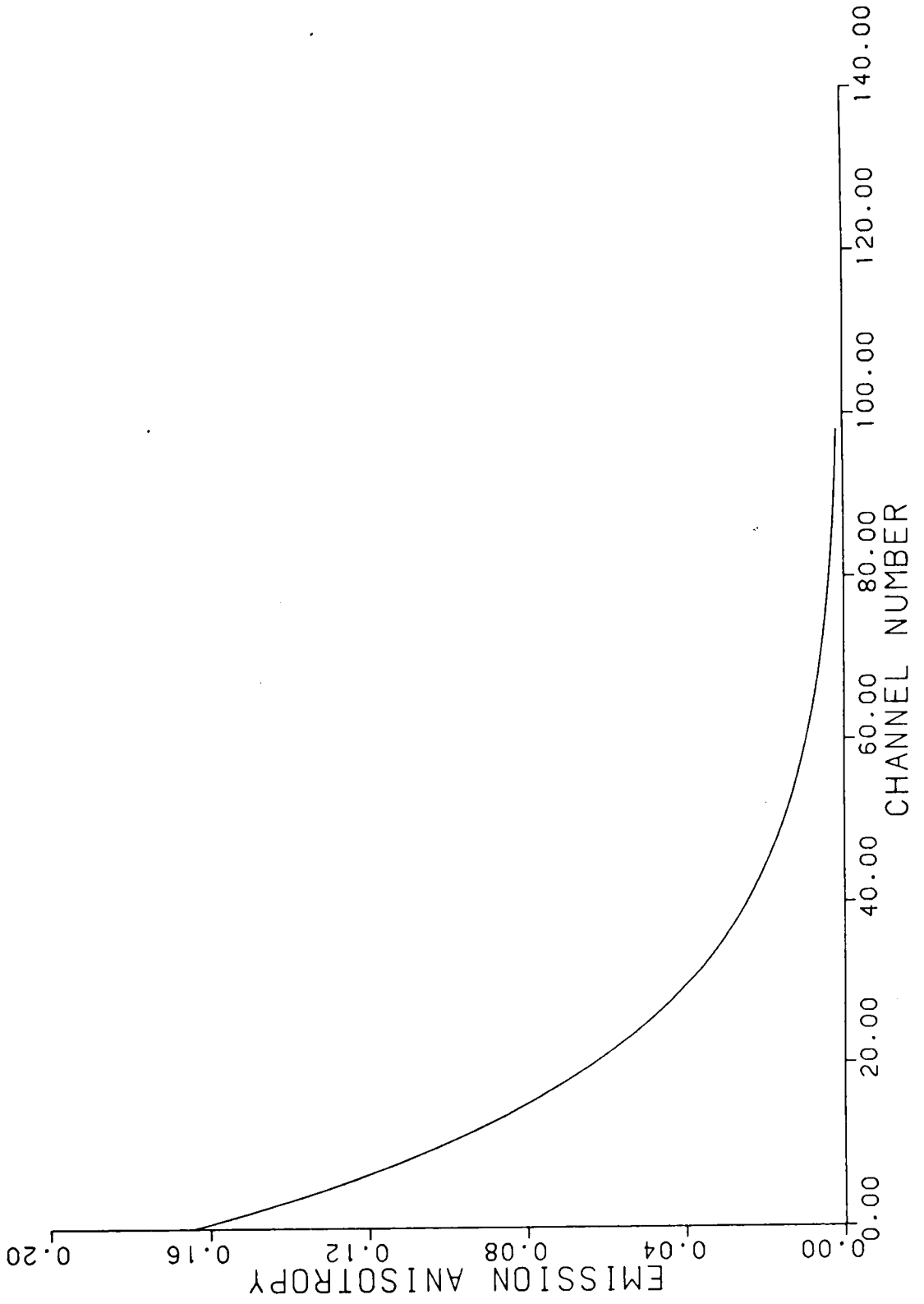
EMISSION ANISOTROPY
0.00
0.04
0.08
0.12
0.16
0.20
0.00
20.00
40.00
60.00
80.00
100.00
120.00
140.00
CHANNEL NUMBER

Fig. III.53.

Fig. III.54. Actual emission anisotropy (r(t)) plotted against channel number for melittin + 0.5 M K_2HPO_4 (see text for more detail). Channel width = 0.168 ns.

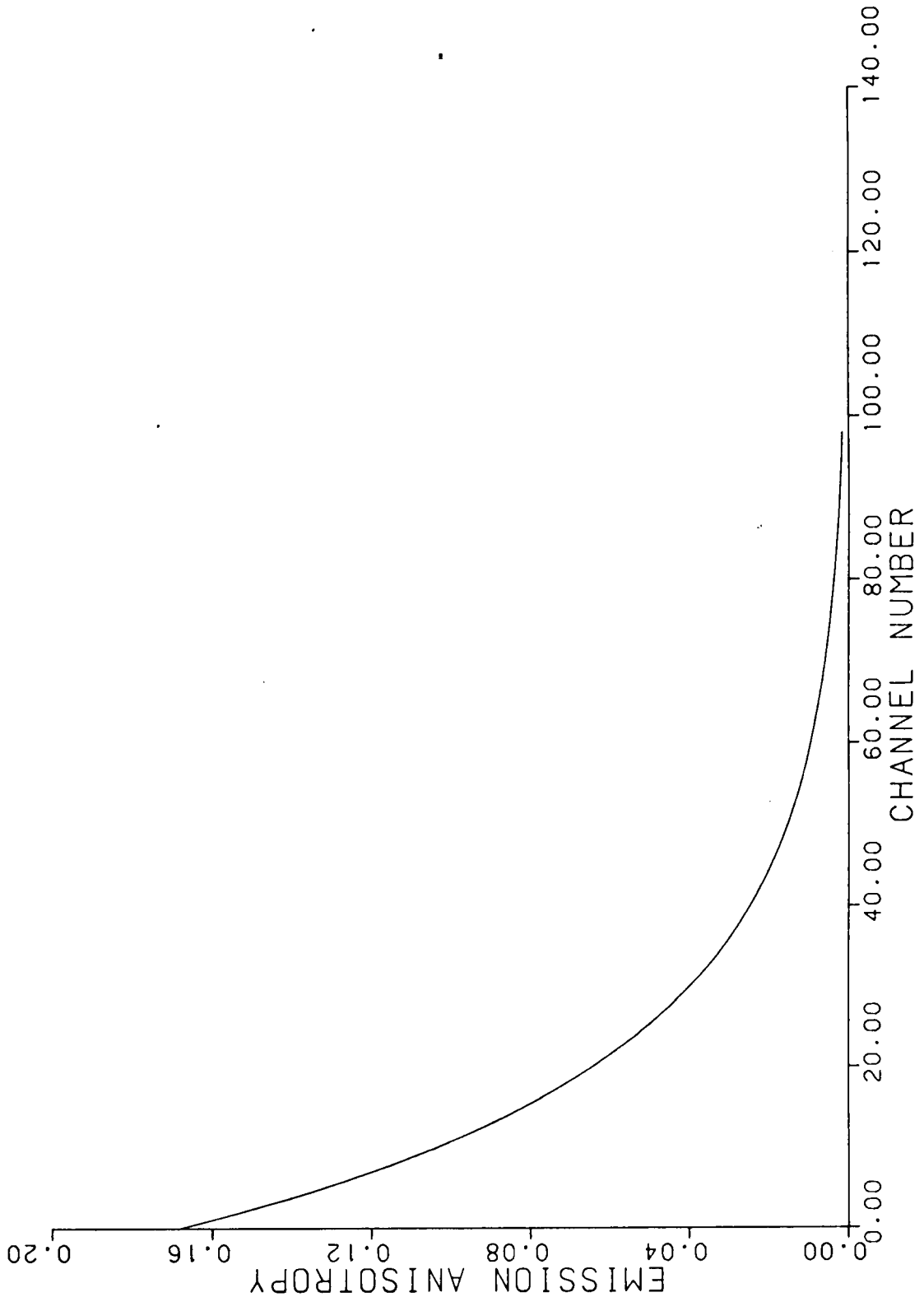
EMISSION ANISOTROPY
0.00
0.04
0.08
0.12
0.16
0.20
0.00
20.00
40.00
60.00
80.00
100.00
120.00
140.00
CHANNEL NUMBER

Fig. III.54.

Fig. III.55. Actual emission anisotropy (r(t)) plotted against channel number for melittin + 0.15 M NaCl (see text for more detail). Channel width = 0.193 ns.

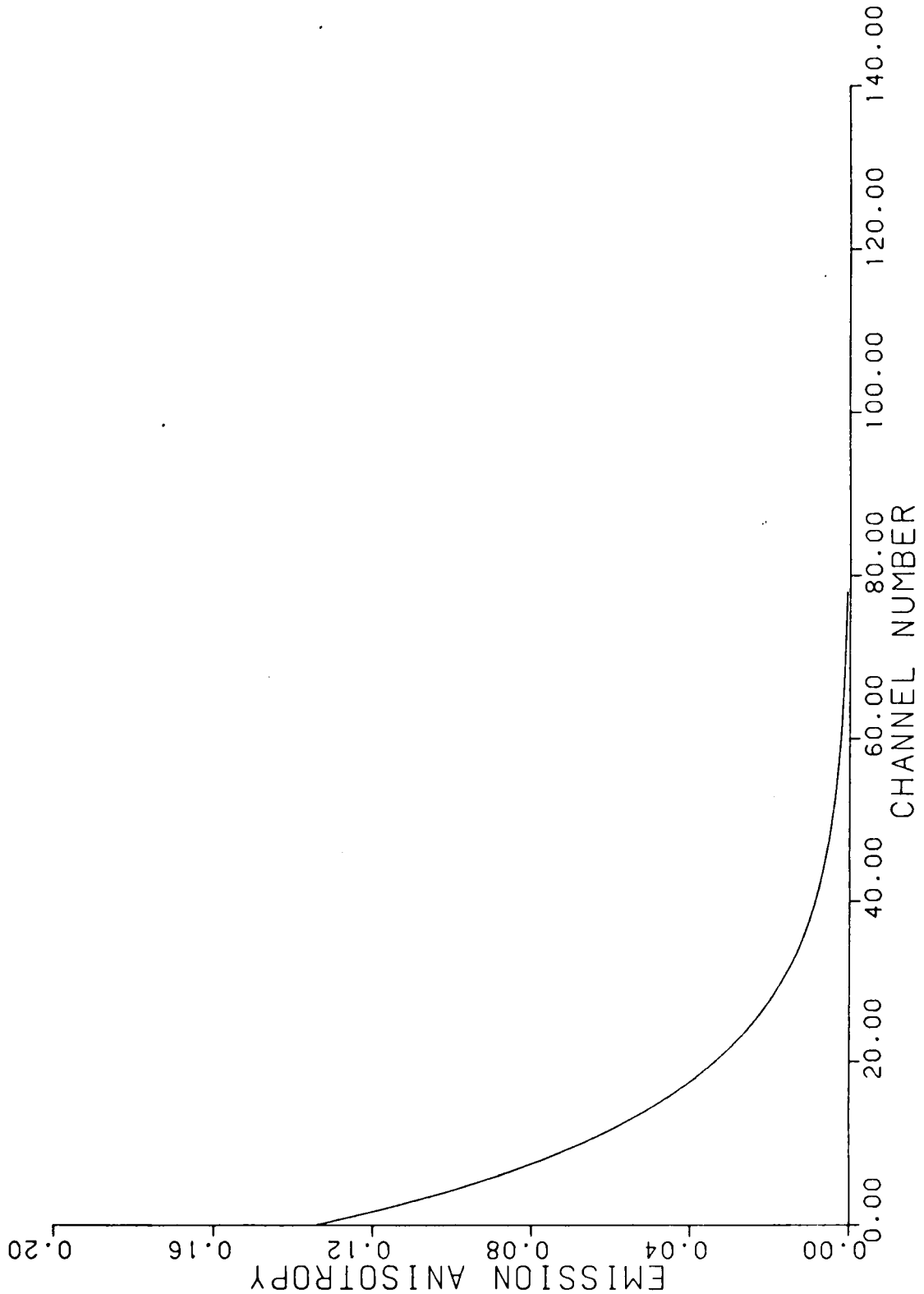
EMISSION ANISOTROPY
0.00
0.04
0.08
0.12
0.16
0.20
0.00
20.00
40.00
60.00
80.00
100.00
120.00
140.00
CHANNEL NUMBER

Fig. III.55.

Fig. III.56. Actual emission anisotropy (r(t)) plotted against channel number for melittin + 1.0 M NaCl (see text for more detail). Channel width = 0.167 ns.

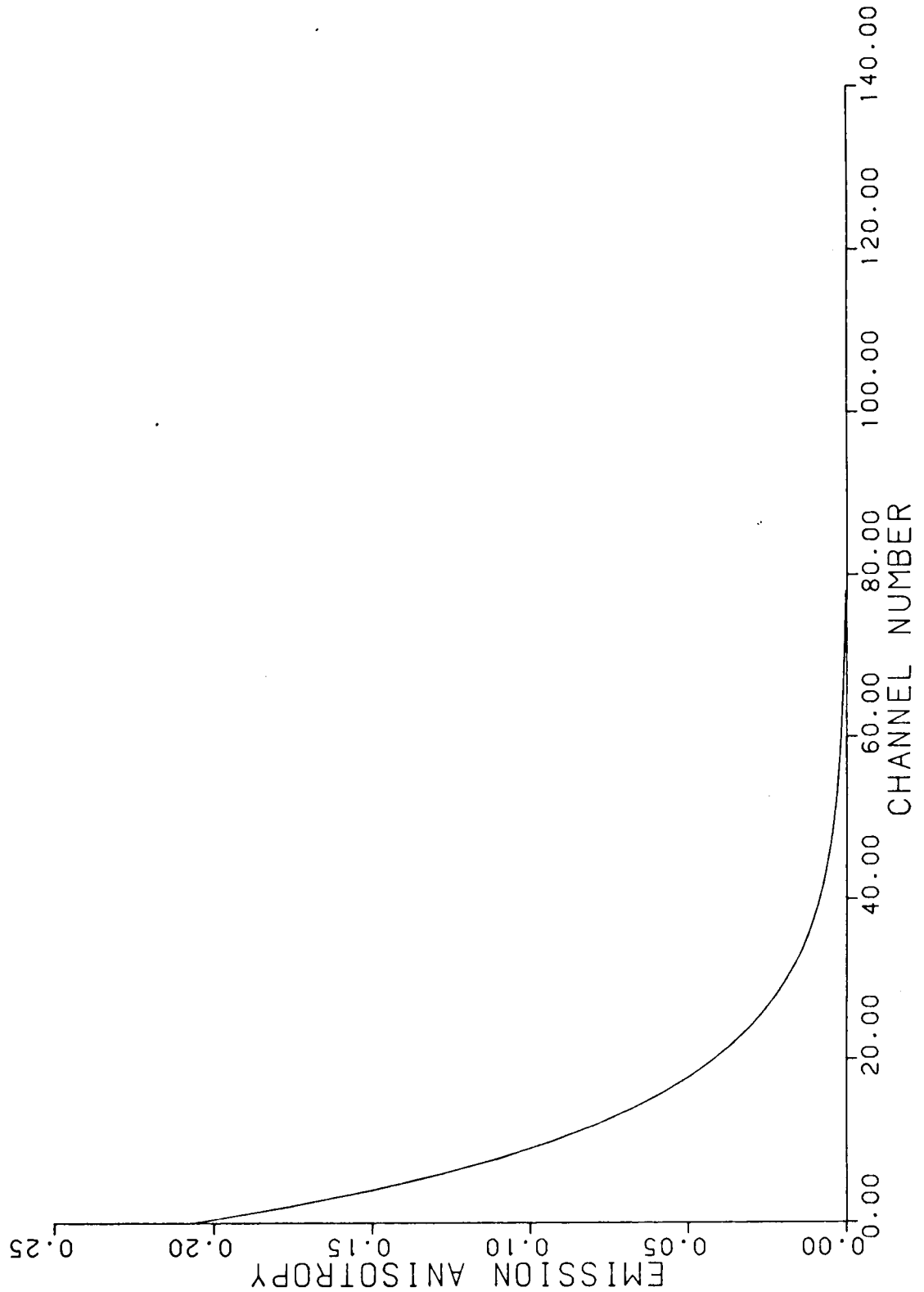
EMISSION ANISOTROPY
0.00
0.05
0.10
0.15
0.20
0.25
0.00
20.00
40.00
60.00
80.00
100.00
120.00
140.00
CHANNEL NUMBER

Fig. III.56.

Fig. III.57. Actual emission anisotropy (r(t)) plotted against channel number for melittin in egg lecithin (see text for more detail). Channel width = 0.190 ns.

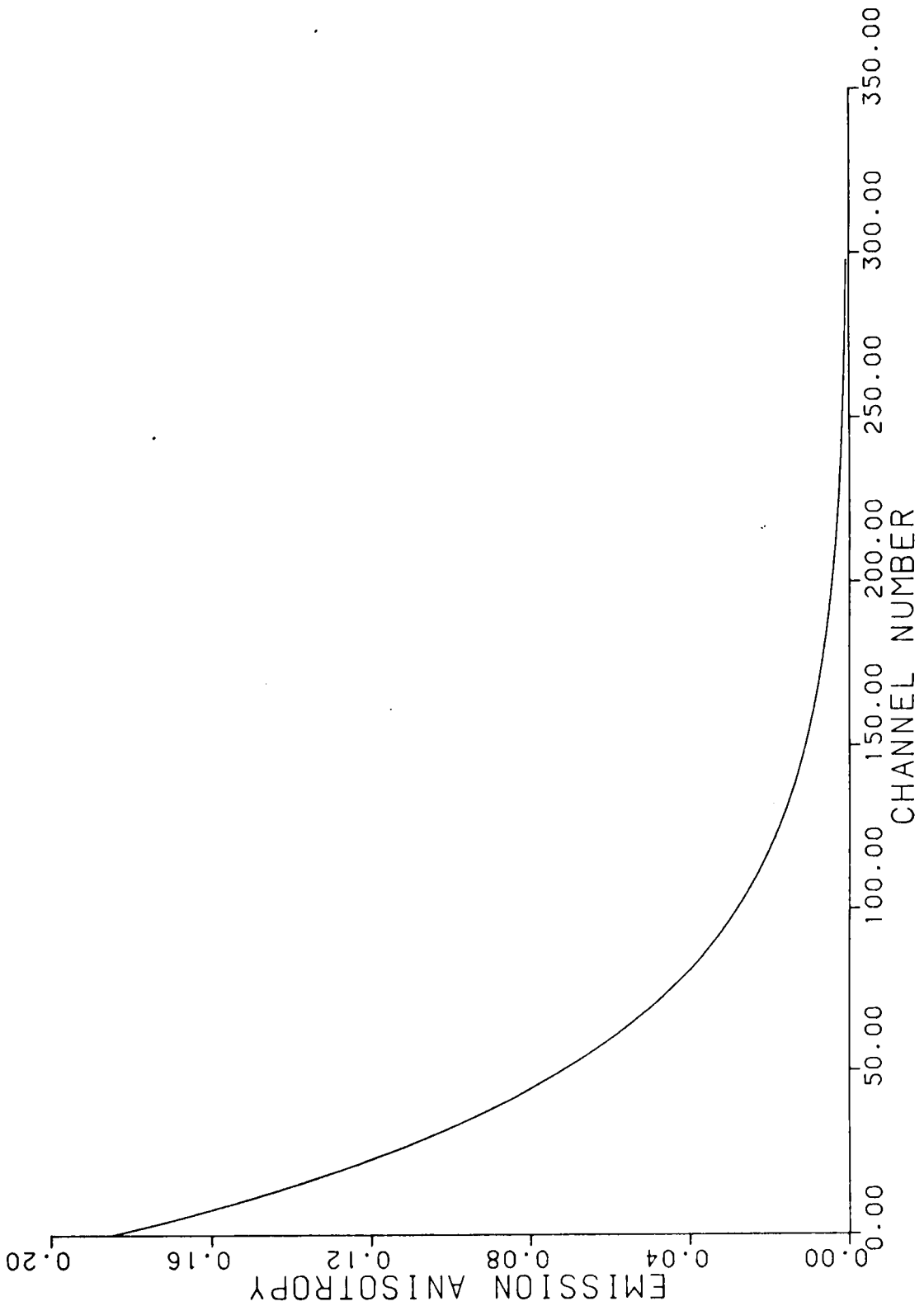
EMISSION ANISOTROPY
0.00
0.04
0.08
0.12
0.16
0.20
0.00
50.00
100.00
150.00
200.00
250.00
300.00
350.00
CHANNEL NUMBER

Fig. III.57.

Fig. III.58. Actual emission anisotropy (r(t)) plotted against channel number for melittin in distearoyllecithin (see text for more detail). Channel width = 0.159 ns.

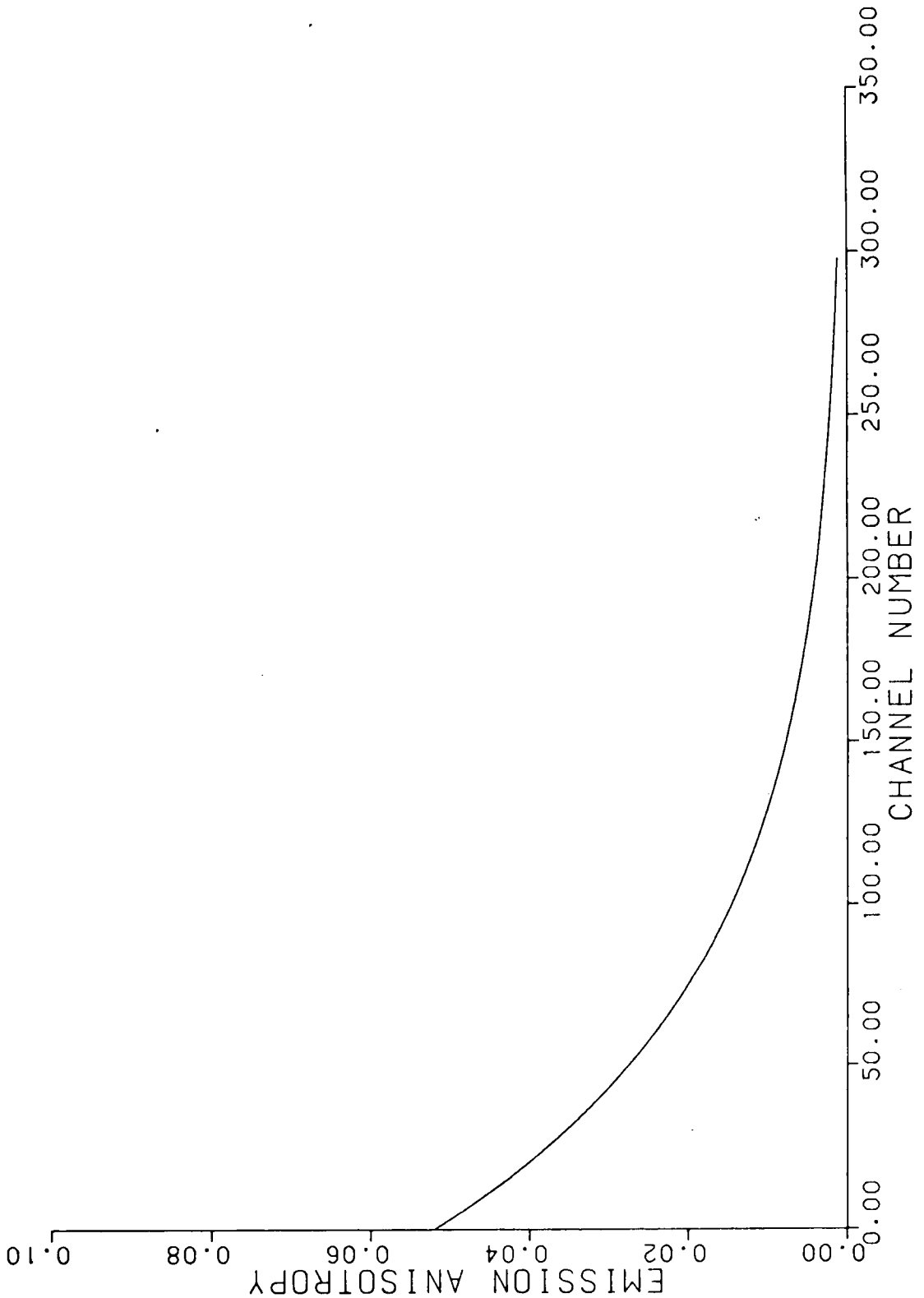
EMISSION ANISOTROPY
0.00
0.02
0.04
0.06
0.08
0.10
0.00
50.00
100.00
150.00
200.00
250.00
300.00
350.00
CHANNEL NUMBER

Fig. III.58.

Fig. III.59. Actual emission anisotropy (r(t)) plotted against channel number for melittin in distearoyllecithin at 61°C (see text for more detail). Channel width = 0.186 ns.

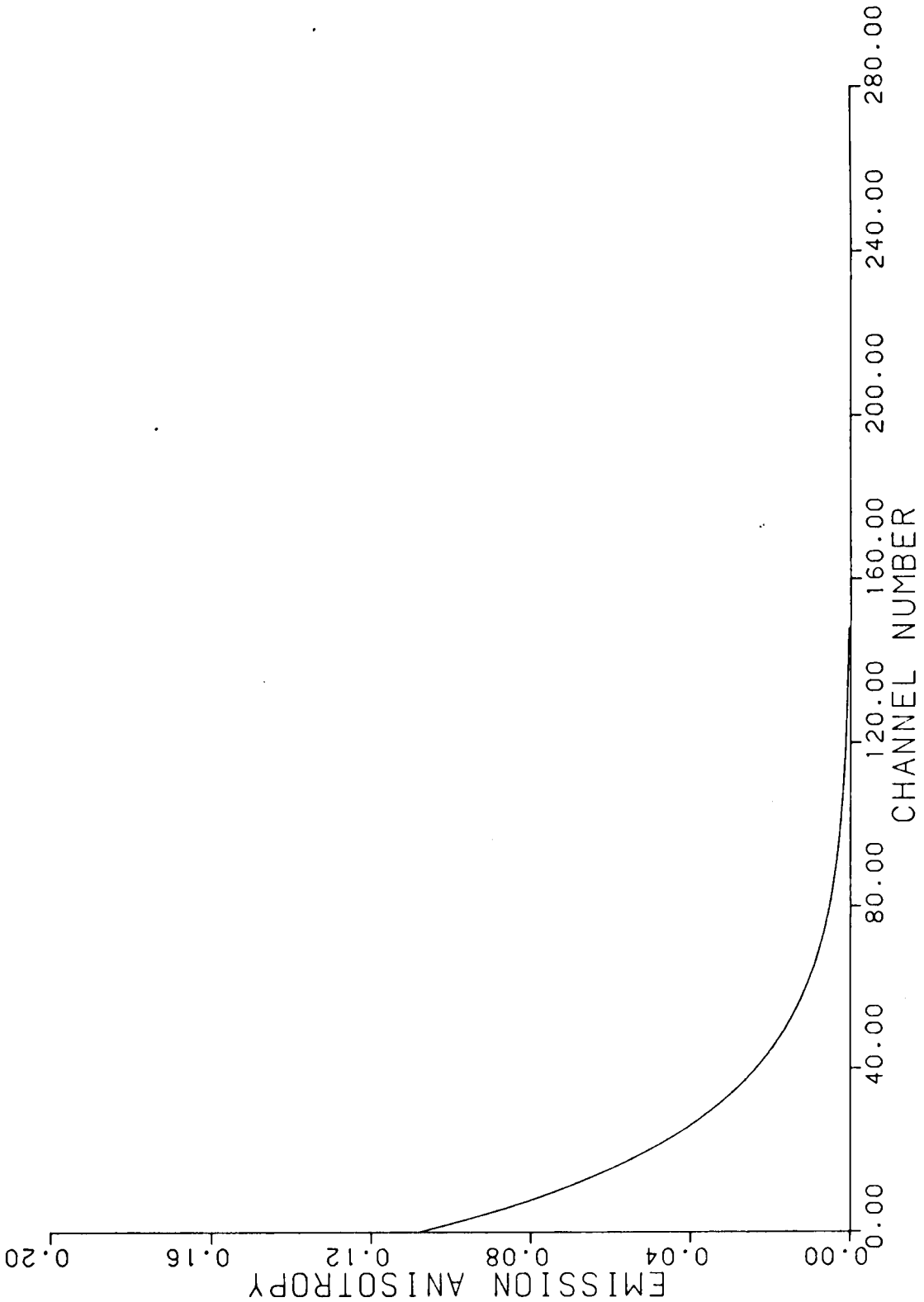
EMISSION ANISOTROPY
0.00
0.04
0.08
0.12
0.16
0.20
0.00
40.00
80.00
120.00
160.00
200.00
240.00
280.00
CHANNEL NUMBER

Fig. III.59.

Table III.2

Depolarization Analysis Parameters

Substance	$I_V(t) - I_H(t)$ τ_o (ns)	A_o	$I_V(t) + 2(I_H(t))$ τ_o (ns)	τ_c (ns)	A_o/A_c	ϕ (ns)	r(o)
Melittin (free)	0.8	0.06	3.2	-	0.34	1.1	0.185
Melittin + 0.15 M K_2HPO_4	1.4	0.09	3.3	1.4	0.85	3.6	0.164
Melittin + 0.5 M K_2HPO_4	1.4	0.10	2.6	0.2	0.63	3.5	0.168
Melittin + 0.15 M NaCl	1.3	0.10	3.1	-	.38	2.8	0.134
Melittin + 1.0 M NaCl	1.2	0.09	2.7	-	0.46	2.1	0.206
Melittin in Egg Lecithin	2.1	0.03	2.7	-	0.14	10.1	0.185
Melittin in D.S.L.	2.5	0.05	3.7	1.2	1.92	12.5	0.052
Melittin in D.S.L. (61°C)	1.4	0.09	2.0	-	0.89	4.9	0.108

plot, the K_{sv} (diffusion-controlled quenching constant) was determined. These plots can be found in Figs. III.60 through III.69. The second-order quenching rate constant, kq, was then obtained from the relation $kq = K_{sv}/\tau_o$, where τ_o is the total fluorescence decay time in the absence of acrylamide. A summary of the quenching parameters and pertinent fluorescence decay times are listed in Table III.3.

Steady-state fluorescence spectra were also taken for melittin in 0.01 M Tris buffer, in inorganic phosphate, in NaCl, and for melittin bound to egg lecithin and distearoylecithin. These spectra can be found in Figs. III.70 through III.72. Melittin in Tris buffer and free tryptophan in Tris buffer exhibited a fluorescence maximum at approximately 352 nm. Upon adding 0.5 M inorganic phosphate, the peak of the spectrum blue-shifted to 337 nm. No more shift was observed upon increasing further the concentration of phosphate. Lower concentrations of phosphate caused smaller blue-shifts. After adding 1.0 M NaCl to melittin, the peak of the spectrum shifted to 336 nm with lesser concentrations of NaCl causing smaller blue-shifts. The limiting concentration of NaCl for spectral shifts was 1.0 M. When melittin was bound to egg lecithin, the peak of the fluorescence spectrum occurred at 338 nm, which was the same as melittin in 0.15 M inorganic phosphate. Melittin bound to distearoyllecithin (below the phase transition temperature) exhibited a peak in the fluorescence spectrum at 335 nm while the peak of the spectrum shifted to 336 nm when the temperature was raised above the phase transition point. The spectrum of melittin in 0.5 M inorganic phosphate and melittin bound to distearoyllecithin at 61°C virtually coincided.

Fig. III.60. Stern-Volmer plot of acrylamide quenching analysis of melittin in Tris buffer. Dotted line represents the Stern-Volmer plot F_o/F vs. [Q]. Solid line represents the modified Stern-Volmer plot $(F_o/F)e^{-V[Q]}$ vs. [Q].

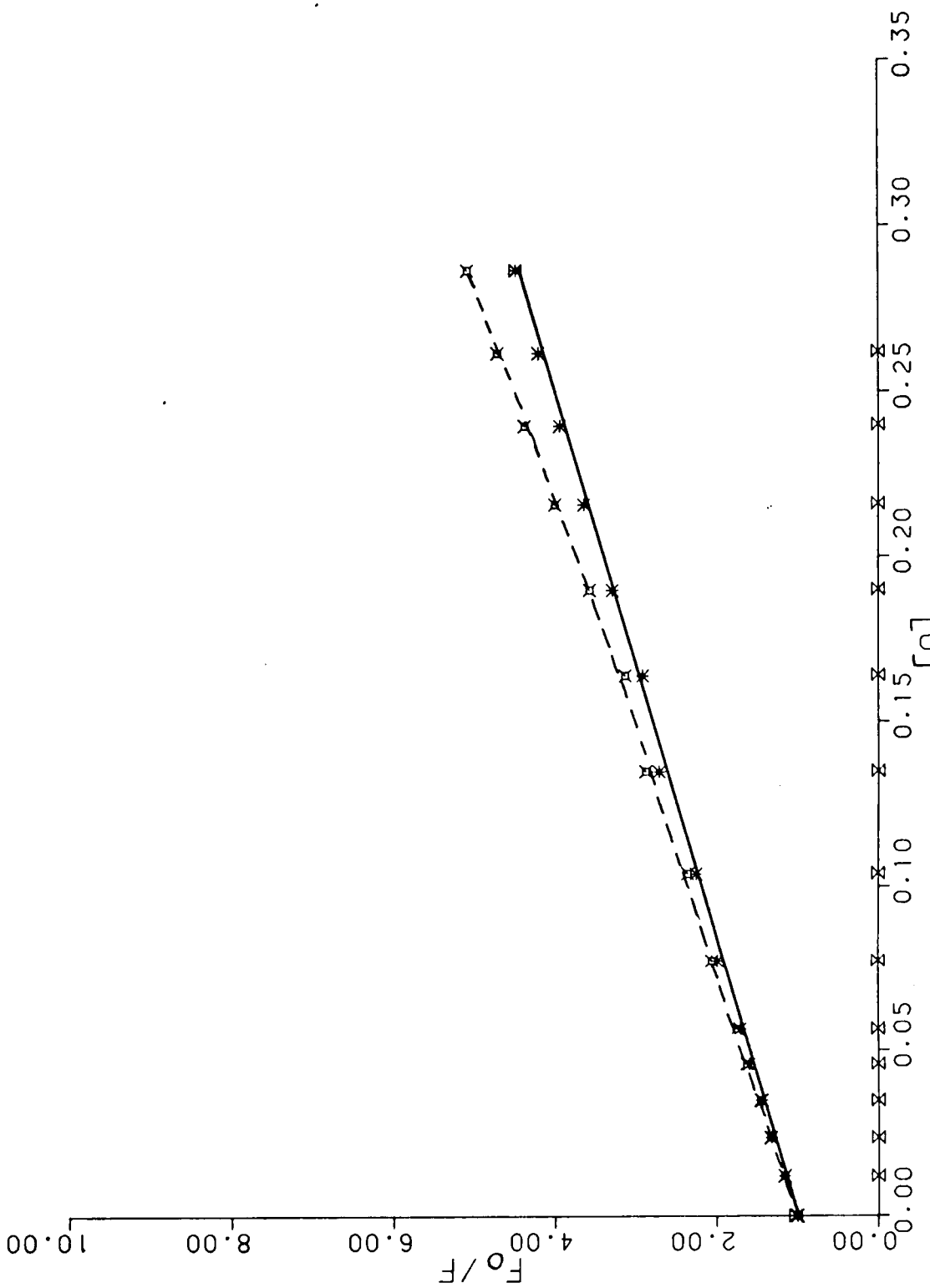

Fig. III.60.

Fig. III.61. Stern-Volmer plot of acrylamide quenching analysis of melittin + 0.15 M K_2HPO_4. Dotted line represents the Stern-Volmer plot F_o/F vs. [Q]. Solid line represents the modified Stern-Volmer plot $(F_o/F)e^{-V[Q]}$ vs. [Q].

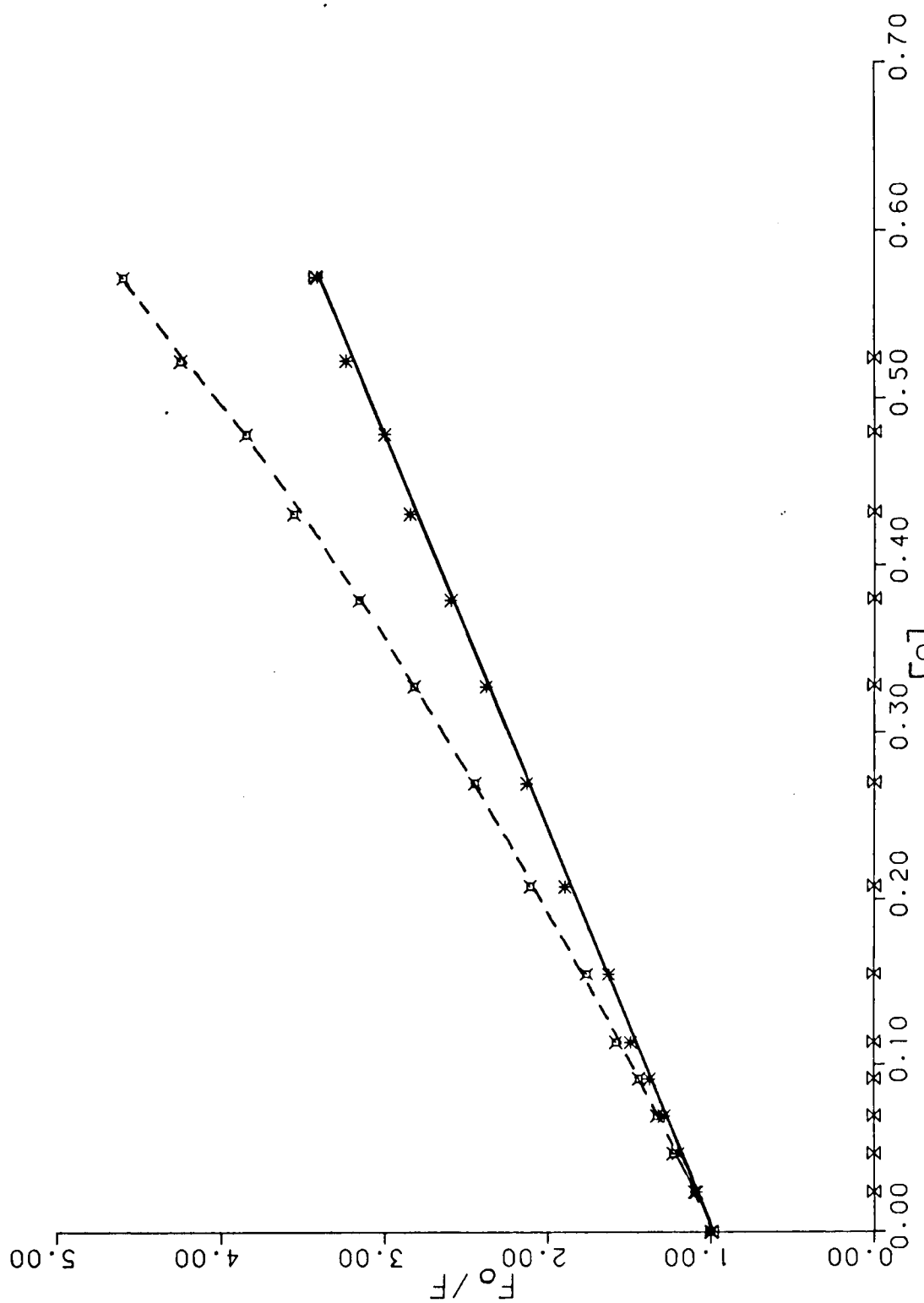

Fig. III.61.

Fig. III.62. Stern-Volmer plot of acrylamide quenching analysis of melittin + 0.5 M K_2HPO_4. Dotted line represents the Stern-Volmer plot F_o/F vs. [Q]. Solid line represents the modified Stern-Volmer plot $(F_o/F)e^{-V[Q]}$ vs. [Q].

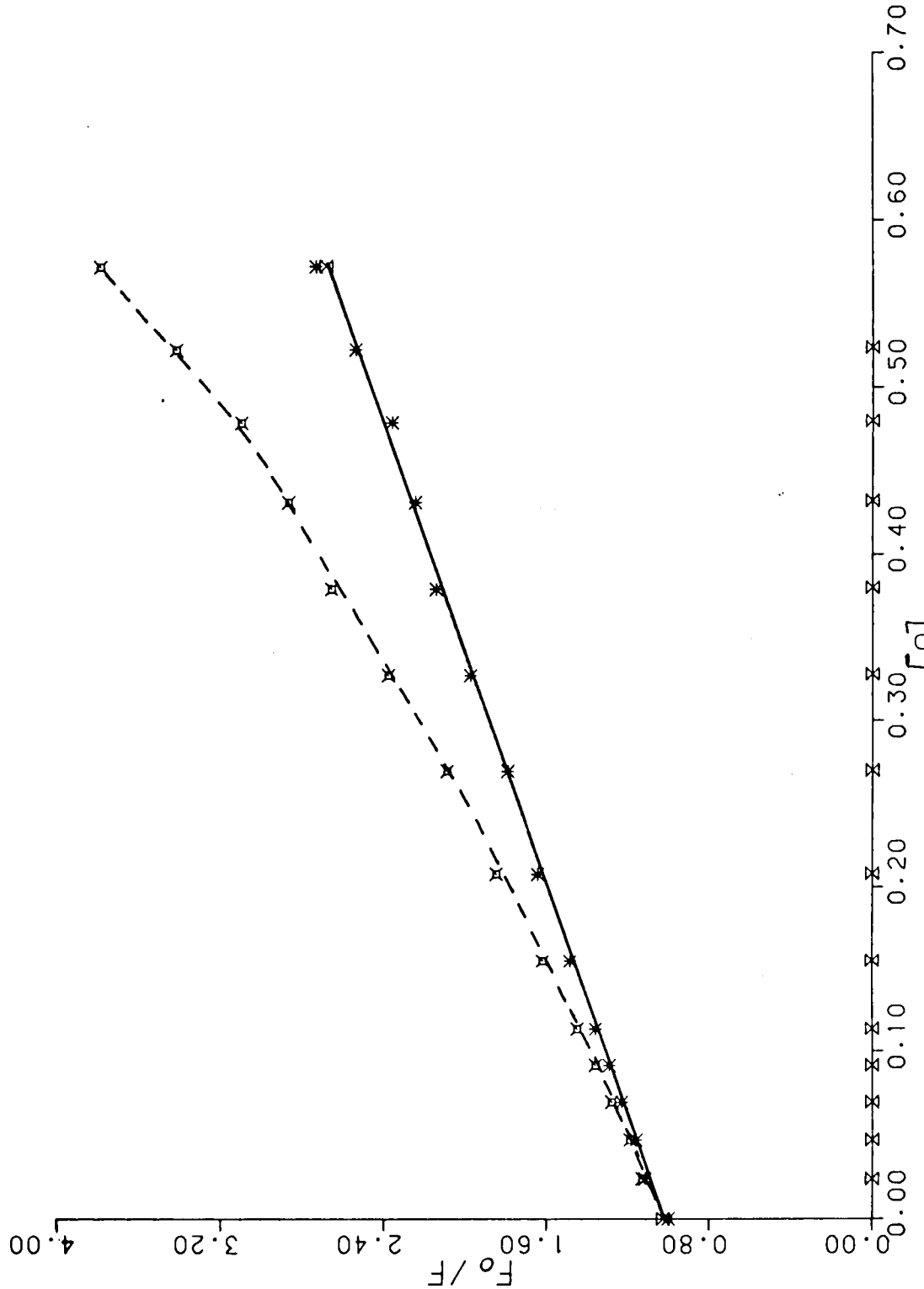

Fig. III.62.

Fig. III.63. Stern-Volmer plot of acrylamide quenching analysis of melittin + 0.15 M NaCl. Dotted line represents the Stern-Volmer plot F_o/F vs. [Q]. Solid line represents the modified Stern-Volmer plot $(F_o/F)e^{-V[Q]}$ vs. [Q].

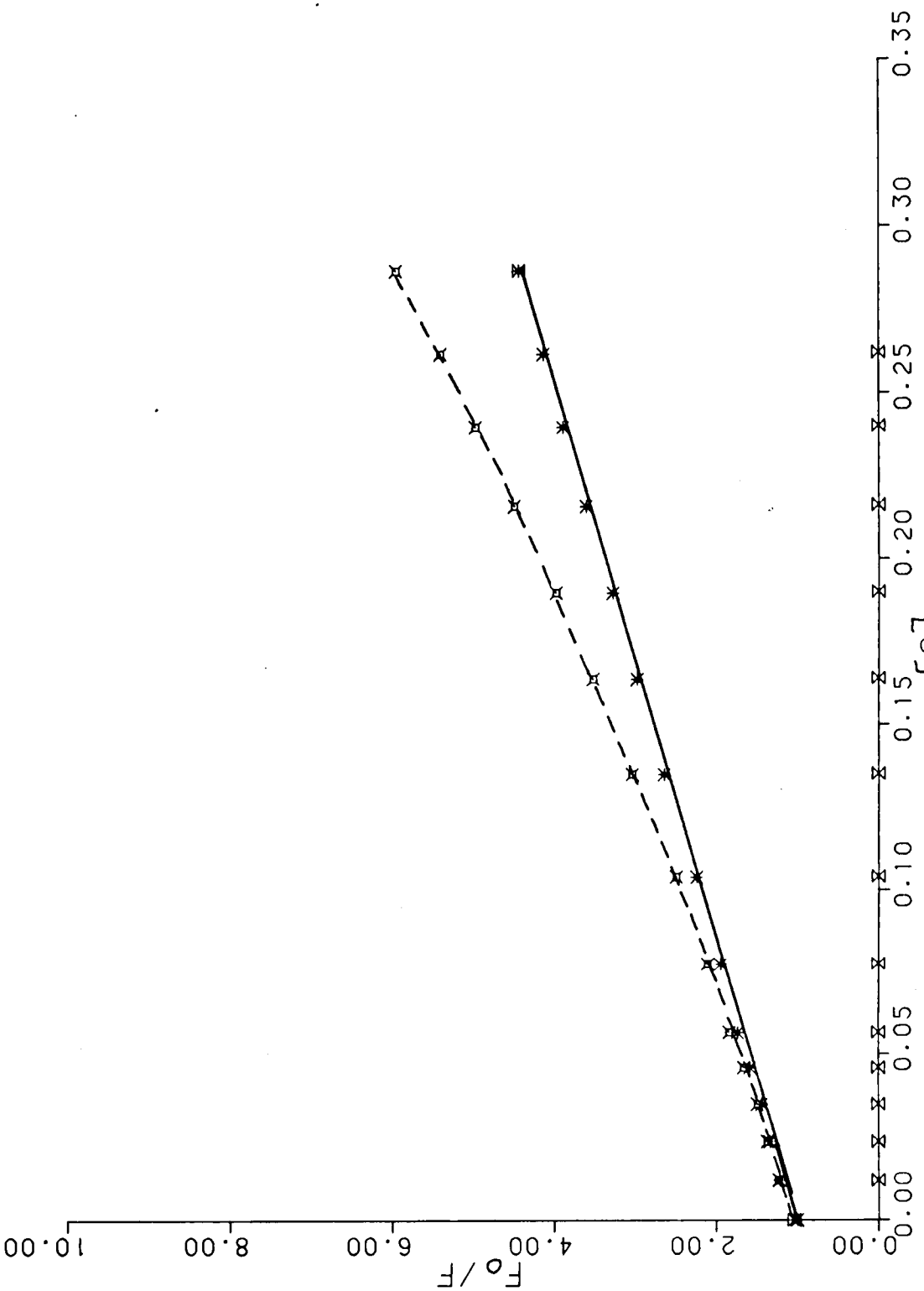

Fig. III.63.

Fig. III.64. Stern-Volmer plot of acrylamide quenching analysis of melittin + 1.0 M NaCl. Dotted line represents the Stern-Volmer plot F_o/F vs. [Q]. Solid line represents the modified Stern-Volmer plot $(F_o/F)e^{-V[Q]}$ vs. [Q].

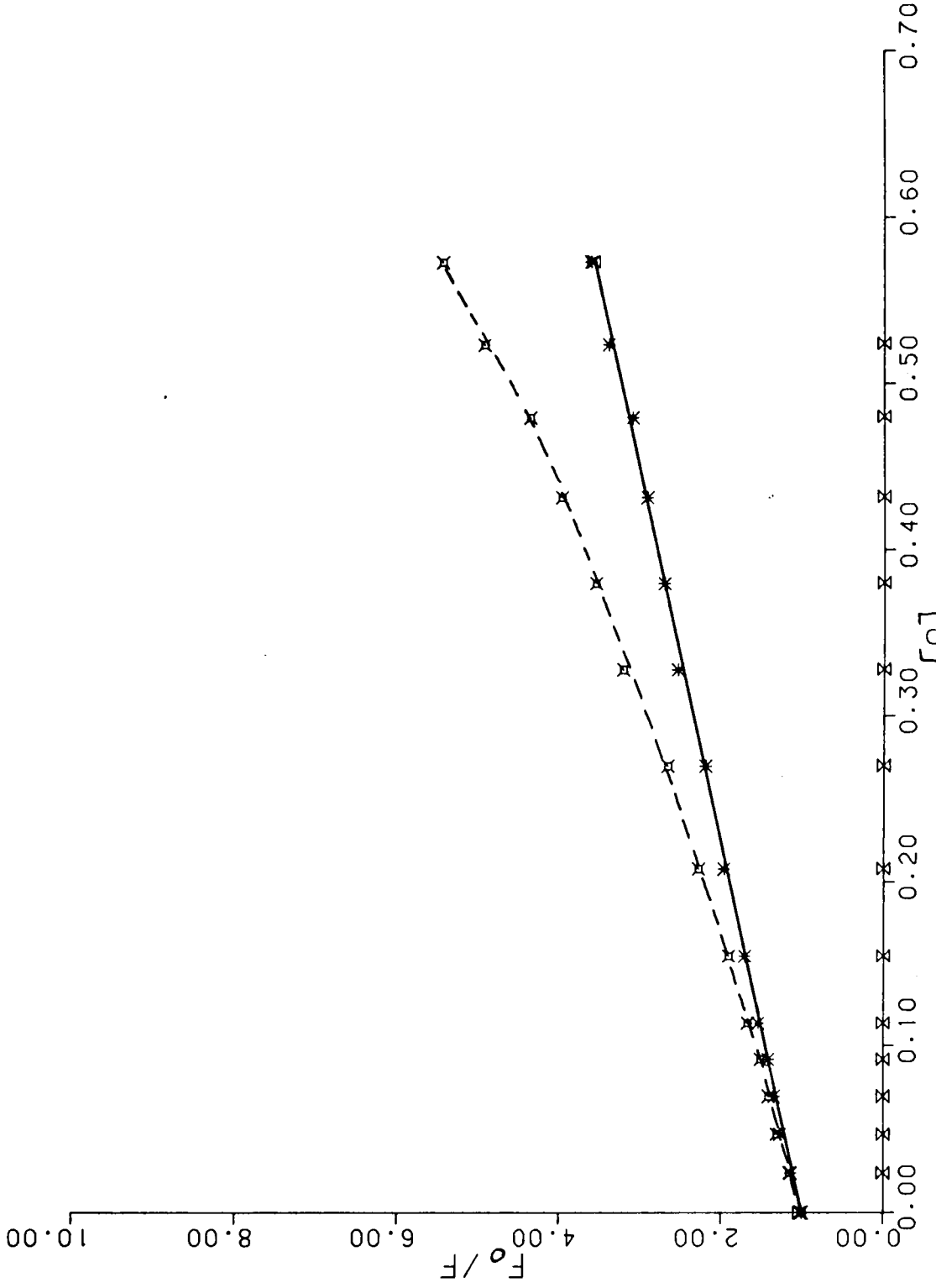

Fig. III.64.

Fig. III.65. Stern-Volmer plot of acrylamide quenching analysis of melittin in egg lecithin. Dotted line represents the Stern-Volmer plot F_0/F vs. [Q]. Solid line represents the modified Stern-Volmer plot $(F_0/F)e^{-V[Q]}$ vs. [Q].

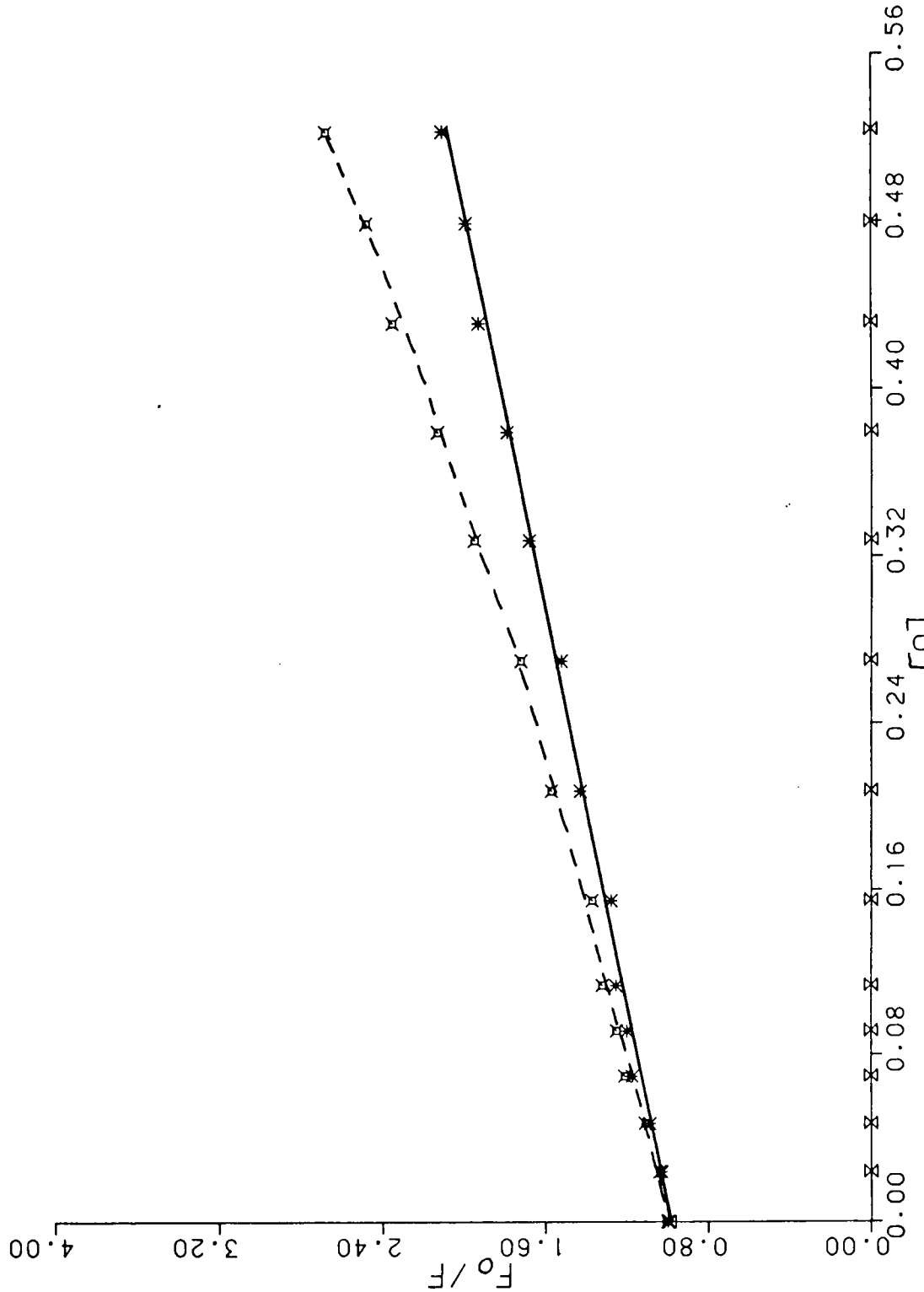

Fig. III.65.

Fig. III.66. Stern-Volmer plot of acrylamide quenching analysis of melittin in distearoyllecithin. Dotted line represents the Stern-Volmer plot F_o/F vs. [Q]. Solid line represents the modified Stern-Volmer plot $(F_o/F)e^{-V[Q]}$ vs. [Q].

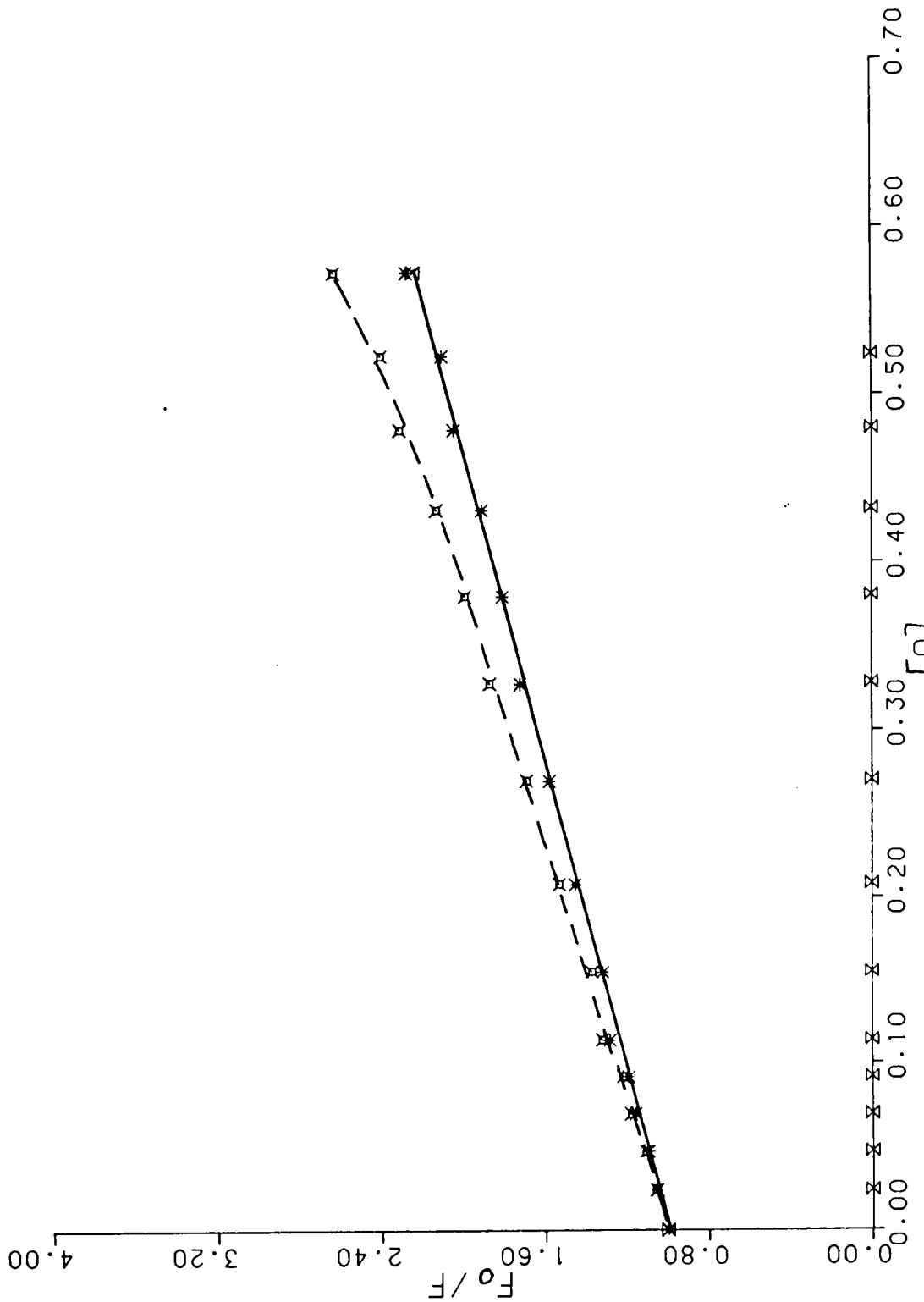

Fig. III.66.

Fig. III.67. Stern-Volmer plot of acrylamide quenching analysis of melittin in distearoyllecithin at 61°C. Dotted line represents the Stern-Volmer plot F_o/F vs [Q]. Solid line represents the modified Stern-Volmer plot $(F_o/F)e^{-V[Q]}$ vs. [Q].

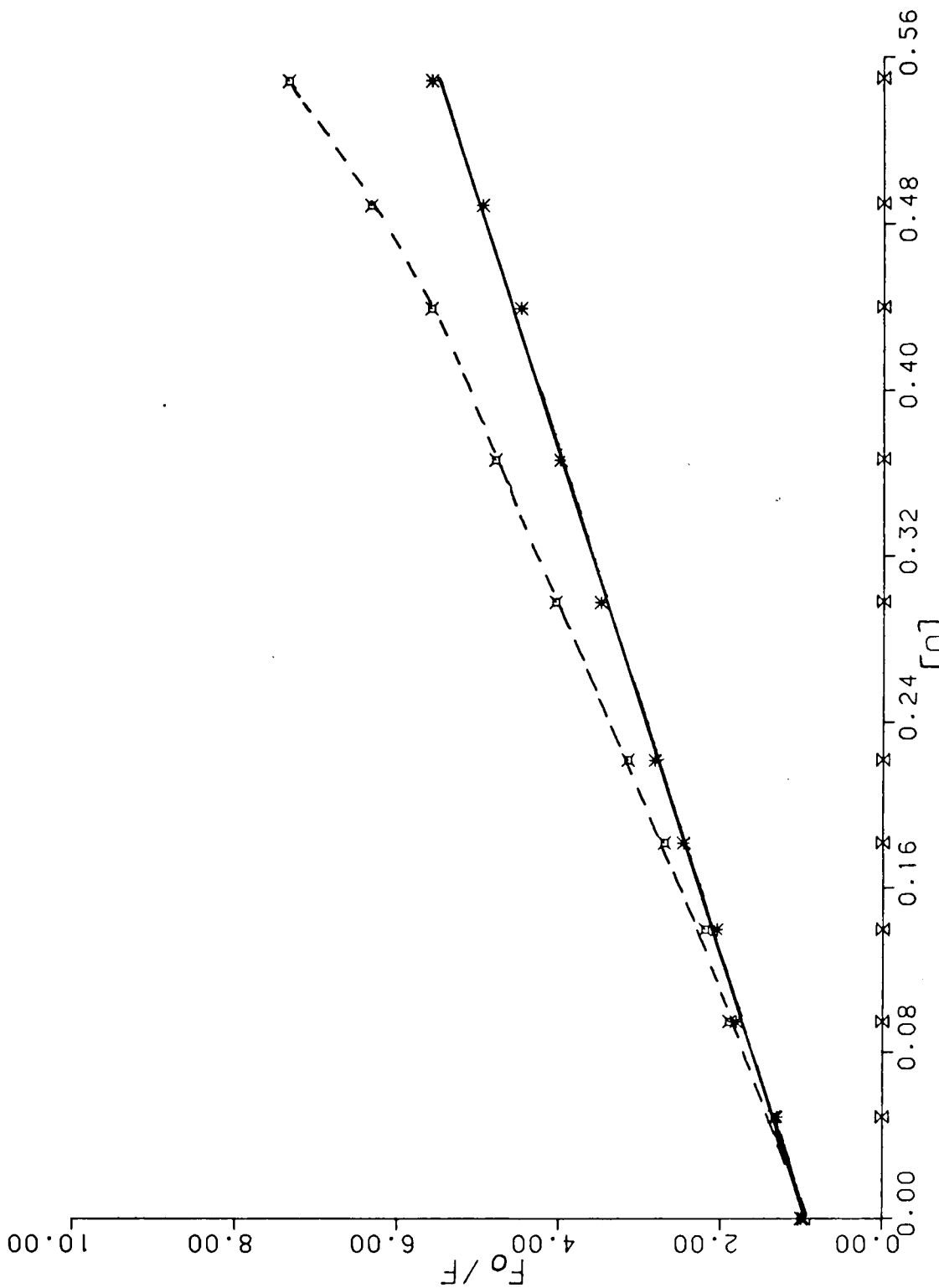

Fig. III.67.

Fig. III.68. Stern-Volmer plot of acrylamide quenching analysis of melittin in egg lecithin + 1.0 M NaCl. Dotted line represents the Stern-Volmer plot F_o/F vs. [Q]. Solid line represents the modified Stern-Volmer plot $(F_o/F)e^{-V[Q]}$ vs. [Q].

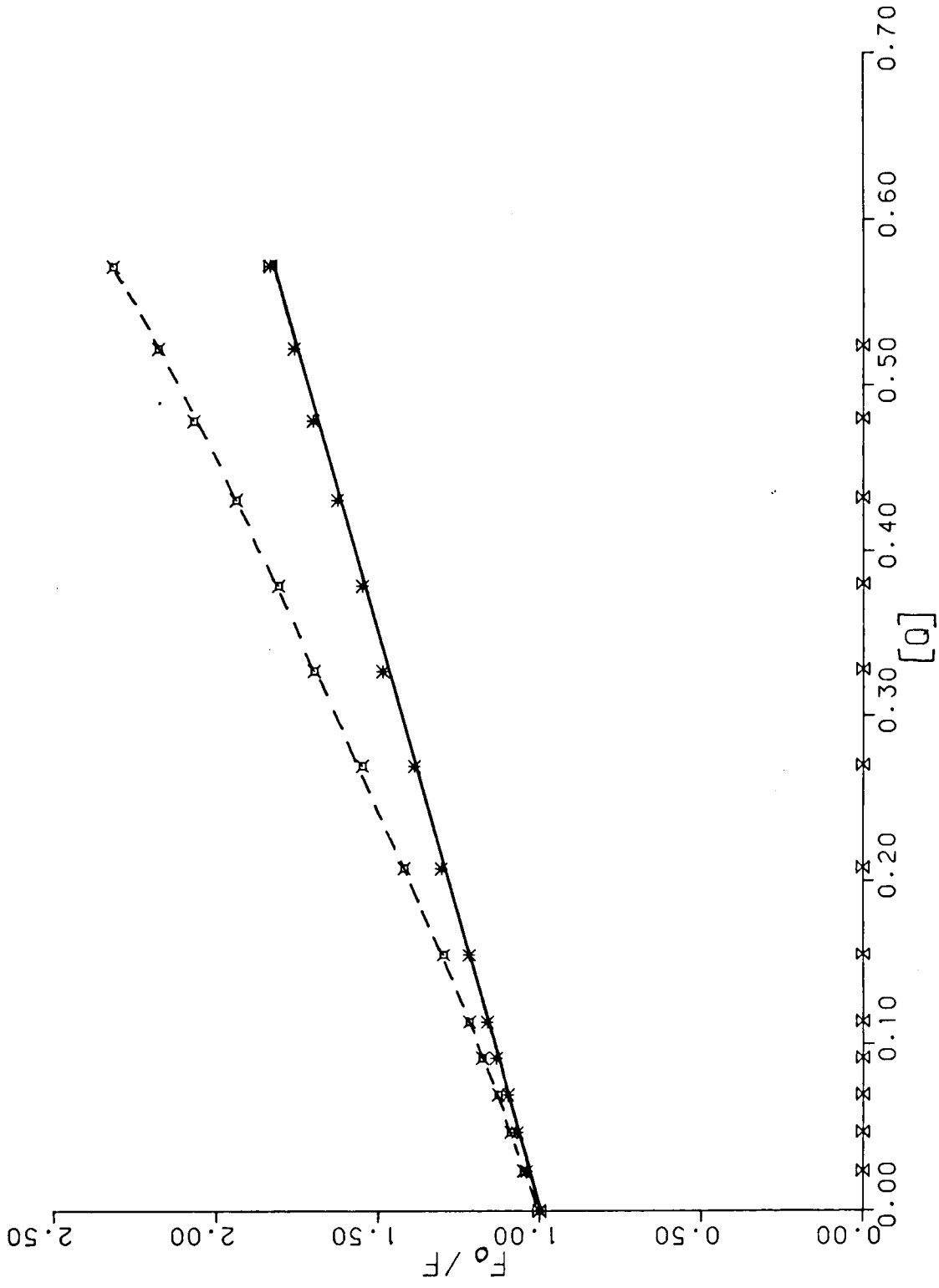

Fig. III.68.

Fig. III.69. Stern-Volmer plot of acrylamide quenching analysis of melittin in Tris buffer at 61°C. Dotted line represents the Stern-Volmer plot F_o/F vs. [Q]. Solid line represents the modified Stern-Volmer plot $(F_o/F)e^{-V[Q]}$ vs. [Q].

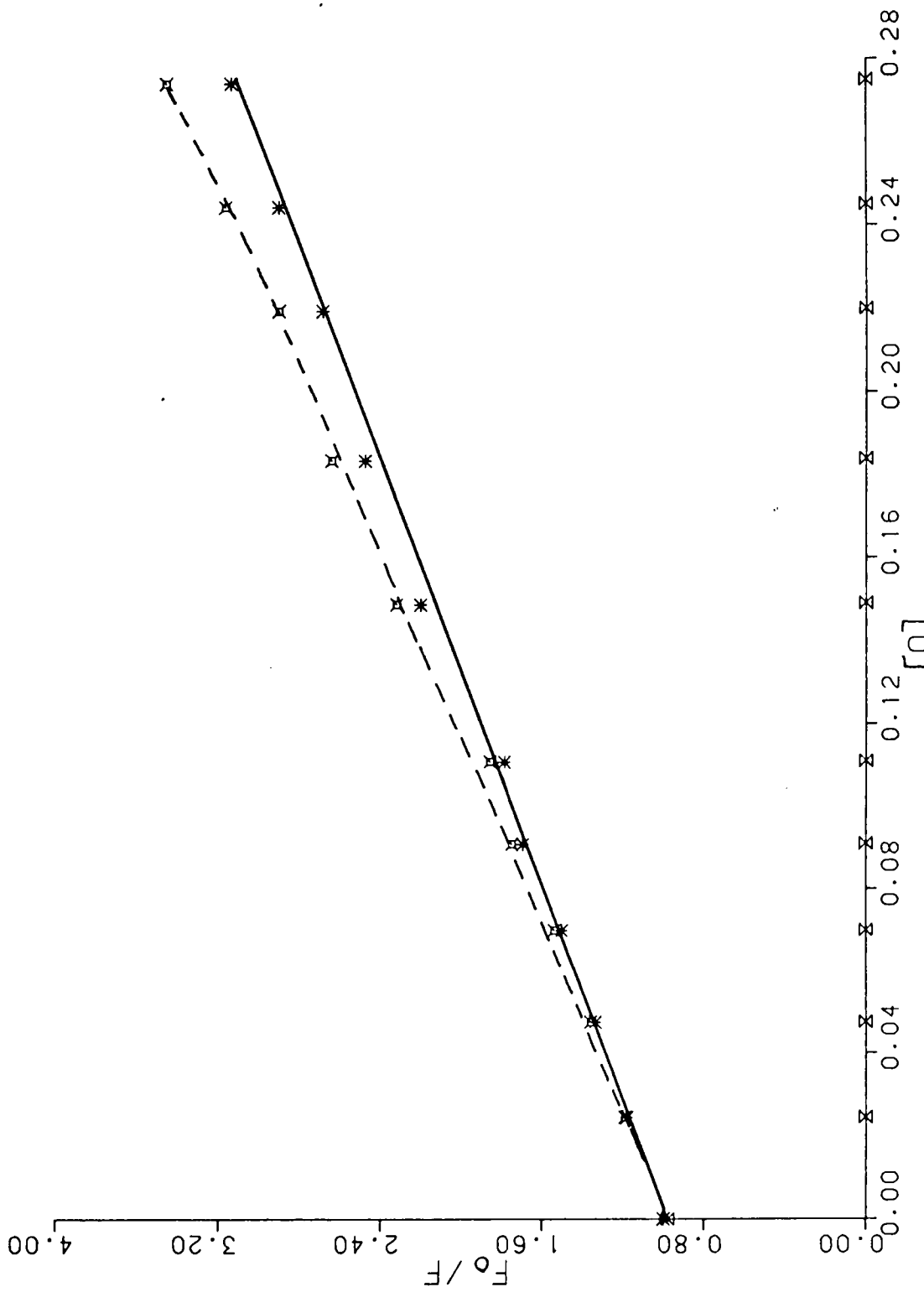
0.00
0.80
1.60
2.40
3.20
4.00
Γ_o / Γ
0.00
0.04
0.08
0.12
0.16
0.20
0.24
0.28
[Q]

Fig. III.69.

Table III.3

Acrylamide Quenching Parameters

Substance	$V(M^{-1})$	$K_{SV}(M^{-1})$	τ_o(ns)*	$K_q \times 10^9$ $(M^{-1}S^{-1})$
Tryptophan	1.2 ± 0.1	16.2 ± 0.5	2.6	6.2
Melittin in 0.01 M Tris buffer	0.44 ± 0.04	12.1 ± 0.5	3.1	3.9
Melittin in 0.15 M K_2HPO_4	0.52 ± 0.03	4.2 ± 0.1	2.3	1.8
Melittin in 0.5 M K_2HPO_4	0.57 ± 0.04	2.9 ± 0.2	2.1	1.4
Melittin in 0.15 M NaCl	1.02 ± 0.1	11.9 ± 0.5	2.9	4.1
Melittin in 1.0 M NaCl	0.72 ± 0.04	4.4 ± 0.2	2.4	1.8
Melittin in Egg Lecithin	0.46 ± 0.03	2.1 ± 0.2	2.2	0.9
Melittin in D.S.L.	0.26 ± 0.03	2.2 ± 0.2	3.2	0.7
Melittin in D.S.L. (61°C)	0.50 ± 0.05	8.2 ± 0.3	2.1	3.9
Melittin in Egg Lecithin plus 1.0 M NaCl	0.41 ± 0.03	1.5 ± 0.1	2.9	0.5
Melittin (61°C)	0.35 ± 0.04	7.9 ± 0.5	1.4	5.6

*The value of τ_o used in this analysis was taken at the peak of the fluorescence spectrum at which wavelength the titration was performed. For double exponential decays an average τ_o was calculated from $\tau_o = \frac{\tau_1(A_1) + \tau_2(A_2)}{A_1 + A_2}$, where τ_1 and τ_2 are the decay times and A_1 and A_2 are the corresponding amplitudes.

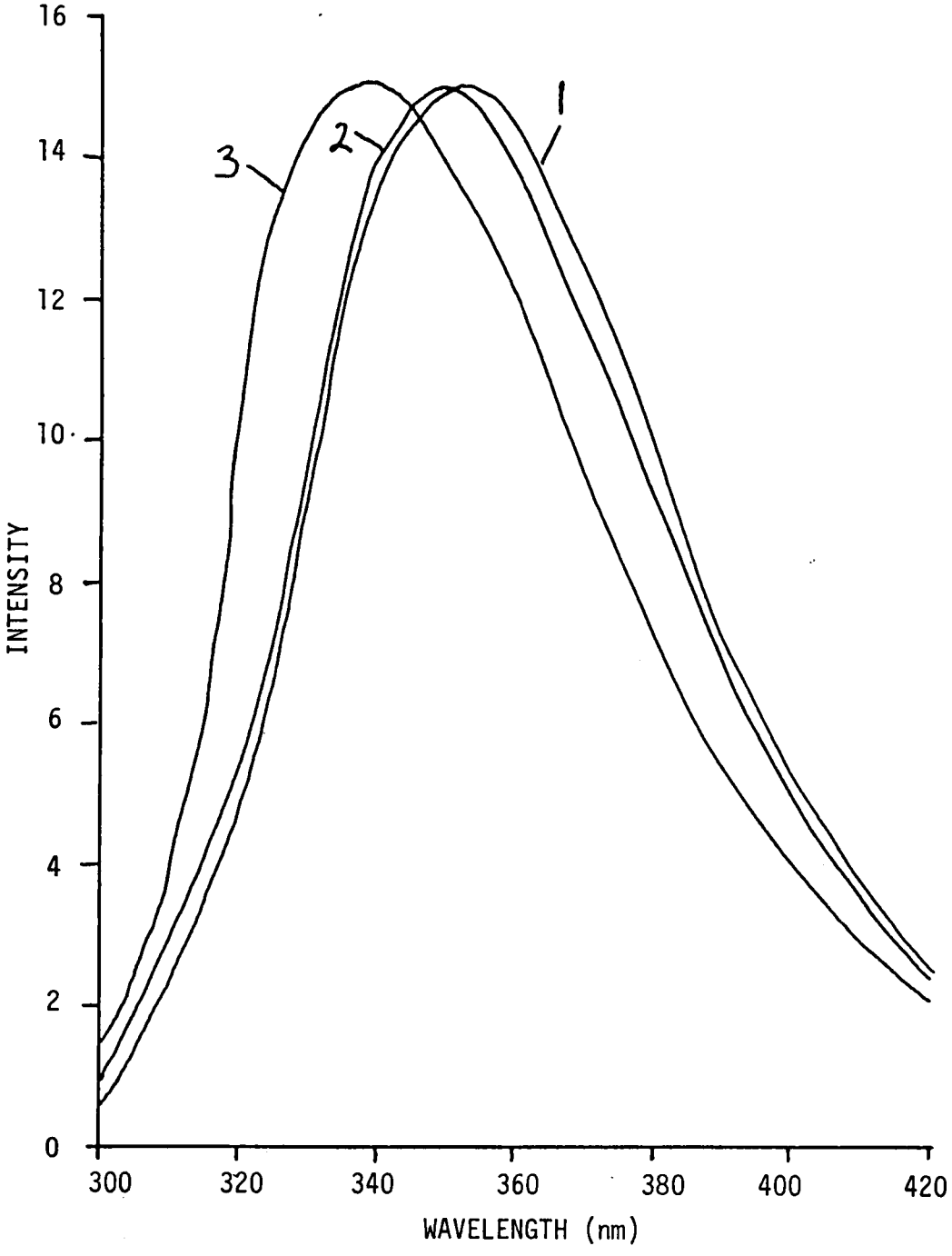

Fig. III.70. Steady-state fluorescence spectra of (1) free melittin, (2) melittin + 0.15 M NaCl, (3) melittin + 1.0 M NaCl.

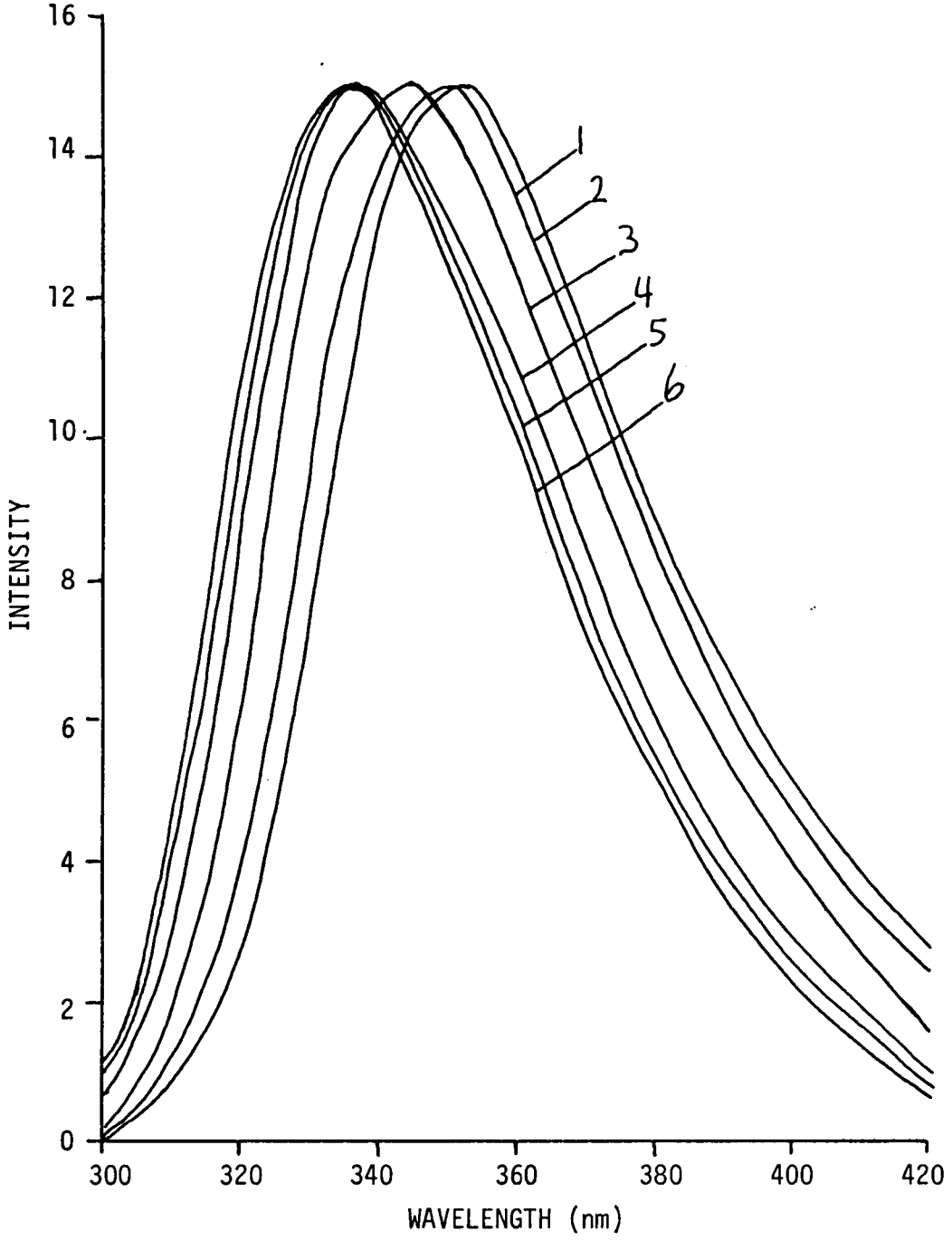

Fig. III.71. Steady-state fluorescence spectra of melittin in various concentrations of inorganic phosphate. (1) free, (2) 0.02 M, (3) 0.04 M, (4) 0.15 M, (5) 0.05 M, and (6) 1.0 M.

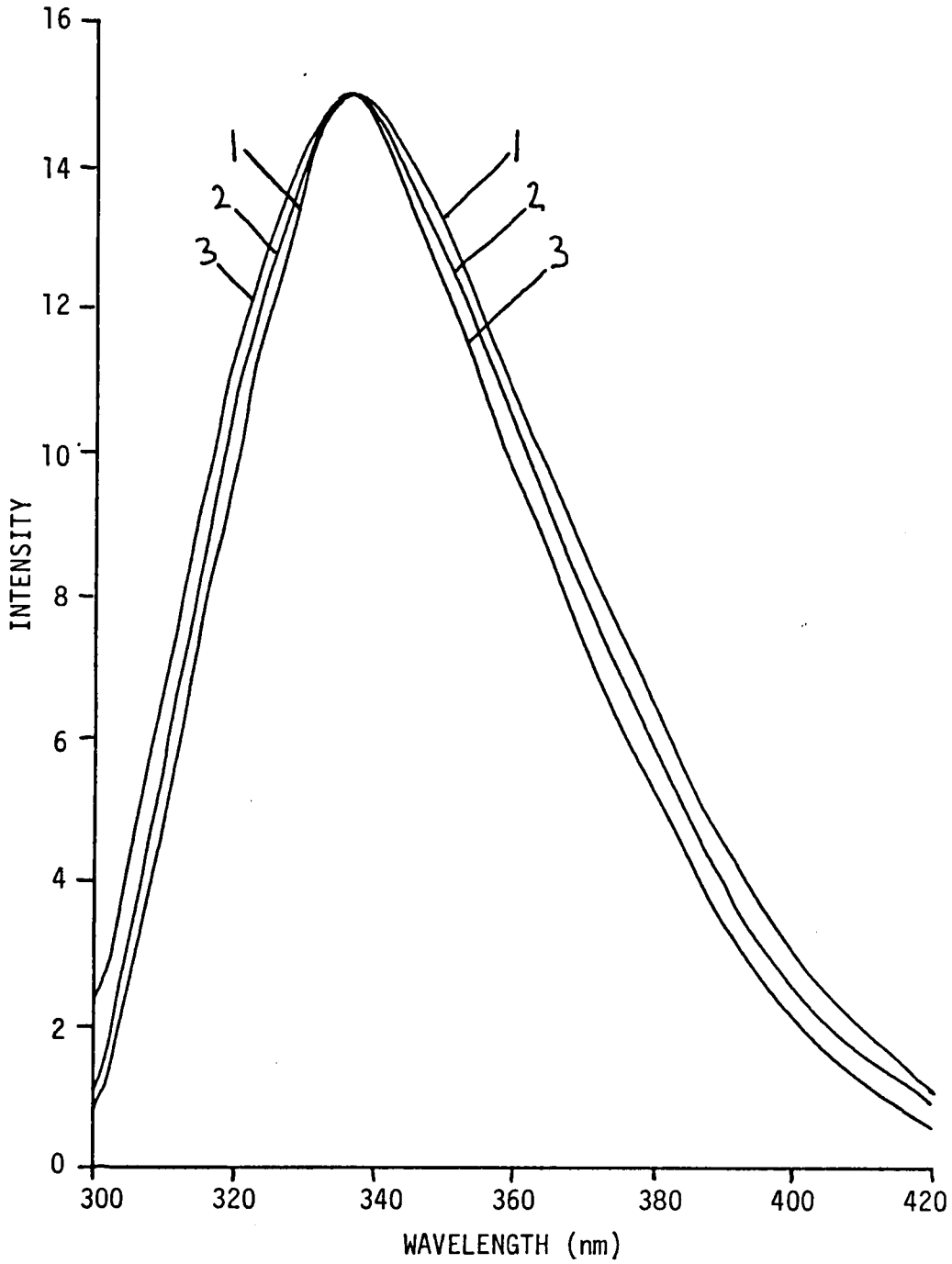

Fig. III.72. Steady-state fluorescence spectra of (1) melittin in egg lecithin, (2) melittin in distearoyllecithin, (3) melittin in distearoylecithin at 61°C. There is the following correspondence between the spectra of melittin in membranes and those of melittin in K_2HPO_4 solutions: (a) egg lecithin with 0.15 M, (b) distearoyl-lecithin at 61°C with 0.5 M, and (c) distearoyllecithin at room temperature with 1.0M.

Absorption spectra were also taken for free melittin, melittin in 0.15 M inorganic phosphate, melittin in 0.5 M inorganic phosphate, and melittin bound to egg lecithin. The absorption spectra are shown in Fig. III.73. The absorption spectra of melittin in 0.15 M phosphate, 0.5 M phosphate, and melittin bound to egg lecithin were virtually identical but were red-shifted 2 nm relative to the spectrum of free melittin.

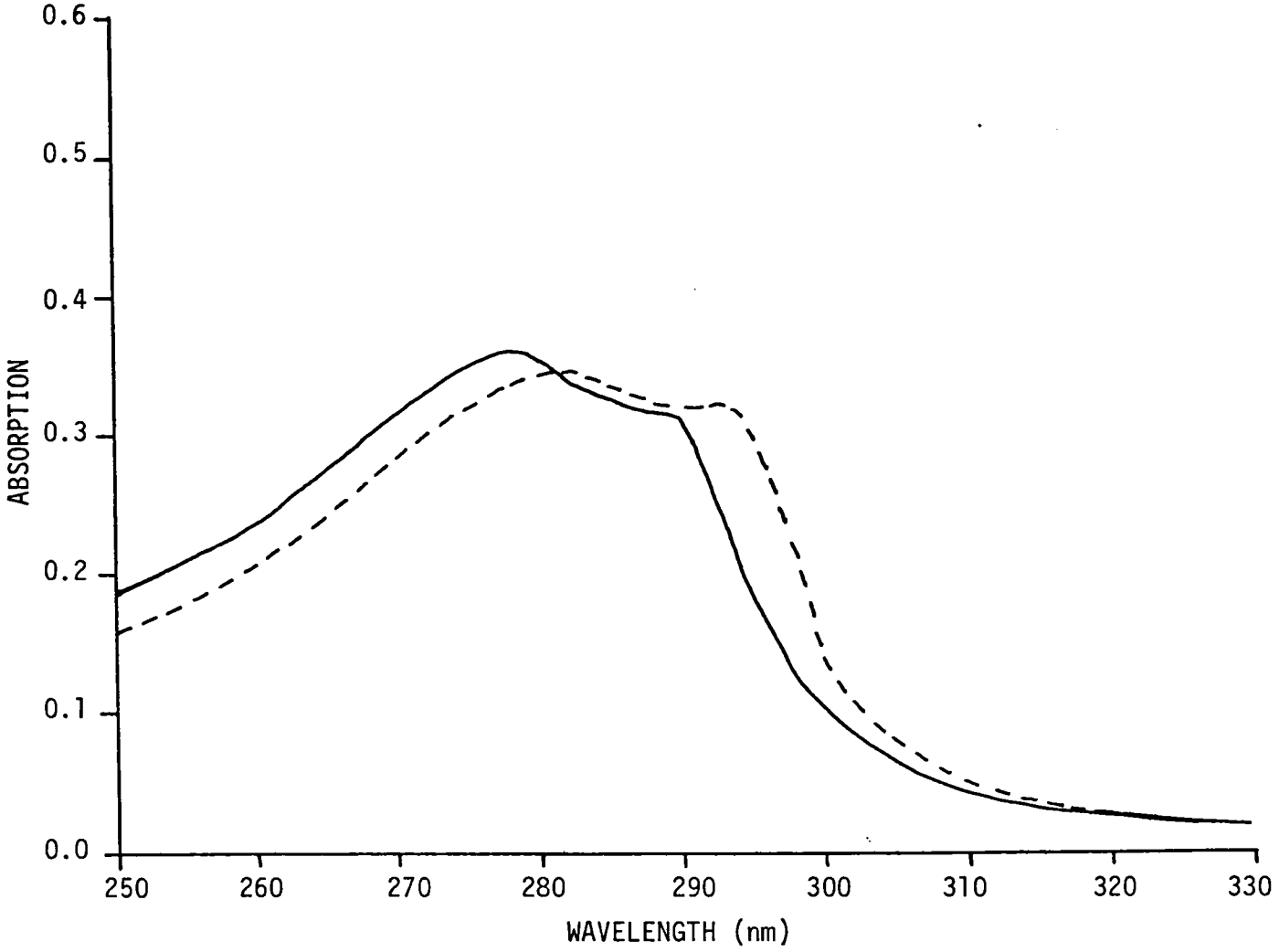

Fig. III.73. Dashed line represents absorption spectra of melittin + 0.15 M K_2HPO_4, melittin + 0.5 M K_2HPO_4, and melittin in egg lecithin. Solid line represents absorption spectrum of free melittin.

CHAPTER IV

DISCUSSION

A recent study indicated that the α-helicity of melittin greatly increased upon binding to egg lecithin (Dawson et al., 1978). A similar effect was observed in 0.15 M inorganic phosphate (Drake and Hider, 1979). Steady-state fluorescence measurements were made in the present study for observing these changes. The fluorescence spectra of the tryptophan residue of melittin and of free tryptophan have been found to be very similar with peaks at 352 nm. After binding melittin to egg lecithin, a shift to the blue was observed with a decrease in the FWHM (Fig. III.72) implying that the environment of the tryptophan residue becomes more hydrophobic. This inference was made based on the optical properties of tryptophan (Teale, 1960). Also, a very good coincidence of spectra was found between melittin in 0.15 M inorganic phosphate and melittin bound to egg lecithin (see Figs. III.71 and III.72). In addition, there was a virtual coincidence of the fluorescence decay time values in the two cases (see Table III.1, p. 87). When melittin was bound to distearoyl-lecithin, a shift to the blue in the spectrum was noted both below and above its phase transition temperature (Fig. III.72). NaCl also caused a blue-shift in the spectrum (Fig. III.70, p. 152).

A change in the absorption spectrum relative to that of free melittin was also observed in salt solutions and in membranes (Fig. III.73). The spectra shifted to the red by about 2 nm. Thus, a structural change in the ground state occurred, in agreement with

previous CD measurements (Drake and Hider, 1979). The fluorescence spectra were found in all cases to be virtually independent of the exciting wavelength, apparently as a result of the very small spectral shift in the absorption spectra relative to that of free melittin.

The question arose as to whether structural changes occurred in the tryptophan residue or in melittin itself, which would possibly cause a change in the tryptophan. To decide between these two possibilities, fluorescence spectra of free tryptophan were taken as a function of inorganic phosphate concentration (data not shown). The shapes and maxima of the spectra were not affected. For melittin, however, large blue-shifts were observed—up to a phosphate concentration of 0.15 M (Fig. III.71, p. 153). Very little change was noted by increasing further the concentration to 0.5 M. Apparently, the protein underwent a structural change affecting, in turn, the tryptophan residue. The protein structural change has been reported to involve an increase in the α-helical content of the protein (Dawson et al., 1978; Drake and Hider, 1979). Another study (DeBony et al., 1979) suggested that at high ionic strength melittin is in a tetrameric form, while at low ionic strength it is in a monomeric form.

In the case of free tryptophan, Szabo and Rayner (1978) and Robinson et al. (1978) reported two overall fluorescence decay components corresponding to decay time of 2.8 ns and 0.5 ns. Robinson (personal communication) later retracted those measurements. He now finds that there is one decay component with another extremely short-lived component that could not be detected with a picosecond streak camera.

A slight emission wavelength-dependence of the fluorescence decay time was observed in the case of melittin in Tris buffer (much the same as in the case of free tryptophan), with the fluorescence decay being monoexponential (see Figs. III.1 through III.3, pp. 17-21 and Figs. III.6 through III.8, pp. 27-31). Upon adding inorganic phosphate, there was a definite wavelength-dependence with the emission of the tryptophan residue decaying as the sum of two exponentials at the emission wavelength of 330 nm (Figs. III.9, p. 33 and III.13, p. 41). In the case of melittin in the presence of 0.15 M phosphate, the decay times were 2.5 ns and 0.6 ns with a ratio of amplitudes equal to 0.58 (Table III.1, p. 87). At 340 nm and longer emission wavelengths, however, the decay process was monoexponential. Such was not the case, however, for NaCl solutions. In the presence of both 0.15 M NaCl and 1.0 M NaCl, melittin decayed monoexponentially for all emission wavelengths. Decay times of 2.6 ns, 3.0 ns, and 3.1 ns were observed for melittin in 0.15 M NaCl at the emission wavelengths of 330 nm, 360 nm, and 390 nm, respectively (Table III.1, p. 87). After adding 1.0 M NaCl to melittin, the fluorescence decay times became 2.2 ns, 2.4 ns, 2.6 ns, and 3.0 ns for emission wavelengths of 330 nm, 340 nm, 360 nm, and 390 nm, respectively (see Table III.1, p. 87). There was appreciable time-resolved dependence with 1.0 M NaCl (Fig. III.40, p. 92). Another important observation concerning the effects of salts on melittin was that very little inorganic phosphate (as low as 0.02 M) caused a detectable change in the structure of melittin (Fig. III.71, p. 153). Because of this, Tris buffer was used in all of the solutions.

Upon binding melittin to egg lecithin or distearoyllecithin, a monoexponential fluorescence decay was observed for all emission wavelengths (see Table III.1, p. 87). Unfortunately, the fluorescence decay for 330 nm could not be studied due to the relatively high amount of scattered light interfering with the fluorescence signal. Time-resolved studies showed that there is a time-dependence in the case of egg lecithin, occurring before 3 ns (Fig. III.41, p. 93). With distearoyllecithin, the time-resolved data indicated a slight time-dependence throughout the time range at both above and below the phase transition temperature (Figs. III.42 and III.43, pp. 94 and 95).

Nanosecond depolarization analysis provided a great deal of information on the nature of binding of melittin to membranes. Melittin in 0.01 M Tris buffer had a rotational correlation time of 1.1 ns (Table III.2, p. 129). After adding 0.15 M inorganic phosphate, the rotational correlation time became 3.6 ns which indicated a structural change. Drake and Hider (1979) observed a change in the ground state by using the CD technique. Above the phase transition temperature of distearoyllecithin, there was more flexibility at the binding site, compared to room temperature, as indicated by the values of the rotational correlation time (4.9 ns versus 12.5 ns at room temperature). In the case of egg lecithin, there was also a relatively high value of the rotational correlation time (10.1 ns) caused by binding to the membrane. While the ϕ values for egg lecithin and distearoyllecithin at room temperature were very similar, there was a drastic decrease in the ϕ value at 61°C, consistent with increased flexibility at the

elevated temperature. It should be noted that there was only a very small change in the emission spectral maximum (Fig. III.72, p. 154) which precludes a major temperature-induced conformational change on the protein and/or change in the mode of binding to the membrane.

The zero point anisotropy (r(ȯ)) values are also important in detecting structural changes. The lowest r(o) value (0.052) was observed when melittin was bound to distearoyllecithin at room temperature. This r(o) value is approximately one-half that of melittin attached to distearoyllecithin at 61°C (see Table III.2, p. 129). Apparently, there is a very fast relaxation process in the subnanosecond range which caused the fast depolarization. All r(o) values are much smaller than the value of 0.24 for free tryptophan which was obtained in propylene glycol at -58°C. This r(o) value of 0.24 is in good agreement with that reported by Valeur and Weber (1977).

Acrylamide quenching studies were also employed to study the binding of melittin to membranes. This quencher was preferred to the charged NaI quencher. Acrylamide did not dissociate the protein. The fluorescence spectrum was found to remain unchanged after enough acrylamide was added to produce 50% quenching. Acrylamide did not even affect the protein as judged by the invariability of the fluorescence spectrum of free melittin and of melittin in a 0.15 M phosphate environment (data not shown). It should also be noted that acrylamide did not penetrate into the membrane—it was a probe of the hydrophilic portion of the protein or membranes due to its $-NH_2$ group. Therefore, if the tryptophan residue of melittin is exposed to the solvent after it

binds to a membrane, fluorescence quenching would take place in the presence of acrylamide.

Eftink and Ghiron (1977) used quenching analysis in determining the degree of exposure of the tryptophan residue in certain proteins. They used an excitation wavelength of 295 nm and had to apply a correction factor due to the absorbance of acrylamide. In working with melittin, I chose an excitation wavelength of 305 nm and adjusted the absorbance of melittin to 0.05. By doing this, no correction factor was necessary because the absorbance of acrylamide at 305 nm was only 0.001. In analyzing the quenching data, F_0/F was plotted against [Q], where F_0 is the fluorescence intensity in the absence of the quencher, F is the fluorescence intensity in the presence of the quencher, and [Q] is the concentration of the quencher. The plots showed upward curvature (Figs. III.60 through III.69, pp. 131-149) due to instantaneous quenching. Apparently, some of the acrylamide molecules were in very close proximity with the tryptophan residue before excitation. Weller (1961) studied theoretically this aspect of fluorescence quenching and showed that by modifying the equation to $(F_0/F)e^{-V[Q]}$ versus [Q], a straight line could be obtained by varying the value of V. V is the quenching constant for instantaneous quenching and is a measure of the degree of accessibility of acrylamide to the tryptophan residue in the ground state.

An important set of observations was made regarding diffusion-controlled quenching versus instantaneous quenching. Total fluorescence decay times were measured in the presence (τ) and absence (τ_0) of a concentration of acrylamide to yield 50% quenching of the

steady-state signal. The ratio of τ_0/τ (3.0 ns/1.8 ns) was determined to be 1.6 in the case of melittin in Tris buffer, 1.7 (τ_0/τ = 2.8 ns/1.6 ns) in the case of melittin in 0.15 M inorganic phosphate, and 1.3 (τ_0/τ = 2.4 ns/1.8 ns) in the case of melittin bound to egg lecithin. If τ_0/τ is equal to 2, then quenching is diffusion-controlled. The findings that the ratios were less than 2 indicate that instantaneous quenching occurs in addition to diffusion-controlled quenching.

It is seen from Table III.3, page 151, that the values of the second-order rate constant (Kq) of acrylamide quenching for free tryptophan and free melittin are comparable. This is in agreement with the red-shifted fluorescence spectrum of that residue indicating its exposure to the solvent (see Fig. III.70, p. 152). In a phosphate environment, Kq decreases implying a conformational change that results in shielding of the residue from the solvent. Interestingly enough, the charge of the phosphate ion is not important because it was found that the optical properties of melittin were identical in the presence of KH_2PO_4 or K_2HPO_4. Quite appreciable values of Kq for egg lecithin and distearoyllecithin at room temperature were obtained. Interestingly, the degree of exposure is very similar in the two cases as indicated by the magnitude of the Kq values.

Clearly there are two possibilities for interpreting the relatively high values of Kq in the case of membranes:

(1) The tryptophan residue does not penetrate into the membrane. The protein undergoes a conformational change with a concomitant increase of the α-helical content and shielding of the tryptophan residue from the solvent.

(2) The tryptophan residue penetrates into the lipid bilayer shielding tryptophan from the solvent. Structural fluctuations in the membrane (which may be brought about by thermal changes) allow exposure of tryptophan to the quencher.

The similarity between the optical properties of the tryptophan residue in salt solutions with those involving membranes suggests that the conformations of the protein are very similar in the two cases and lends strong support for mechanism (1). The fact that tryptophan is situated next to the hydrophilic residues (Dawson et al., 1978) is in harmony with this inference. Previous workers (Mollay and Kreil, 1973) favored (2) on the basis of the emission spectral maximum. As Eftink and Ghiron (1976a and 1977) emphasized, however, that criterion can be quite misleading, with acrylamide quenching yielding much more reliable information.

Above the phase transition temperature of distearoyllecithin, Kq increased much more than the observed increase of Kq of free melittin upon going to that temperature (see Table III.3, p. 151). This implies a conformational change in the membrane that allows a greater degree of accessibility of tryptophan by the quencher.

Addition of 1.0 M NaCl to egg lecithin resulted in a reduction of the Kq value which, however, paralleled the reduction in Kq when 1.0 M NaCl was added to free melittin (see Table III.3, p. 151). This indicates that the major effect of NaCl is on the protein and not on the membrane.

The values of V are now briefly discussed. It is seen from Table III.3, page 151, that V obtains its highest value for free

tryptophan. This is to be expected, for V is a measure of the accessibility of tryptophan to the quencher in the ground state. From all other cases, melittin in NaCl has the highest V value. Thus, NaCl appears to affect the conformation of the protein differently than K_2HPO_4. Another indication of differences in the effects of these two salts is provided by the finding that the fluorescence decay profile of the tryptophan residue at 330 nm is monoexponential in NaCl but double exponential in K_2HPO_4 (see Table III.1, p. 87). For membranes, distearoyllecithin at room temperature has the lowest V value.

In interpreting the nanosecond optical properties of melittin, it is important to note that free melittin exhibited a behavior very similar to that of free tryptophan (see Fig. III.70, p. 152). The emission wavelength-dependence of the decay time and the time-dependence of the emission spectra in the nanosecond range for salt solutions and membranes could then arise from:

(1) aggregation of melittin as was proposed by DeBony et al. (1979), or

(2) heterogeneous population of the tryptophan residue in monomeric protein.

The increase in the rotational correlation time, ϕ, nevertheless, can still be taken to support mechanism (1) on the following ground: the transition from random-coil to α-helix upon addition of 0.15 M inorganic phosphate (Drake and Hider, 1979) would have resulted in a lower value of ϕ according to mechanism (2), contrary to the experimental observations. The fact, however, that the shape of melittin is not globular makes such

comparisons not very reliable. Determination of the molecular weight of melittin in different environments by the ultracentrifuge method would provide a more direct test of the aggregation hypothesis.

These results demonstrate that the optical techniques employed in this study are able to follow the structural changes melittin undergoes in the presence of salts or when it binds to membranes. The macromolecule changes structurally in inorganic phosphate in a manner similar to that when it binds to membrane. This implies that electrostatic interaction occurs between basic amino acid residues, e.g. arginine or lysine, of melittin and the membrane phosphate groups.

NaCl seems to cause a structural change in melittin, also. Melittin in a NaCl environment has optical properties that are very similar to those in membranes. As was discussed above, these observations may imply that salt (free or part of the membrane structure) causes aggregation of the protein.

Egg lecithin and distearoyllecithin were used in this research project because they were found to be the least turbid after melittin was added. It would be interesting to see how melittin binds to a membrane with an overall negative charge, e.g. phosphatidylserine, since egg lecithin and distearoyllecithin are zwitterionic.

REFERENCES

REFERENCES

Badea, M. G. and Georghiou, S. (1976) Rev. Scient. Instrum. 47, 314.

Birks, J. B. (1970) Photophysics of Aromatic Molecules, John Wiley, New York.

Cogan, V., Shinitzky, M., Weber, G., and Nishida, T. (1973) Biochemistry 12, 521.

Dawson, C. R., Drake, A. F., Helliwell, J., and Hider, R. C. (1978) Biochem. Biophys. Acta 510, 75.

Dayhoff, M. D. and Eck, R. V. (1968) Atlas of Protein Sequence and Structure, National Biomedical Research Foundation, Silver Spring, Maryland.

Drake, A. F. and Hider, R. C. (1979) Biochem. Biophys. Acta 555, 371.

DeBony, J., Dufourcq, J., and Chin, B. (1979) Biochim. Biophys. Acta 552, 531.

Defourcq, J. and Faucon, J. F. (1977) Biochim. Biophys. 467, 1.

Eftink, M. R. and Ghiron, C. A. (1976a) Biochemistry, 15, 672.

Eftink, M. R. and Ghiron, C. A. (1976b) J. Phys. Chem. 80, 486.

Eftink, M. R. and Ghiron, C. A. (1977) Biochemistry, 16, 5546.

Georghiou, S. (1975) Photochem. Photobiol. 22, 103.

Grinvald, A. and Steinberg, I. Z. (1974) Anal. Biochem. 59, 583.

Grinvald, A. (1976) Anal. Biochem. 75, 260.

Kawato, S., Kinosita, K., and Ikegami, A. (1977) Biochemistry, 16, 2319.

Lianos, P. C. "Photophysical Properties of Pyrene of Biophysical Importance," Diss. Univ. of Tennessee, 1978.

Mollay, C. and Kreil, G. (1973) Biochim. Biophys. Acta 316, 196.

Mollay, C., Kreil, G., and Berger, H. (1976) Biochim. Biophys. Acta 426, 317.

Robinson, G. W., Fleming, G. R., Morris, J. M., Robbins, R. J., Woolfe, G. J., and Thistlethwaite, P. J. (1978) Proc. Nat. Acad. Sci. 75, 4652.

Sessa, G., Freer, J. H., Colacicco, G., and Weissmann, G. (1969) J. Biol. Chem. 244, 3575.

Szabo, A. G. and Rayner, D. M. (1978) Can. J. Chem. 56, 743.

Teale, F. W. J. (1960) J. Biochem. 76, 381.

Valeur, B. and Weber, G. (1977) Photochem. Photobiol. 25, 441.

Walker, M. S., Bednar, T. W., and Lumry, R. (1967) J. Chem. Phys. 47, 1020.

Weller, A. (1961) Prog. React. Kinet. 1, 187.

VITA

Michael L. Thompson was born on March 31, 1954, in Ithaca, New York. The oldest of three sons of Dr. Walter and Doris Thompson, he grew up in Greeneville, North Carolina. He attended J. H. Rose High School in Greenville until December 1970. After the family moved to Hixson, Tennessee, he enrolled at Hixson High School from where he was graduated in June 1972. In September of 1972, he entered The University of Tennessee at Knoxville and was graduated in December 1976 with a major in Cell Biology. He then entered the Graduate School at The University of Tennessee to pursue a degree in the Institute of Radiation Biology. He received his Master of Science in December 1980 and will attend the College of Dentistry at The University of Tennessee Center for the Health Sciences in the fall of 1980.